Proceedings of the 54th Annual Ohio River Valley Soils Seminar

Water in Geotechnical Engineering

November 13, 2024
Great American Ball Park
100 Joe Nuxhall Way
Cincinnati, Ohio

ORVSS LIV Planning Committee:

Suraj Khadka, P.E. (UES)
Nick Kloenne, P.E. (Goettle)
Sudip Khadka, P.E. (S&ME)
Donald Thelen, P.E. (UES, Retired)
Rebecca Scherzinger, P.E. (UES)
Russ Gatermann, P.E. (Geopier, a division of CMC)
Aaron Klingshirn, P.E. (Goettle)

Agenda – Tuesday, November 13, 2024

6:30-7:15 am	Exhibitor Setup
7:15-7:50 am	**Attendee Sign-In/Registration**
7:50-8:00 am	**Welcome Remarks**
8:00-8:50 am	Paddy's Run: Levee Under-Seepage Design and Monitoring *Adam Hacker, P.E., and Matthias Lindenbauer, P.E. (HDR)*
8:50-9:40 am	Interferometric Synthetic Aperture Radar to Monitor Slow Moving Ground Deformation *Stuart Edwards, P.E., LM. ASCE*
9:40-10:00 am	**Coffee Break**
10:00-11:00 am	Case Study: Underwater Retrogressive Slope Failure: Observation and Analysis *Timothy D. Stark, F. ASCE, D.GE, University of Illinois*
11:00-11:50 am	The Effects of Porewater Pressure on Driven Pile Installation in the Ohio Valley *Ben White, P.E., and Bradley Klausing, E.I.T. (GRL Engineers)*
11:50-12:50 pm	**Lunch Break**
12:50-12:55 pm	Keynote Speaker Introduction
12:55-1:55 pm	**Keynote Speaker:** Soil and Water: An appreciation of People, Places and Experiences *Mark T. Bowers, PhD, P.E.* (Professor Emeritus, University of Cincinnati)*
1:55-2:45 pm	From PFMs to PZ Readings: Considerations for a Dam Seepage Modification *Kyle Blakley, P.E. (Stantec)*
2:45-3:05 pm	**Coffee Break**
3:05-3:55 pm	Bifurcation and Repurposing of a Lime Sludge Lagoon *Daniel Woeste, P.E., (Geosyntec) and David Mueller, P.E. (Goettle)*
3:55-4:45 pm	Near-Surface Geophysical Methods for Subsurface Characterization Across River Channels *John M. Schneider, P.G., Adam Gostic, P.G., Amber K. Lacy (S&ME)*
4:45-4:50 pm	**Closing Remarks**
5:00-6:00 pm	**Happy Hour**

Table of Contents

**Keynote Speaker-ORVSS LIV*

Paddy's Run: Levee Under-Seepage Design and Monitoring

Adam Hacker, P.E., and Matthias Lindenbauer, P.E.

Abstract: The Louisville Metro Levee System reduces flood risk to the City of Louisville, Kentucky, and was constructed by the U.S. Army Corps of Engineers (USACE). It is now operated and maintained by the local sponsor, Louisville and Jefferson County Metropolitan Sewer District (MSD). MSD determined the need to construct a new flood pump station within the existing levee prism along the Ohio River. The existing subsurface configuration, consisting of a clay blanket overlaying alluvial sand and bedrock formation, puts attention towards under-seepage potential failure mode (PFM) concerns related to the levee system impacted by the new flood pump station design. A diaphragm wall structure serves as the temporary support of excavation (SOE), and subsequently as a permanent foundation for the new flood pump station. The diaphragm wall system follows the footprint of the new flood pump station and extends through blanket and alluvial material into the underlying bedrock. This configuration will provide a localized under-seepage cutoff beneath the levee. However, the diaphragm walls introduce end-around effects around the corners of the cutoff structure. High seepage gradients are the result at the structure's corners. Elevated pore water pressures on the land side of the levee would remain if an additional system was not constructed to address this concern. Further design selected a new relief well system as risk reduction measure to mitigate elevated pore water pressures on the land side of the levee. The under-seepage design considered both features complementing each other, the effects of the diaphragm wall cutoff and the new relief well system. The design was conducted in accordance with current USACE engineering criteria. Finite element section and plan view seepage analyses supported the design efforts. In addition, a PowerBI Dashboard was created for all stakeholders involved to observe in-place slope inclinometer and vibrating wire piezometer data collected during construction on-site and in real-time. This contributes to levee safety throughout the project duration and creates long-term benefits to validate the finite-element modeling efforts performed. It also benefits the further understanding of finite element modeling used for relief well design, as part of current draft version of engineering manual EM 1110-2-1914.

Introduction

The Louisville Metro Levee System reduces flood risk to the City of Louisville, Kentucky. The levee system was constructed by the U.S. Army Corps of Engineers (USACE) and is now operated and maintained by the local sponsor, the Louisville and Jefferson County Metropolitan Sewer District (MSD). The levee system has a total length of 26.1 miles, consisting of concrete floodwalls and an earthen levee with sixteen flood pump stations for flood risk reduction.

In the 1950's, USACE built the Paddy's Run Flood Pump Station in the western portion of Jefferson County, Kentucky as one of sixteen flood pump stations constructed to support flood risk reduction efforts for the Louisville Metro Levee System. Paddy's Run Flood Pump Station pumps the combined sewer water from the western metropolitan area of

Louisville through water discharge pipes over the levee into the Ohio River. Combined sewer water from the Southwestern Outfall Sewer flows into the existing station's wet well. Surface runoff water reaches the existing Paddy's Run Flood Pump Station through Paddy's Run Creek, flowing into the station's wet well. Additional storm water is collected in a ponding area, land side of the levee, during extreme rain events when the wet well reaches capacity. The Southwestern Sewage Outfall conveys water from the western metropolitan area under the levee to Closure Structure 118. The discharges from the outfall flow into the Ohio River when the Ohio River is not elevated. The pump station is only active when the Ohio River is elevated, and Closure Structure 118 closes its floodgate to prevent inland backflow through the Southwestern Outfall Structure caused by the head-differential between the Ohio River and the land side ponding area water elevation. A closed closure structure prevents gravity outflow resulting in any interior inflow to be pumped over the levee.

Holistic Project Design Approach

Recently, MSD determined the need to upgrade the existing Paddy's Run Flood Pump Station's capacity to reduce the risk of interior flooding. MSD determined the new flood pump station capacity would need to increase existing capacity from 875 million gallons a day (MGD) to 1,900 MGD to account for 2035 projected storm event using 10-year, 24-hour storm event (5.0 inches in 24 hours). Due to the age and complications associated with upgrading the existing pump station, a new pump station was selected as preferred approach. In 2021, MSD initiated the Paddy's Run Flood Pump Station Capacity Upgrade (PRFPSCU) project to construct the new flood pump station. The new flood pump station is being constructed within the existing levee prism of the Louisville Metro Levee System. Portions of the existing station will be selectively demolished after the new station goes into operation.

Soil and Site Conditions

Geotechnical exploration performed at the project site found the subsurface characterization consists of up to 60 feet of compacted lean clay fill for the levee embankment, overlying in order of occurrence, 20 feet of native silty lean clay, 40 feet of sands and gravels that are part of the glacial outwash overlying bedrock, identified as New Albany Shale. A 12-inch-thick layer gravel blanket beneath the levee embankment was noted on USACE's as-built drawings of levee construction (USACE). The gravel blanket was only encountered beneath portions of the levee embankment and samples retrieved showed coarse gravel with high fines content. The native silty lean clay with some sands from recent alluvial deposits was identified as the clay blanket over the deeper sands and gravels from the glacial outwash. The glacial outwash deposit makes up the aquifer system located over majority of western and downtown Louisville. The glacial outwash was noted to have an upper and a lower zone. The upper zone consisted of looser and finer sands with some gravels, silts, and clays, while the deeper deposit consisted of coarse and dense sands and gravels. These layers are identified in this paper as the upper and lower alluvial sands. Figure 1 below schematically shows the soil lithology derived from the subsurface exploration results and the proposed flood pump station, including diaphragm foundation walls acting as cutoff. The cutoff feature is explained in detail later in this paper.

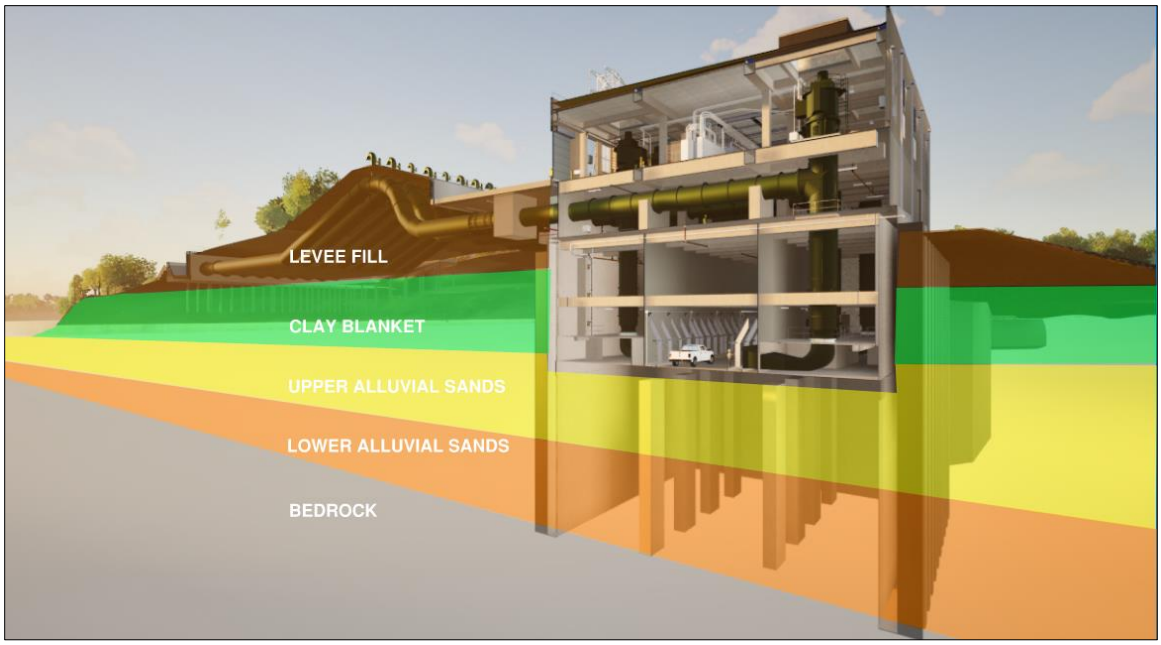

Figure 1: Normalized Soil Lithology

An extensive laboratory testing campaign was conducted to estimate the soil's seepage and shear strength material parameters, as well as bedrock foundation characteristics. Table 1 below summarizes the hydraulic parameters relevant for the seepage analysis conduct as part of this project and herein.

Table 1: Hydraulic Parameters for Seepage Analysis

Material	**Vertical Hydraulic Conductivity K_v (cm/s)**	**Anisotropy K_h/K_v**	**Residual Water Content (%)**	**Volumetric Water Content (%)**
Levee Fill (Layer A)	5×10^{-8}	4	9	34
Gravel Blanket (Layer B) [(1)]	5×10^{-4}	1	2	24
Clay Blanket (Layer C)	1×10^{-7}	10	9	38
Upper Alluvial Sands (Layer D1)	1×10^{-3}	10	-- [(2)]	29
Lower Alluvial Sands (Layer D2)	1×10^{-3}	10	-- [(2)]	13

[(1)] Layer B is eliminated for the seepage assessment presented below. Refer to Section Modeling Assumptions*"*

[(2)] Layer D1 & D2 are below the groundwater table and always saturated. GeoStudio's SEEP/W "Saturated Only" material model was assigned during seepage analysis and requires no residual water content.

Existing Geometry

The existing levee embankment has a hydraulic height of nearly 50 feet with an approximate (appr.) crest width of 15 feet at elevation 460.0 feet. The river side of the

embankment is sloped 3 horizontal to 1 vertical (3H:1V) to an elevation of appr. 410.0 feet at the river side toe. A bench exists on the land side slope of the levee embankment at elevation 450.0 feet. The land side embankment slopes at 3H:1V to the bench and continues at a steeper slope of appr. 1H:1V to the land side toe of the embankment, located within the ponding area.

A typical cross-section is presented below for seepage and slope stability analyses, shown in Figure 2 below. The critical cross-section was determined by reviewing the variability in the subsurface stratigraphy regarding the thickness of the clay blanket within the former Paddy's Run Creek Area. The clay blanket was encountered at lower elevations in the northern area of the levee when compared to the rest of the site. The location of the former Paddy's Run Creek was determined to be the reason for this encounter variance. Figure 3 displays the contours of the estimated location of the original Paddy's Run Creek before the construction of the levee in 1953. As a result, the depth of levee fill material in the northern area of the project site, at former location of the Paddy's Run Creek, were found deeper than compared to the rest of the project area.

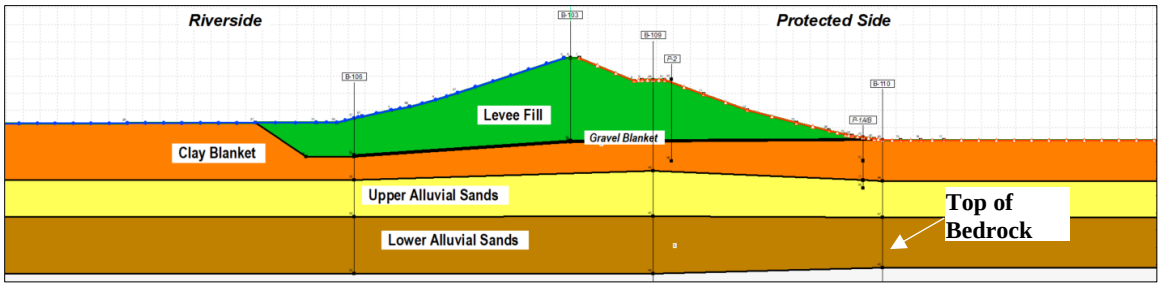

Figure 2: Typical cross-section

Pre-Construction Seepage Analysis

A preliminary analysis of the existing levee embankment was performed to understand the relationship between elevated Ohio River levels and how much pore water pressure increases beneath the clay blanket land side of the levee. It concluded that Ohio River flood events are highly influential to the pore water pressures that develop within the alluvial sands. Additionally, the elevated pore water pressures on the bottom of the clay blanket were found to show unfavorable conditions that could develop into seepage exit along the land side of the levee.

The seepage model analyses were performed using GeoStudio SEEP/W. GeoStudio SEEP/W uses finite element-based modeling to estimate the water gradients and pore water pressure distribution. The software allows the user to input problem geometry, boundary conditions, and soil properties to either compute hydraulic head or flow rate conditions for nodal points within the modeled mesh.

Modeling Assumptions

Key assumptions were determined when reviewing available information at the project site. The following assumptions were used when modeling the under-seepage:

- The gravel zone mentioned earlier between levee fill material and clay blanket was not considered an active drainage layer for the purpose of the seepage analyses. Four borings within the area of the gravel blanket did not retrieve any gravel material, two borings retrieved traces of fine to medium gravel material and three confirmed a gravel blanket with a total thickness of less than 12 inches. Figure 3 below shows the expected extent of the gravel layer from available as-built drawings outlined in red. The area of the previously existing Paddy's Run Creek outlined in blue. In addition, laboratory testing of the gravel blanket material retrieved, determined a fines content for the material of more than 21 percent. These findings support the gravel blanket does not act as an active drainage layer and does not support a notion to implement this layer in seepage modeling.

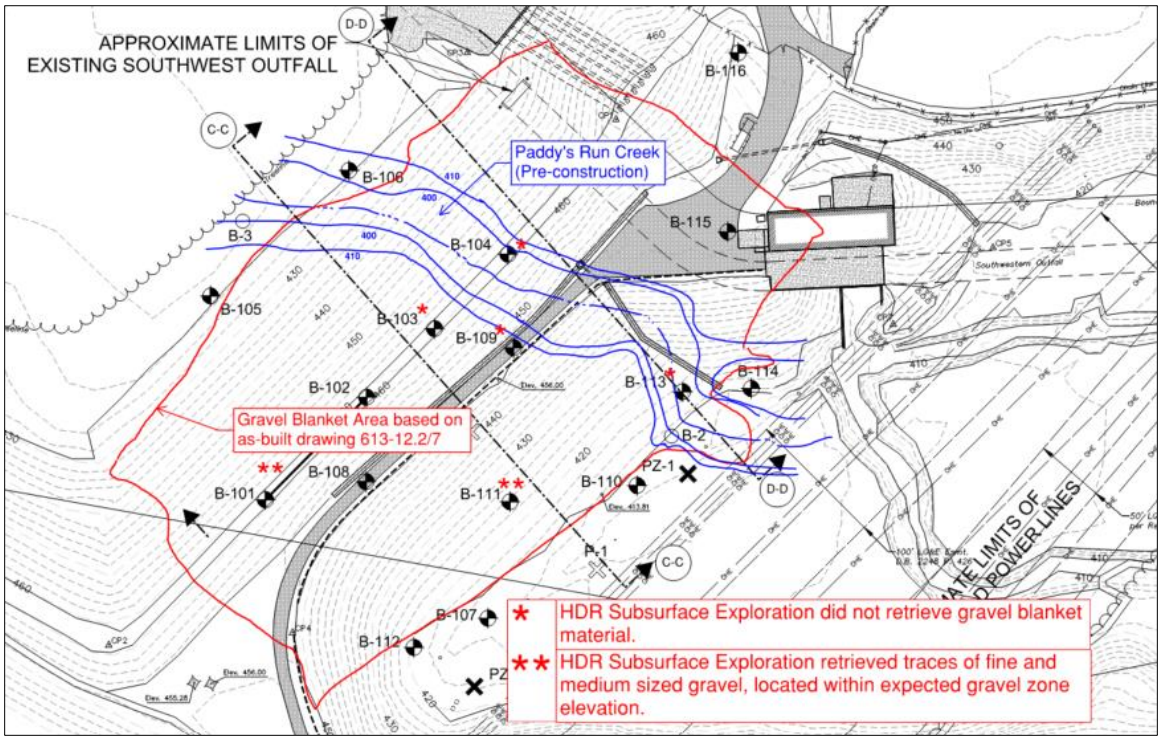

Figure 3: Gravel zone (in red) and former Paddy's Run Creek area (in blue) sketched on HDR's as-drilled drawing. Modeled cross-section C-C is shown as dotted black line.

- Existing relief wells on the land side were considered not to be functioning. At the time of initial construction in 1953 seven passive relief wells were installed on the land side levee toe. Data collected from existing vibrating wire piezometers between 2016 and 2019 shows elevated pore water pressures during flood events at the land side levee toe. As shown in Figure 4, piezometers P-1A (within clay blanket) and P-1B (in alluvial sands) show elevated pore pressures towards the end of February flood event in 2018. The pore pressures were approximately five feet above the ground surface supporting the assumption that the relief wells are likely not functioning at the design capacity. Additionally, no records of routine relief well maintenance were found which further

justified the concern that the relief wells are not functioning at the design capacity. The quick rise in piezometer P-1A shown in Figure 4 at this same time was assumed to be caused by the land side ponding area significantly flooding during this storm event. An aerial google image shown in Figure 9 shows the water elevation in the ponding area during this flood event.

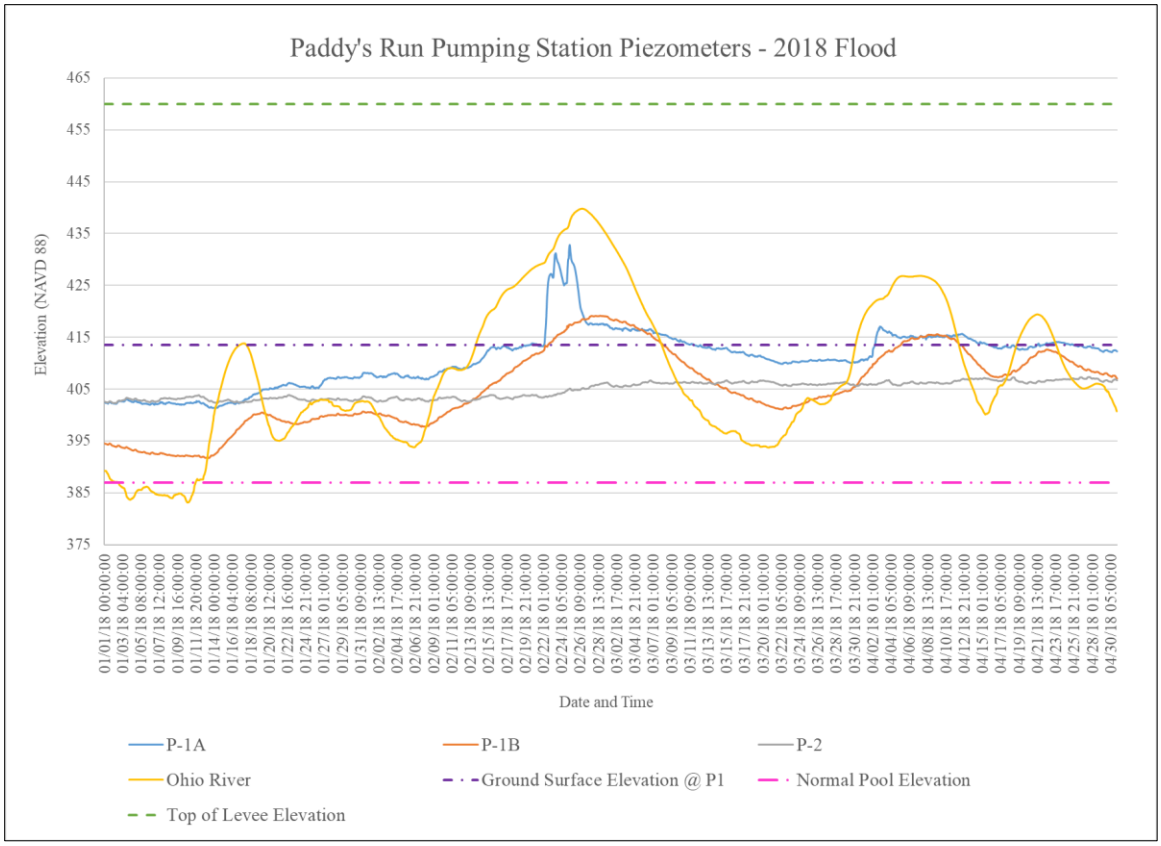

Figure 4: Piezometer data recorded during the 2018 flood event.

Boundary Conditions

USACE engineering manuals dictate the Ohio River elevation be set at crest of levee (El. 460 ft) at steady state conditions. This is approximately three feet higher than the flood of record from 1937. The groundwater elevation within the project boundaries was determined from surrounding wells to be approximately 393.0 feet during normal low water elevations of the Ohio River (El. 386.0 feet). However, it is important to recognize the groundwater elevation is dependent on Ohio River levels and land side rainfall events within the entire aquifer system. Figure 5 below shows the plan view seepage model water total head results prior to construction of the new flood pump station. The model results show water total head values between 440.0 feet and 445.0 feet on the land side levee toe. This level of elevated pore water pressure has the potential for seepage outbreaks.

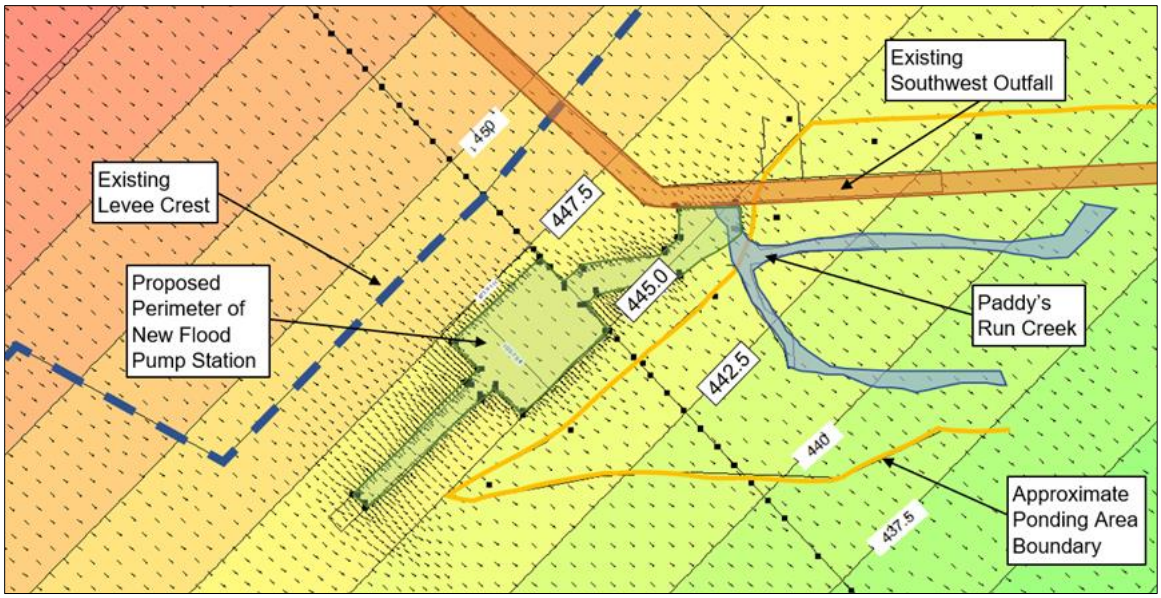

Figure 5: Aquifer plan view seepage model without under-seepage mitigation features (existing condition).

Subsequently, the pressure points calculated from the plan view model were implemented into the 2-dimensional cross-section model by using the water total head results from the plan view model at locations along cross-section. Model results were collected and inserted in the section model as node boundary conditions at the top of the aquifer, between upper alluvial sands and clay blanket layer. The cross-section model was compared to vibrating wire piezometers measurements to confirm the model was calibrated.

Seepage Modeling Verification

An additional step to evaluate the model was done by comparing the model results to in-field vibrating wire piezometer data. The flood events on the Ohio River are typically short events. As a result, the levee embankment will likely not reach a steady-state seepage condition. It just happens as to our benefit that available field data from the vibrating wire piezometers was collected during the 2018 flood event. During this flood event in 2018, the Ohio River crested at approximately El. 440.0 feet which is the highest event in 25 years. Accounting for the change in Ohio River over time, transient seepage analysis was utilized to model this event. The intent of comparing model results with field measured data was to evaluate the assumed input parameters, such as material characteristics and boundary conditions. Comparison to field measured data also increases the confidence to predict behavior of the system as accurately as possible and provides a sense for the margin of predictive error. It also allows the modeling of a variety of similar load case scenarios, including the prediction of transient seepage and slope stability parameters.

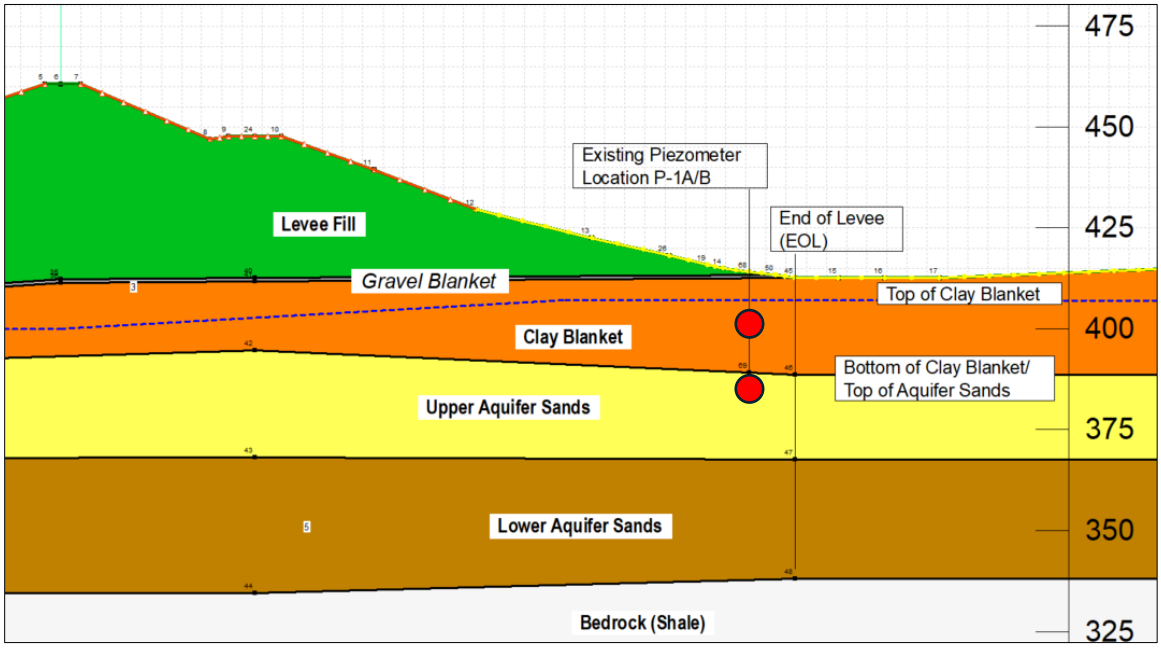

Figure 6: Typical cross section with piezometer locations P-1A and P-1B marked in red.

Vibrating wire piezometer PZ-1A is located at an elevation of 400.4 feet in the clay blanket layer, and PZ-1B is located at an elevation of 384.5 feet in the upper alluvial sands. Figure 6 above shows the location of the piezometers and stratigraphy of the levee section. Both piezometers measured a change in pore water pressure during the 2018 flood event.

Boundary conditions used for this model were the Ohio River, groundwater, and ponding area water levels. The Ohio River hydrograph measured at Lower McAlpine Lock during the 2018 flood event was implemented as a water total head function for the riverside boundary condition. The total duration of the flood event modeled was 59 days with time-stepping in one day increments. The initial water level condition on the riverside was implemented as 385.0 feet according to hydrograph data obtained before the 2018 flood event. The boundary condition representing the groundwater level landside 2000.0 feet from the levee crest was set to 396.0 feet. The landside boundary condition is based on studies from the U.S. Geological Survey (USGS) for the aquifer in the Louisville region (Lyverse, Starn, & Unthank, 1996). Studies have shown that the aquifer in the Louisville region functions as a homogenous unit and is primarily recharged by consolidated rocks in the eastern area of the valley, direct infiltration through the floodplain, small streams, and temporary infiltration from elevated Ohio River conditions. For reference, Figure 7 below shows the generalized cross-section of the alluvial aquifer at Louisville developed by Rorabaugh and others in 1953 (Lyverse, Starn, & Unthank, 1996).

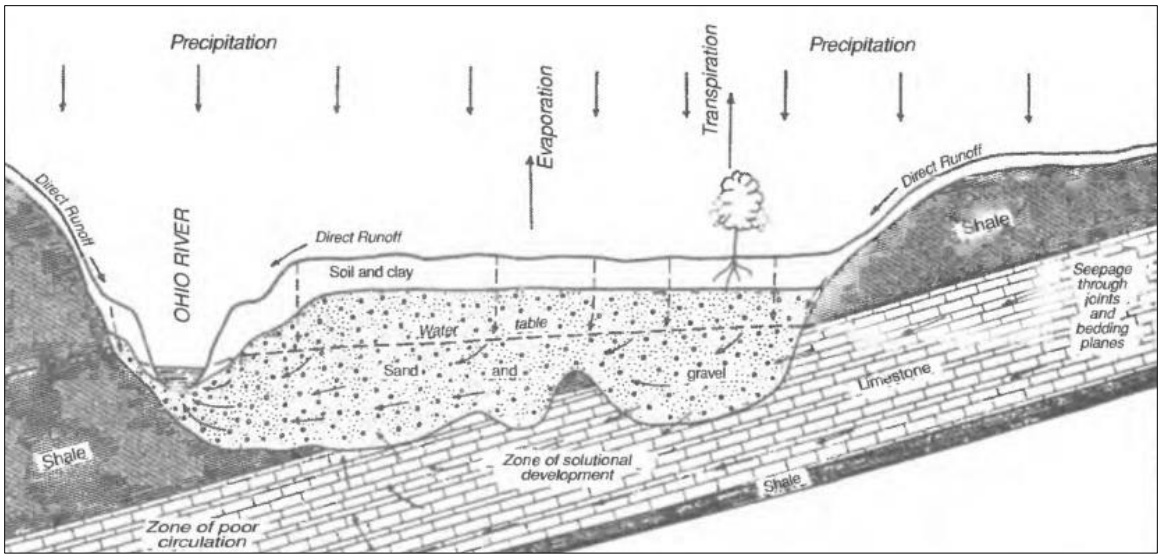

Figure 7: Generalized hydrologic cross-section of the alluvial aquifer at Louisville (Lyverse, Starn, & Unthank, 1996).

Minimum rainfall occurred leading up to the 2018 flood event, and Ohio River elevation levels were low, fluctuating by less than 5 feet. These conditions likely led to near steady-state conditions within the aquifer, which likely resulted in horizontal water flow from the bedrock boundaries in the east of the valley to the Ohio River.

Figure 8 below summarizes the 2018 Ohio River flood event data with the measured pore water pressures in P-1A and P-1B along with the calculated pore water pressure results from the model.

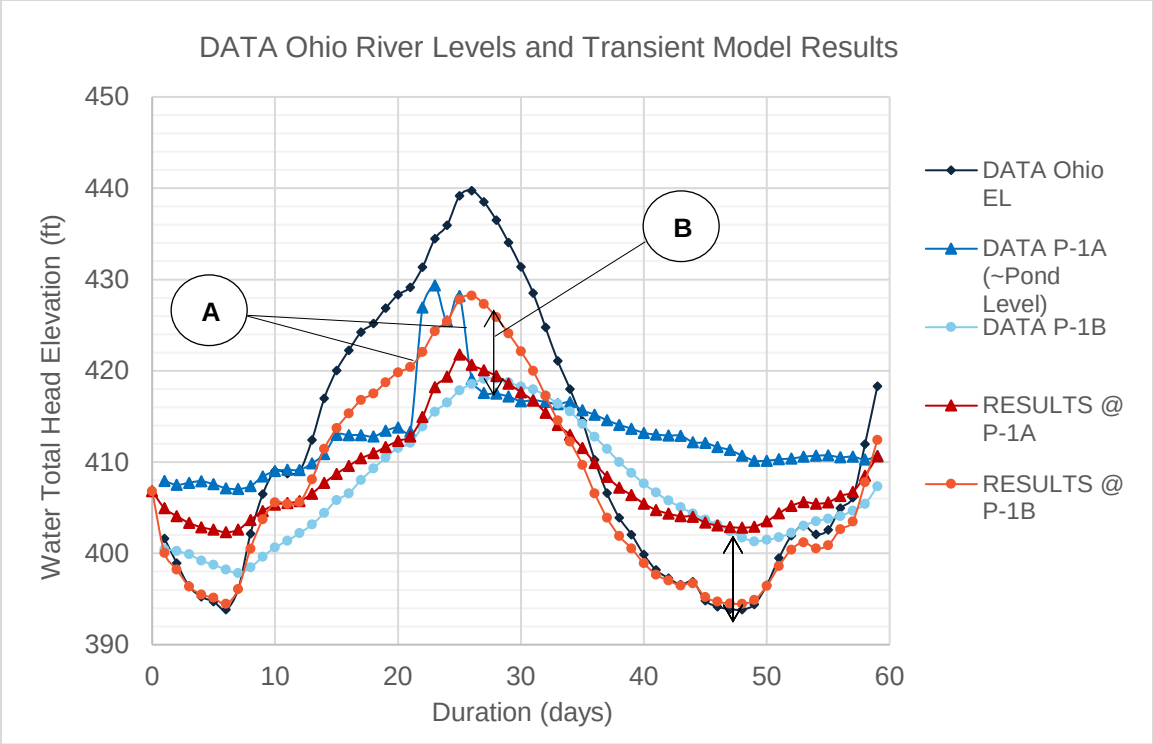

Figure 8: The Ohio River Hydrograph (black), in-field piezometer readings (blueish) and transient results at piezometer locations for the 2018 flood (reddish).

As mentioned above, P-1A records pore water pressures within the clay blanket. The model estimates the pore water pressures within the clay blanket during the time of elevated water levels in the ponding area. This data is coherent with Google Earth images at the time of elevated water levels in the ponding area during the 2018 flood event (Google, 2018). Figure 9 below shows the outline of sediment remains after the ponding area filled to approximately 430.0 feet on February 23, 2018. The estimated pore water pressure from the model for location PZ-1A estimated a difference of approximately 7.0 feet compared to the measured pore water pressure in the field. Additionally, the model does not show the spike and drop in pore water pressure measured by P-1A, as shown in Figure 8, Point A. This situation is due to the model not accounting for the ponding area quickly filling from the storm event and subsequently being drained by the existing flood pump station. The transient seepage model only recognizes changes in water pore pressures, not additional effective stress applied by the weight of the water in the ponding area.

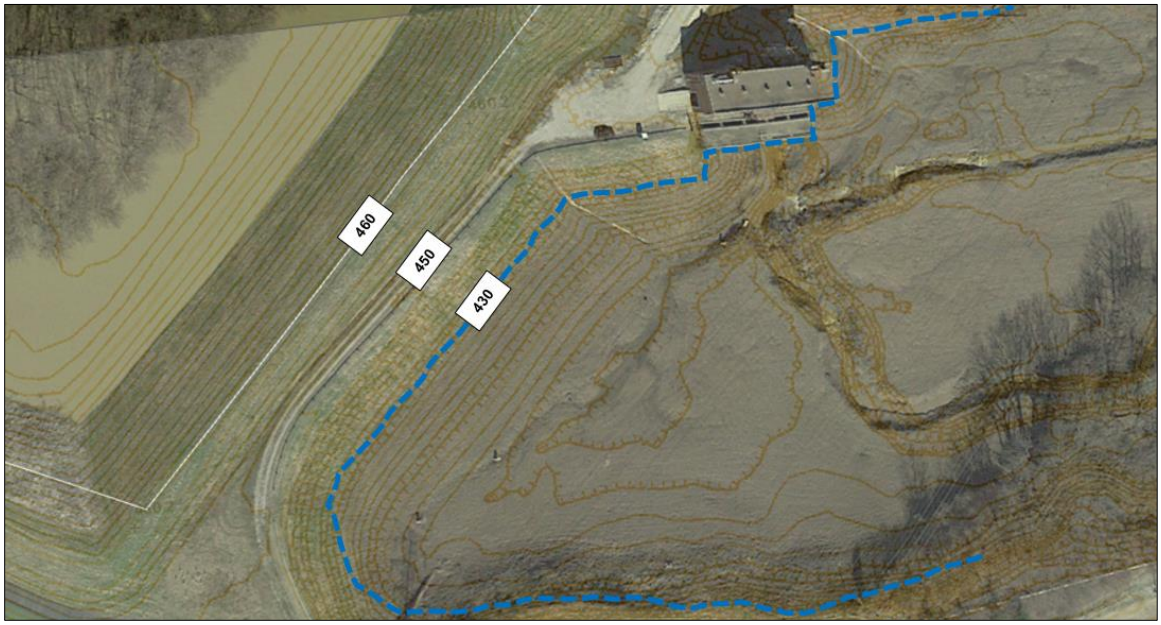

Figure 9: Aerial view of the ponding area on February 28, 2018, five days after the maximum P-1A reading of 429.36 feet (Google, 2018).

The aquifer pressures at the bottom of the clay blanket are measured by piezometer P-1B. The piezometer data of PZ-1B shows the immediate connection between alluvial sand pressures and Ohio River water levels. The transient seepage analysis models the same behavior of pore water pressure distribution within the alluvial sands when flood loads are applied on the riverside. However, the comparison of data shows that there is a discrepancy between pore water pressures measured in the field versus the estimated pore water pressures in the model. The maximum difference between the field measurement and estimated value during the peak of the flood event in 2018 was 9.1 feet as shown in Figure 8, Point B. This discrepancy is likely due to the transient seepage models not having an exact representation of the behavior happening in the field. However, the model is a conservative estimate for flood cases at a project location. The soil stratigraphy is assumed to be homogenous and potential variability could lead to false results. In addition, the hydrograph used for the boundary condition on the riverside was recorded upstream of the project site at McAlpine Lock, which creates an additional margin for error or delay of boundary conditions. The flood event implemented on the ponding side is not an accurate representation of the actual ponding area elevations.

Piezometer P-1A data shows more consistent water pore pressures before and after the flood, excluding the 27 days when the Ohio River peaked during the 2018 flood event. P-1A measured less impact by the Ohio River fluctuations but recognized water pore pressures caused by a saturated or filled ponding area. This condition could be the result of unknown degrees of saturation in the clay blanket that cannot be implemented into the model, or localized permeability material characteristics of the soil that develop a better connectivity to the ground surface than to the alluvial sands; therefore, subjecting P-1A primarily to loads caused by ponding area levels.

The likely explanation of the discrepancy is the regional aquifer effects at the project site. As shown in Figure 10, measured field data for Piezometer P-1B showed a slower rise than the model results using a constant groundwater elevation. This measured field data likely represents the aquifer being charged by the Ohio River. The opposite effect can be noted from the measured field data for Piezometer P-1B shows the water head above the Ohio River when it is receding. Again, this effect is likely from the aquifer draining back to the Ohio River. This connection between the Ohio River and the aquifer in the Louisville region was discussed earlier. The process of charging and discharging the aquifer is influenced by effects beyond the extent of the project site; such effects are unknown, and the exact time-dependent behavior of the aquifer response tough to model. An attempt to understand this effect was estimated by applying a time-stepped water flux boundary condition to the model. Figure 10 presents the model result with groundwater flow which closely matches the measured field data from Piezometer P-1B. The estimated groundwater flow ranged from 0 to 50 feet per day. This landside boundary condition is within the range of flowrates found in studies from the USGS for the aquifer in the Louisville region (Lyverse, Starn, & Unthank, 1996). However, as discussed previously, this charging and discharging effect is variable based on the flood events, recent rains in the region, and previous conditions of the aquifer prior to that flood event. The model results using reasonable flowrates further increase the confidence of the model.

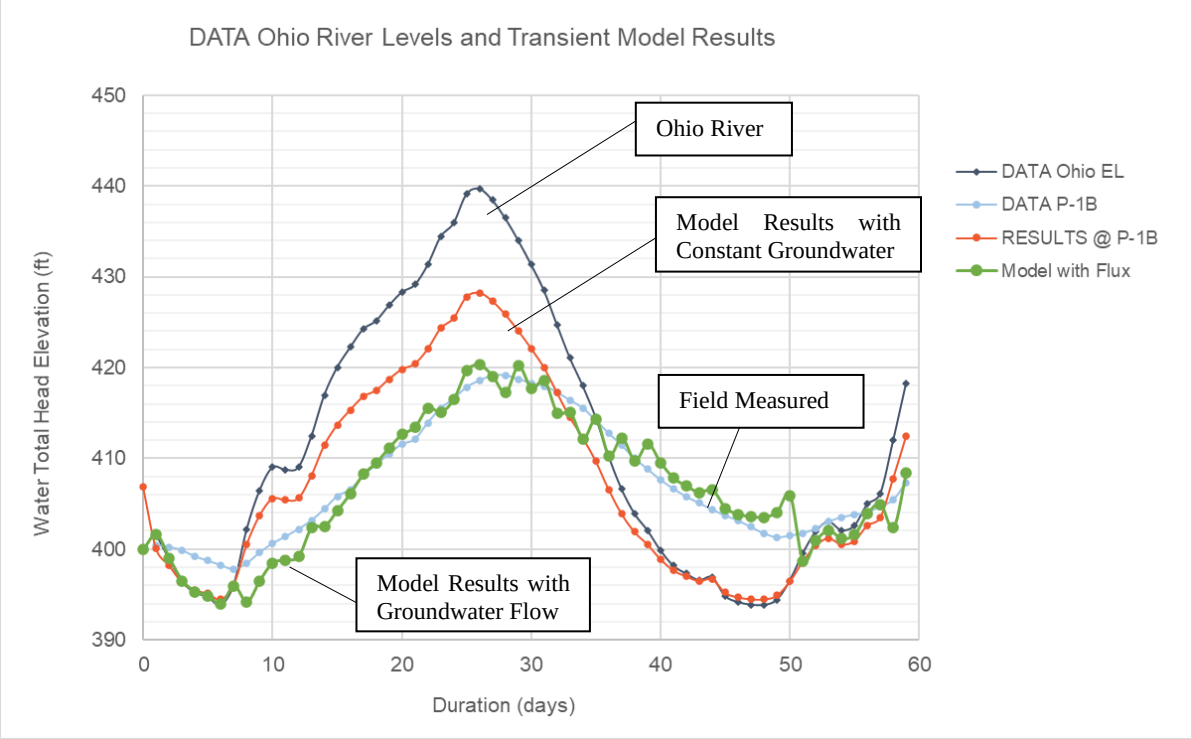

Figure 10: The Ohio River Hydrograph, in-field piezometer readings and transient results at piezometer locations for the 2018 flood.

New Flood Pump Station

The new Paddy's Run Flood Pump Station will be located within the existing levee embankment and will require support of excavation (SOE) during construction. The excavation for the new flood pump station is located within the alluvial sands. This would create a large risk to the project attempting to dewater for the excavation and addressing levee safety during construction. The design team determined the SOE system would need to be taken to bedrock to provide a cutoff of groundwater during excavation. The design team determined a concrete diaphragm wall system tied into bedrock would be best suited to address this design. The diaphragm wall's elements were designed to form a continuous wall around the perimeter of the proposed flood pump station shown in Figure 11. This approach would provide means of excavation without the need of active dewatering, provide a permanent seepage cutoff beneath this segment of levee, and incorporate structural elements to serve the purpose of a temporary SOE, permanent structural walls, and foundation elements.

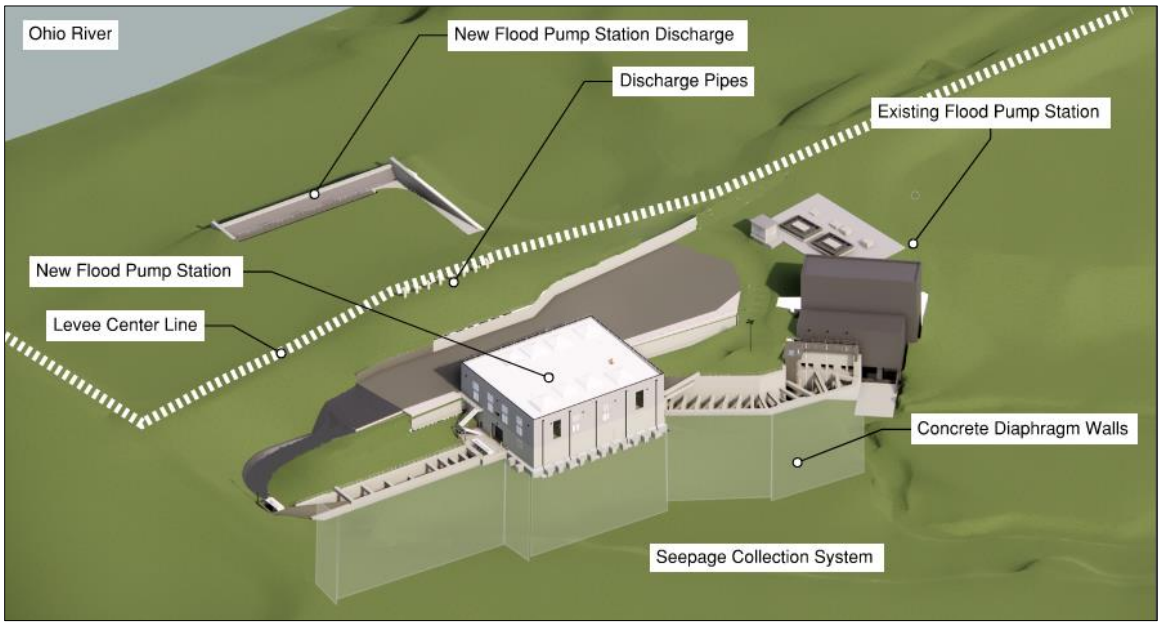

Figure 11: Paddy's Run Pump Station Capacity Upgrade Project

Support of Excavation Cutoff Wall

As previously mentioned, the SOE creates a cutoff to bedrock and addresses some of the existing seepage concerns. Further, a permanent cutoff to bedrock, SOE structure will address the upwelling from the seepage and levee instability concerns during construction and post project completion. The SOE structure consists of structural concrete diaphragm wall elements constructed five feet into bedrock following the perimeter of the proposed pump station. The riverside diaphragm wall elements function as a cutoff wall for alluvial sand under-seepage from the fluctuating Ohio River water levels. Plan view seepage analysis was conducted to assess the impact of the diaphragm wall SOE structure on seepage behavior. Figure 12 shows the alluvial sand pore water pressure distribution

calculated in GeoStudio SEEP/W with the SOE structure installed. The modeled load case accounts for a maximum flood load to the levee crest at 460.0 feet and an empty ponding area on the land side. The SEEP/W plan view model shows the seepage end-around effects created at the northern and southern corner of the diaphragm walls with increased hydraulic gradients, labelled as areas A and B in Figure 12. The SOE is acting as cutoff wall and contributes to a decrease of the water total head at the bottom of the clay blanket on the land side. Previous plan view model results shown in Figure 5 indicated water total head conditions around 445.0 feet on the land side toe. The SOE structure reduces the water total head pressure within the project boundaries to approximately 437.5 feet to 442.5 feet. However, as discussed further later, this reduction is not significant enough to mitigate the risk for seepage out breaks. As a result, additional risk reduction efforts to mitigate land side pore water pressure will be needed.

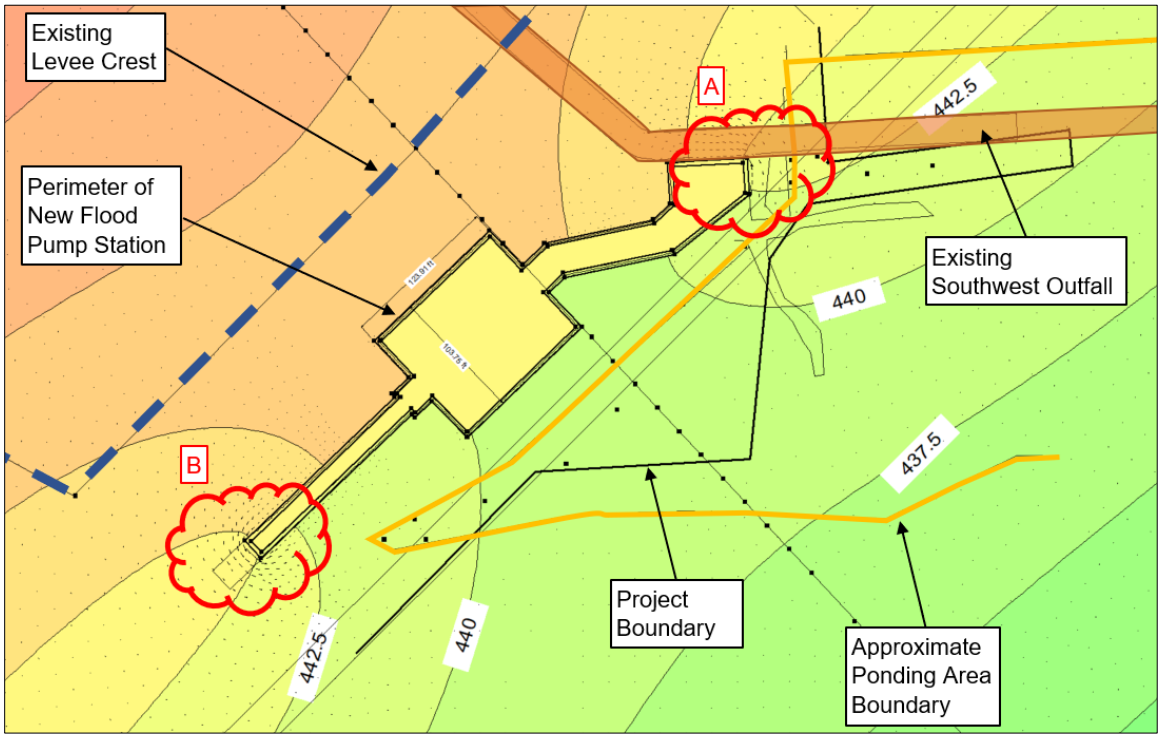

Figure 12: GeoStudio SEEP/W aquifer plan view analysis with diaphragm wall structure (under-seepage cutoff wall).

Relief Well System

Relief wells were selected as the additional risk reduction measure to reduce pore water pressures on the land side levee toe. The relief well system design was based on the USACE guidelines per current EM 1110-2-1914 (1992). Design approaches and results were compared to the EM 1110-2-1914 (2022) draft version and optimized with finite element aquifer seepage results obtained with GeoStudio SEEP/W. The relief wells are designed to be located on the land side of the existing Paddy's Run Levee approximately between Station 571+63 and 576+60 along the Levee Reach. The proposed relief well system consists of 11 relief wells. The relief wells will relieve excess pore water pressure into the

existing Paddy's Run Creek through collector pipes at elevation 408.0 feet. The relief wells must have sufficient depth to intercept the upper layer of alluvial aquifer sands and provide sufficient inflow area into the relief well pipe.

Design Loads and Allowable Water Total Head

The maximum flood case was also considered for the relief well design per current EM 1110-2-1914 (1992). The maximum flood load accounts for an Ohio River elevation to the crest of the levee (El. 460.0 feet) with no standing water land side of the levee using steady state conditions.

Calculations of allowable head for heave (vertical effective stress) and uplift (vertical gradient) show that the required factors of safety are not met after the diaphragm wall construction. For the relief well system design, the maximum water total head at the bottom of the clay blanket was calculated in respect to vertical effective stress and vertical gradient in coherence with EM 1110-2-1914 (1992) Design, Construction, and Maintenance of Relief Wells to meet minimum requirements per EM 1110-2-1913 Design and Construction of Levees.

The allowable water total head on the land side levee toe beneath the clay blanket was determined to be 423.5 feet for the average elevation of ground surface at 412.0 feet. The critical allowable water total head of 416.2 feet is identified within the area of the thinner clay blanket along the existing Paddy's Run Creek and governs the relief well design.

Proposed Location of Relief Wells

The proposed locations for the relief wells were selected based on the outer project boundaries, construction means and methods, calculation results per EM 1110-2-1914 (1992) relief well design approach for an infinite line of wells with an impervious top stratum and complemented with iterative finite element plan view seepage analysis results. Figure 13 shows 11 proposed relief well locations along the land side levee toe in plan. Figure 13 also shows the outlines of project boundaries, as well as areas affected by overhead powerlines. However, the proposed diameter for relief wells allows the use of smaller drilling equipment that is not restricted by an allowable maximum operating height under the overhead powerlines. The proposed relief well locations are within the proposed project boundaries. End-around seepage effects created by the diaphragm wall support of excavation structure are mitigated in the northern area of the project by three closely spaced relief wells.

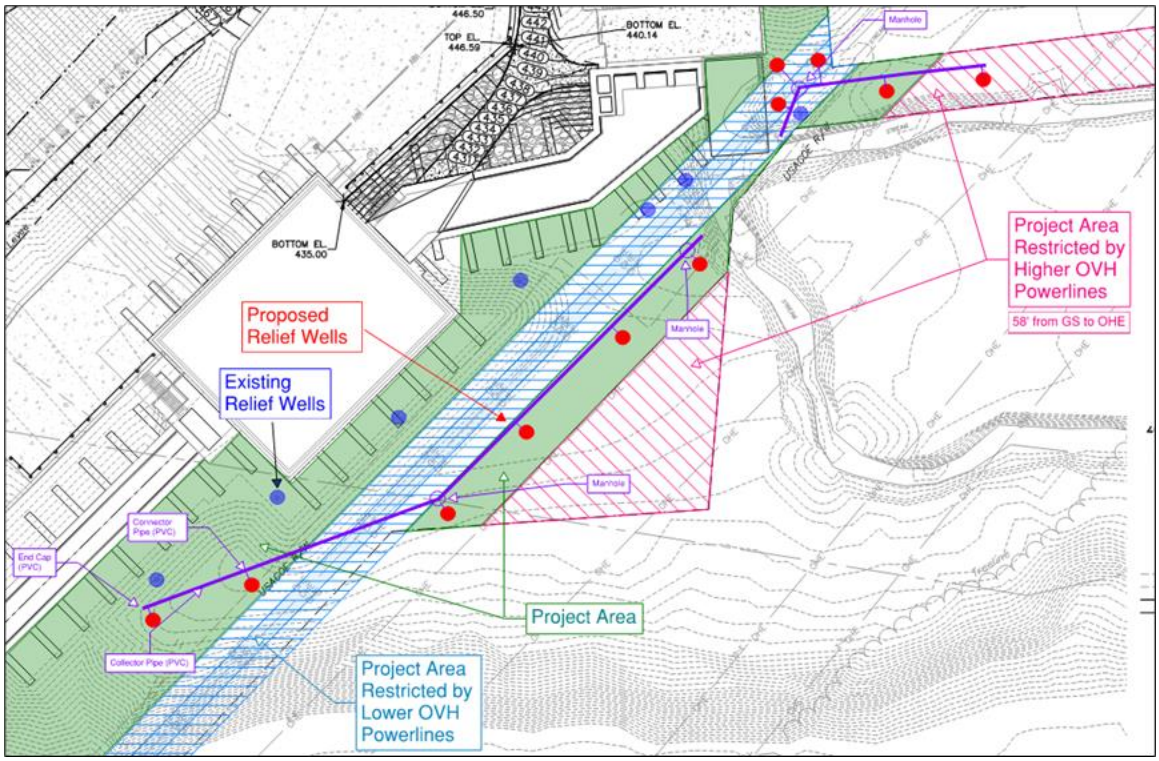

Figure 13: Sketch of proposed relief well locations and project boundaries in plan view.

SEEP/W Plan View Approach to Support Relief Well Design

In addition to the design requirements per current EM 1110-2-1914 (1992) for the design, construction, and maintenance of relief wells, the design was complemented by seepage plan view analysis incorporating the effect of relief wells.

The relief well plan view analysis was conducted in a similar manner to the analyses presented above with and without the cutoff wall for the loading case of an extreme flood event (Ohio River elevation at 460.0 feet). The effect of relief wells was accounted for by implementing nodal total water head boundary conditions at proposed relief well locations within the finite element mesh. The maximum water total boundary conditions were selected in close collaboration with site and civil engineering efforts to determine appropriate depths of collector pipe systems. The collector system is designed to divert excess water collected per relief well system to the existing Paddy's Run Creek. The elevation of water total head relief, meaning the invert location of the collector pipe at each relief well, represents the governing variable to be used in the model as nodal water total head boundary condition.

The result of the relief well plan view seepage analysis is shown in Figure 14 below. While the effects of the diaphragm cutoff wall were taken into consideration in the model geometry, the relief wells were appropriately sized to meet the requirements stated in section above. The critical allowable water total head of 416.2 feet identified for the area

of the thinner clay blanket along the existing Paddy's Run Creek is met based on seepage modeling results.

A closer look reveals the difficulty of mitigating the elevated gradients around the corners of the diaphragm wall structure. Although the allowable water total head is met for most of the land side project area, a small zone at the corner of the structure remained slightly elevated. This area of concern was mitigated by an increased slab thickness to counteract heave and uplift pressures, as well as jet grouting efforts between the corner of new construction and the existing Southwestern Outfall Sewer.

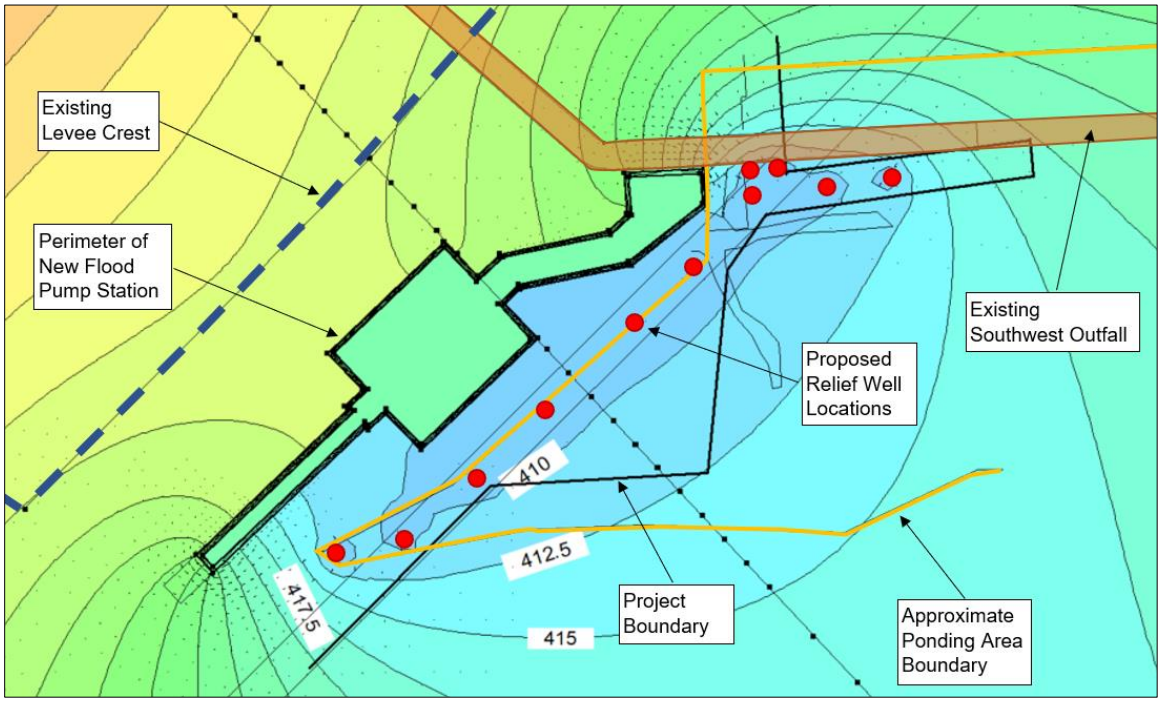

Figure 14: GeoStudio SEEP/W Aquifer Seepage Results.

Additionally, the analytical calculation following the current USACE EM 1110-2-1913 approach for an infinite line of relief wells with an impervious top stratum was compared to the SEEP/W results. The calculation per analytical infinite line approach does not account for seepage end-around effects caused by the cutoff walls, and therefore higher flow rates at several relief wells near the corner locations of the proposed structure were found with the plan view seepage model. The intent for this evaluation is to account for post-construction conditions with an active seepage cutoff diaphragm wall in place. The results found the analytical infinite line approach estimates a maximum inflow of 16 gpm per relief well. In contrast, a maximum inflow of 92 gpm for the relief wells at the corners based on SEEP/W results was determined. This is caused by the cutoff wall redirecting seepage around the corners of the diaphragm wall structure and the inflow into the northern and southern relief well locations. For the analytical approach, the maximum distance d_{max} between relief well points was set to the maximum distance between relief wells existing in the plan view seepage model. Based on distance d_{max}, the maximum pressure head

between the relief well points was evaluated and it was determined that requirements per current engineering manual are met. Figure 15 schematically shows the analytical infinite lines approach on the left and the plan view seepage model on the right.

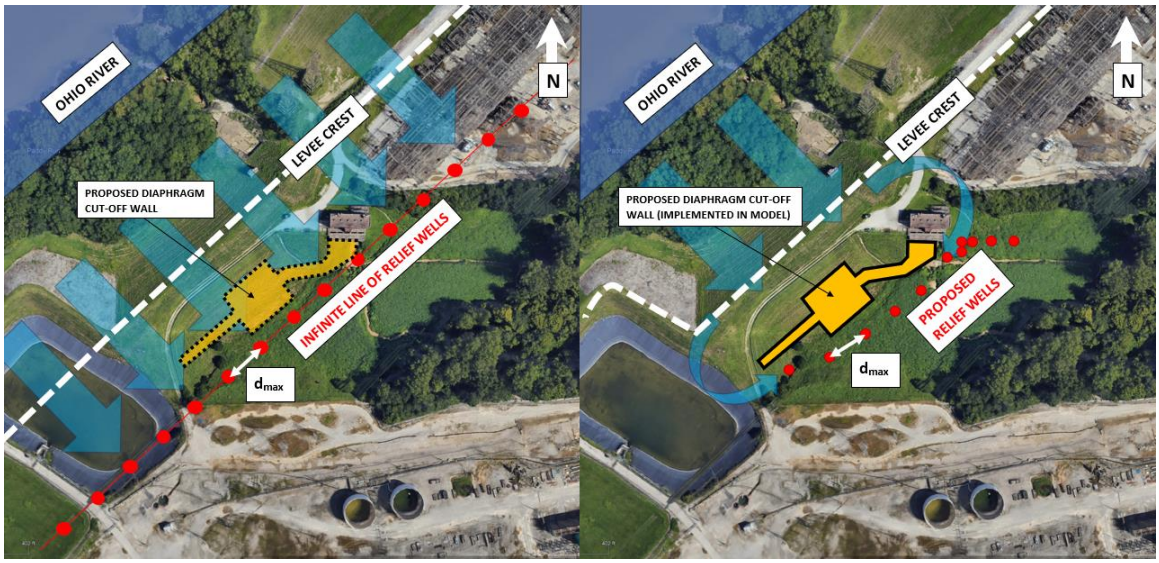

Figure 15: Schematic seepage paths for the analytical approach with an infinite line of relief wells (left) and finite element approach (right).

Design Conclusion

The approach to design and construct the new flood pump station within the levee embankment adds a level of complexity to the overall design. In addition, the diaphragm cutoff wall and relief well system features contribute an increased level of complexity when interacting with under-seepage conditions. The following conclusions were identified as important findings:

- Calibration and verification of seepage models in plan view and cross-section is a crucial step to increase confidence in model results and understand the margin of predictive error.
- Seepage modeling in plan view is a great approach to complement traditional two-dimensional cross-section analysis. Two-dimensional seepage analysis does not account for aquifer system relationships that have a regional impact on the model results.
- Seepage modeling in plan view can be implemented when a homogeneous soil stratigraphy like the glacial outwash is present for your project. However, this modeling approach requires the subsurface to be normalized and it is important to understand the impacts of normalizing the subsurface layering.
- The plan view seepage analysis provides the advantage of confirming adequate invert elevations and quantities for relief wells accomplishing the desired maximum water total head within the project area. It allows to incorporate seepage barriers that would have three-dimensional impacts to the seepage flow paths, such as cutoff wall features.

- Analytical approaches for relief well design, such as the infinite line approach, use simplified inputs to determine the relief well spacing. These simplified inputs do not account for subsurface features that may impact the flow rates at individual relief wells.
- Finite-element seepage models can be a helpful tool; And consistent with USACE engineering manuals, approaching the under-seepage with steady-state conditions will likely provide adequate pore water pressures used for the design of under-seepage mitigation features in homogeneous soil stratigraphy's and without considerable seepage barriers.
- Conducting sensitivity models in plan and cross-section, such as considering the transient impacts from fluctuating river levels, regional groundwater impacts, and three-dimensional effects of cutoff walls are beneficial to understand the impact on pore water pressures development and can be a helpful method to optimize design features.

An instrumentation program was developed and installed for the project to further evaluate the design. Future papers will be published after comparing future field measurements with the design.

Seepage Monitoring Efforts During and Post-Construction

As part of the PRFPSCU project, in-place slope inclinometers (IPIs) at three locations (B-117, B-118, B-119), and vibrating wire piezometers (VWPZs) at six locations (B-117, B-118, B-119, B-120, B-121, and B-122) were installed within the project area, as schematically shown in Figure 16 below.

In addition, vibrating wire piezometers were set and grouted in-place at two open well locations (PZ-1 and PZ-2). The well locations were installed during the project's initial geotechnical subsurface exploration phase.

Figure 16: In-place slope inclinometer (IPI) and vibrating wire piezometer (VWPZ) locations.

Instrument Locations, Installation, and Schedule

The instruments were placed at locations that were previously evaluated to support levee performance observations. The levee performance could be impacted by project construction activities. Specifically, construction activities may have an impact on the stability of the existing levee embankment, as well as on aquifer pore water pressure development beneath the levee embankment and land side of the levee toe. Further, levee performance during flood events, while construction activities are in process, will be observed. Flood events may cause reason for levee safety concerns during critical construction activities, such as overall levee performance subjected to a combination of elevated Ohio River water levels and diaphragm wall slurry trench excavations.

Instrument Locations B-117, B-118, and B-119

For instrument location B-117 between the adjacent chemical pond and the proposed working platform, and locations B-118 and B-119 along the existing levee embankment, hollow stem augers were advanced from the ground surface to top of bedrock (appr. El. 335.0 feet). Subsequently, slope inclinometer (SI) casings were installed and grouted in-place to later be equipped with in-place-inclinometer (IPI) instruments. Individual IPIs were setup using 10 feet probes that were strung together to create the IPI instrument for a single location that is referenced at each location B-117, B-118, and B-119. Refer to Figure 17 on the right for a schematic representation of the individual probes' setup within the SI casing. Each probe measures the temperature and tilt in parallel and perpendicular direction to the levee crest over the length of the probe at the depth of the individual probe. Once the instruments are set into the SI casing and an initial tilt and temperature baseline reading is taken for all instruments along the string, data is collected every four hours. Throughout the period of data collection, the tilt at each probe along the string may change. The horizontal deflection at a specific depth or location of probe is estimated by calculating the difference in actual tilt compared to the baseline tilt reading of the probe over its length.

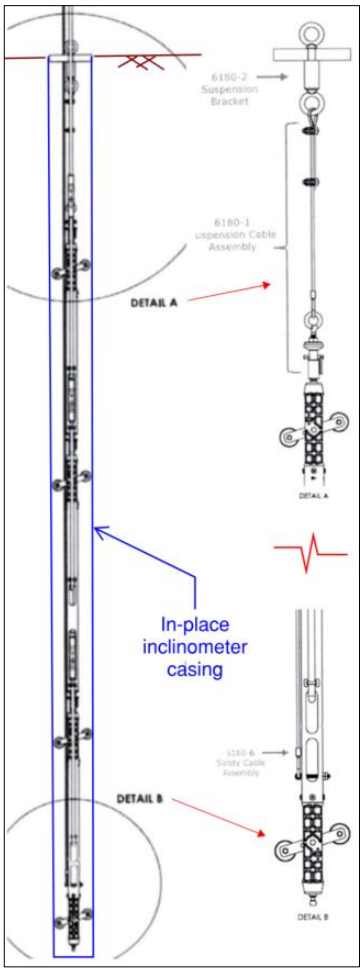

Figure 17: In-Place Slope Inclinometer Schematics (GEOKON-6180 Worksheet)

In addition, vibrating wire piezometer (VWPZ) instruments were installed at two different elevations on the outside of the SI casings before lowering the casings into the borehole. At each boring location, one upper VWPZ instrument was placed within the clay blanket material and one lower VWPZ instrument was placed within the aquifer sands.

Instrument Locations B-120, B-121, and B-122

At location B-120, close to the existing pump station, and instrument locations B-121 and B-122, hollow stem augers were advanced approximately five to ten feet beneath the bottom of the clay blanket (appr. El. 395.0 feet) into the underlaying aquifer sand formation. Like the previous borings, B120, B-121, and B-122 were equipped with VWPZ instruments at two different elevations, whereas one upper instrument is located within the clay blanket and the lower instrument is located within the aquifer sands, but no IPI instruments were installed at these locations.

Instrument Locations PZ-1 and PZ-2

At location PZ-1 and PZ-2, existing open well points, installed during the previous subsurface exploration campaign, were each equipped with one VWP instrument to be

located beneath the clay blanket. All VWP instruments were grouted in-place with a bentonite mixture.

In-Place-Inclinometer and Vibrating Wire Piezometer Instruments

GEOKON equipment was selected for the monitoring instruments described above. GEOKON's 4500S-350KPA model was used as the vibrating wire piezometer and the GEOKON 6180 instruments were utilized for the in-place slope inclinometers. The VWPZ and IPI data collection is automated through an on-site mesh connection between five battery powered data loggers that are continuously collecting data from the instruments. The data is uploaded into GEOKON's network through a solar powered cellular gateway and can be accessed as soon as data is uploaded. HDR furnished an automated online dashboard that is updated every four hours with data from the GEOKON network through an API connection. The dashboard allows a user-friendly and quick overview of the collected data. Figure 18 below shows a typical dashboard view.

Figure 18: Typical BI Dashboard View of the Monitoring Data Collection

References

AECOM . (2019). *Potentiometric Surface Map* . Louisville, KY: Third Rock Conultants, LLC.

Department of Interior Bureau of Reclamation (USBR). (2014). *Embankment Dams.* Washington D.C.: Department of Interior Bureau of Reclamation (USBR).

GEO-SLOPE International Ltd. (2012). *Seepage Modeling with SEEP/W.* Calgary, Canada: GEO-SLOPE International Ltd.

Google. (2018). *Google Earth Imaging.* Google.

Lyverse, Starn, & Unthank. (1996). *Hydrogeology and Simulation of Ground-Water Flow in the Alluvial Aquifer at Louisville, KY.* Louisville, KY: U.S. Department of the Interior.

Stantec Conulting Services, Inc. (2015). *Paddy's Run Flood Pumping Station Seepage Evaluation.* Stantec Conulting Services, Inc.

U.S. Army Corps of Engineers (USACE). (1992). *Design, Construction, and Maintenance of Relief Wells.* Washington D.C.: U.S. Army Corps of Engineers (USACE).

U.S. Army Corps of Engineers (USACE). (2000). *Design and Construction of Levees.* Washington D.C.: U.S. Army Corps of Engineers (USACE).

U.S. Army Corps of Engineers (USACE). (2022). *Design, Construction, and Maintenance of Relief Wells (DRAFT).* Washington D.C.: U.S. Army Corps of Engineers (USACE).

USACE. (n.d.). *Drawing Nos. 613 - 12.2 / 7 and 48 - Flood Protection, Louisville, Ky Section E - As Built Drawings.*

Interferometric Synthetic Aperture Radar to Monitor Slow Moving Ground Deformation

Stuart Edwards, P.E., LM. ASCE[1]

Abstract: A large number of landslides world-wide are triggered - at least in part - by water; usually resulting from a storm event that produces unusually intense precipitation. It is also true that many, if not most are either reactivations of earlier failures, or the final dramatic phase of an unstable condition that developed slowly over a long period of time. This presentation introduces Interferometric Synthetic Aperture Radar (InSAR), satellite-based technology that, although developed more than 30 years ago, is finally emerging as a viable tool for geoscience professionals interested in detecting and monitoring slow moving landslides. InSAR's ability to detect ground surface displacements on the order of millimeters/year has long been appreciated. However, the complexity of analysis and substantial computing requirements had a chilling effect on its adoption as an everyday tool. Only recently has there been an major effort on the part of space agencies in Europe and the US to post-process InSAR data to a higher level where it can now be used by disciplines that lack an intimate knowledge of satellite radiometry. The general principles of InSAR are briefly presented and the workflow to produce a ground motion analysis is illustrated. Some examples of monitoring results at slow moving landslides are shown, followed by a look to the future opportunities that the 'Eye in the Sky' may represent for geoscientists and engineers.

Introduction

This paper presents a *very* brief introduction to Interferometric Synthetic Aperture Radar (InSAR) and, specifically, its potential relevance in geotechnical engineering. This space-based technology has been hiding in plain sight for more than 30 years, but only recently has it become accessible to those who are not specialists in satellite telemetry or radar physics and who do not generally publish in (or read) IEEE journals. The broad capabilities of InSAR are presented together with a description of the underlying technology and a generalized workflow for its use. Some examples of its application in geotechnical engineering and earth science are illustrated.

[1] Senior Geotechnical Consultant, Lead Geotechnical Engineer on the Michael Baker's QAM Team of Corridor H Design Build Project, West Virginia Email: sedwards@verdantenv.com

InSAR - what is it?

InSAR technology is described at varying levels of detail in the technical papers in which it features, and in the numerous manuals and training material published by space agencies generating SAR data in the US and EU (e.g. [1]). A succinct and descriptive (non-technical) characterization of InSAR can be found in Wikipedia [2]:

Interferometric synthetic aperture radar, abbreviated InSAR, is a radar technique used in geodesy and remote sensing. This geodetic method uses two or more synthetic aperture radar (SAR) images to generate maps of surface deformation or digital elevation, using differences in the phase of the waves returning to the satellite or aircraft. The technique can potentially measure millimetre-scale changes in deformation over spans of days to years. It has applications for geophysical monitoring of natural hazards, for example earthquakes, volcanoes and landslides, and in structural engineering, in particular monitoring of subsidence and structural stability.

SAR systems were originally deployed in space to generate ground surface imagery, having an advantage over optical alternatives that were limited by darkness and cloud cover. InSAR evolved from the observation that return signals on successive passes over the same point sometimes were out of phase with those recorded on previous occasions, leading to the conclusion that the line-of-sight (los) distance from the satellite to that point on the ground must have changed. This phase difference is the basis for our current ability to detect what are sometimes very subtle los differences, and to translate them into ground motion velocities and magnitudes.

Sentinel 1, a European Space Agency (ESA) satellite with SAR capability, flying at an altitude of about 700 km above the ground is currently imaging the earth with a repeat cycle of 12 days, allowing creation of deformation and velocity mapping with a resolution of 40 meters on the order of 30 times per year. Time series analysis of these data create a record of ground motion history that can be used to assess past activities - natural and anthropogenic - and in some cases be part of an alert mechanism based on continuously updated acceleration / deceleration rates.

How does InSAR work?

Radar waves are sinusoidal and so can be characterized by amplitude, wavelength, frequency and phase. In the case of SAR data generated by Sentinel 1, the wavelength is 5.6cm ('C' band), the frequency is ~5.4 GH_z (microwave) and the phase is the location of any observation within the 0 - 2π radian period. Amplitude is considered on a relative basis, comparing the strength of the outgoing pulse with that of the return signal as a measure of

reflectivity of the target. Single SAR images can be used to create ground surface visualizations that are generally similar to (clear sky, daytime) photographic images.

To perform interferometric analysis requires multiple (at least two) SAR acquisitions. As successive reflected signals are received from a given point on the ground their phases can be compared, the difference quantified and used to determine a key property known as the 'phase velocity' i.e. how fast is the phase change occurring? The general concept is depicted in Figure 1. With appropriate corrections for topography and climatic conditions the phase velocity can be plotted to form interferograms at which point the process has transitioned from SAR to InSAR.

Figure 1 - Illustration of Radar Phase Change and Deformation

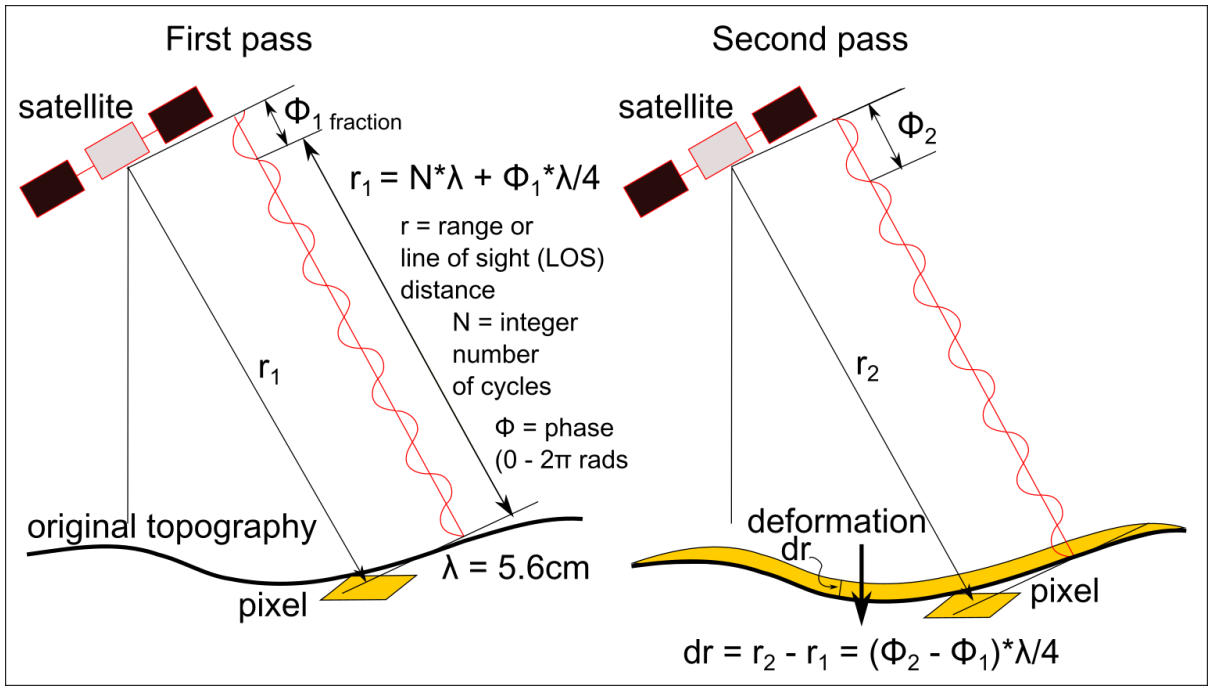

If deformation is rapid, the resulting phase difference from one orbit to the next may exceed π radians, in which case the data become ambiguous - is the deformation one wavelength or two, or even more? This problem is solved using some mathematical sophistication known as 'phase unwrapping' that attempts to assign correct values to the deformation represented by each phase velocity. The final result is a data set that includes line of sight (los) velocity and displacement values for each pixel at a typical resolution of 40 m (~130 ft) this is ready for the analysis planned by the user.

Examples of InSAR use in a geotechnical engineering context

Landslide monitoring: Many of the published use cases for InSAR involve monitoring slow moving landslides, for which it is ideal. In this example (Figure 2) taken from [3], data from two locations within an area of interest are analyzed to produce a multi-year displacement time series and average velocity estimate at a resolution of mm/yr. As with any landslide monitoring program, once identified, the main purpose is to detect changes that may suggest transition from slow moving to a catastrophic failure. In the first case (lower left), the slight increase in velocity mid-way through the time series could have been a sign of acceleration but appears to have stabilize at a constant rate subsequently.

Figure 2 - LOS Displacement from InSAR data [from 3]

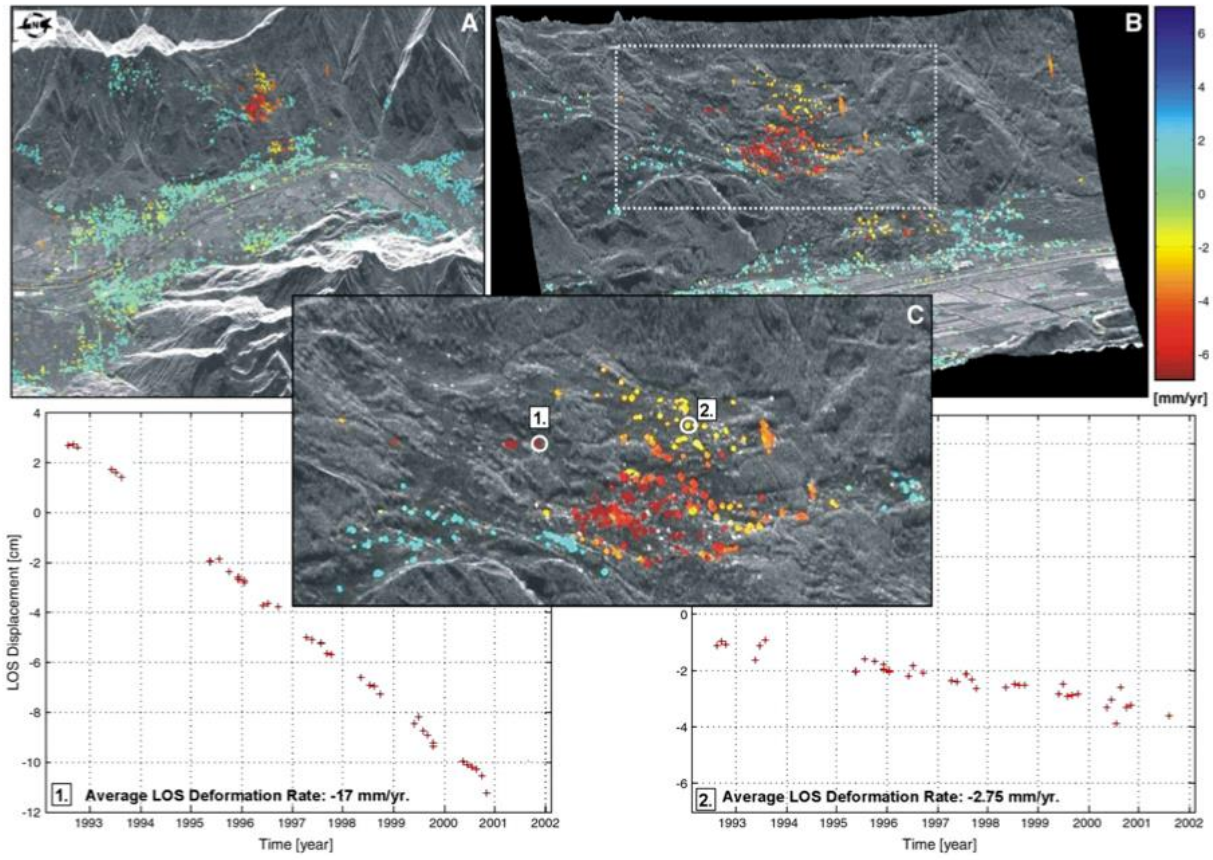

A subset of slope failures involves deep open pit mines where pit walls may be hundreds of meters high. Ground based radar systems are being used at some mines to monitor these

slopes using interferometric technology. Space based InSAR could be a useful addition or replacement at these and other mine sites.

Settlement monitoring: Low displacements can indicate either horizontal or vertical movement, or a combination of both. Distinguishing between them mathematically is currently not possible with the Sentinel 1 data in the absence of additional information. For example, landslides generally move more laterally than vertically, and in the direction of the maximum slope dip. That then becomes a reasonable assumption when interpreting displacement data at landslides. Conversely, if settlement is the concern, vertical displacement should be expected.

For projects where AASHTO criteria may require inclusion of drag loads on shafts or piles, the settlement of newly constructed approach embankments becomes a critical design element. If the foundations are constructed at a time when less than 0.4-inches of settlement remains, drag loads need not be applied. InSAR can be very useful to supplement conventional settlement monitoring during long duration pre- or project loading programs where future settlement trends must be projected.

Infrastructure Monitoring: Routine inspection of infrastructure located in geohazard-prone areas is an application for which InSAR is well suited. This could include cut and fill slope stability inspection along freeways, pipeline corridors, earthen dams and levees, railroads and airports. Subtle changes in ground conditions can be detected early in their development and provide the opportunity for corrective measures to be implemented before the onset of a failure.

Subsidence and Rebound: Subsidence in areas where underground mining was formerly conducted is difficult to predict and monitor. Long term trends argue for the natural elimination of significant voids which may occur as roof supports decay (timber) or pillars of coal deteriorate or suffer bearing failures. The only certainty is the ultimate end point; but timing is completely indeterminate. InSAR surveys can provide community leaders and regulatory agencies with the means to assess subsidence trends on an ongoing basis.

Figure 3 - Subsidence and Rebound

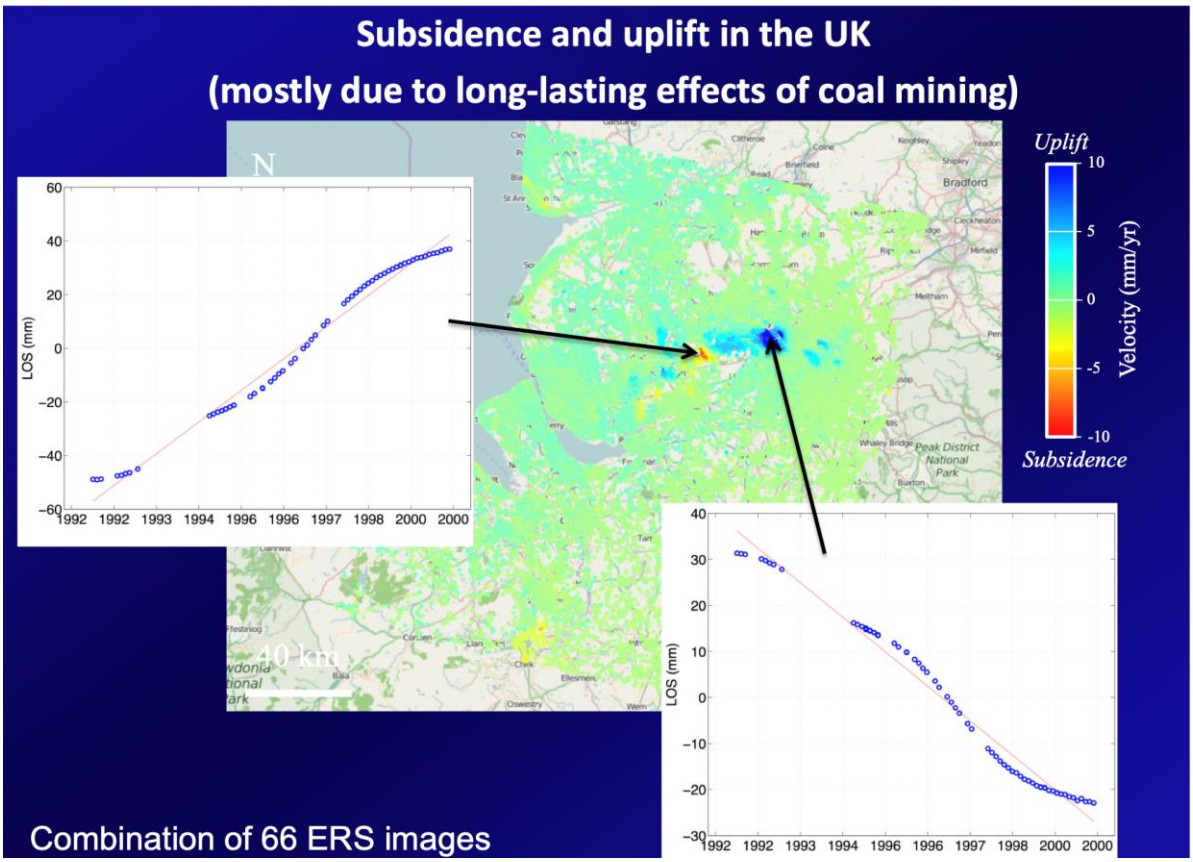

Paradoxically, there may be post-mining trends in the opposite direction as well. During operation, deep underground mines require groundwater extraction that create landscape-scale zones of depressed piezometric pressure. The resulting increase in effective overburden stress causes compression of the rock - which is a form of subsidence, although fairly minor. When the mine closes, the pumps are shut off and the groundwater system is slowly restored. Now there is an opposite change in effectives stress (reduction) as the overburden regains its buoyancy and rebounds. This phenomenon was observed at closed coal mines in norther Europe [4] using InSAR (Figure 3) and has subsequently been observed by the writer at a site in the Appalachian Basin.

Regional and sub-regional subsidence can be effectively monitored in areas where groundwater or hydrocarbon extraction is occurring.

How can a geotechnical engineer learn, access and work with InSAR?

Four or five years ago, at the start of the writer's interest in InSAR, it was difficult to work in this field. There was adequate software provided by ESA (the SNAP toolbox), but each scene (or granule as they are known) was a 5 GB download and at least 2 were required just to make one interferogram. A good internet connection and lots of storage were essential - together with a lot of patience. Things took a long time and if a mistake was made or the granules turned out not to be suitable, that time was all wasted.

Early in 2022 things changed as NASA became involved, using the Alaska Satellite Facility (ASF) at Fairbanks AK, and starting on a path to make InSAR more accessible to the scientific community at large. ASF is a Distributed Active Archive Center (DAAC) that specializes in SAR data and contains all of ESA's radar data. In addition, they have developed software in the form of Jupyter Notebooks to prepare data for analysis and to then conduct time-series analysis. They provide training [5][2] - there were over 700 applicants for the virtual 2024 InSAR course of which 170 qualified to participate.

ASF's Vertex Search system [6] is a (relatively) easy to use graphical interface where searches can be conducted for granules covering any location on the planet (Figure 4). These can then be ordered at no cost and downloaded. But they are still 5 GB granules.... A year or so later a beta program, that is now permanent, let the user select an interferogram option in the search, and then identified suitable pairs of granules that can be downloaded - or processed directly by ASF to create interferograms. The output with all options selected is about 1 GB per interferogram and the user need never touch the 10 GB of source granules. Now short temporal baseline time-series analysis is feasible with a modest computer set-up. The Sentinel 1 data are available back to about 2016, so an 8-year time series will involve ~240 interferograms, or 240 GB of output that is typically available for download within 24 hours. Downloading it can be time consuming depending on internet speed, and best performed at night.

Each 1GB interferogram directory contains 36 individual files that include raw and processed data. The next step is to process the 'stack' of interferograms so that they all have the same boundaries that are subset to the user's area of interest. This can be done using one of ASF's Jupyter notebooks which can be downloaded from Github.[7] Then the time-series can be run using readily available open-source software. There are several, but

2 This reference links to the lecture videos and notebooks from ASF's August 2024 training program and provides a wealth of relevant information

ASF favors MintPy [8] - also available as a Jupyter notebook from Github - MintPy is usually very fast and trouble free.

Figure 4 - Vertex InSAR Granule Search Screen

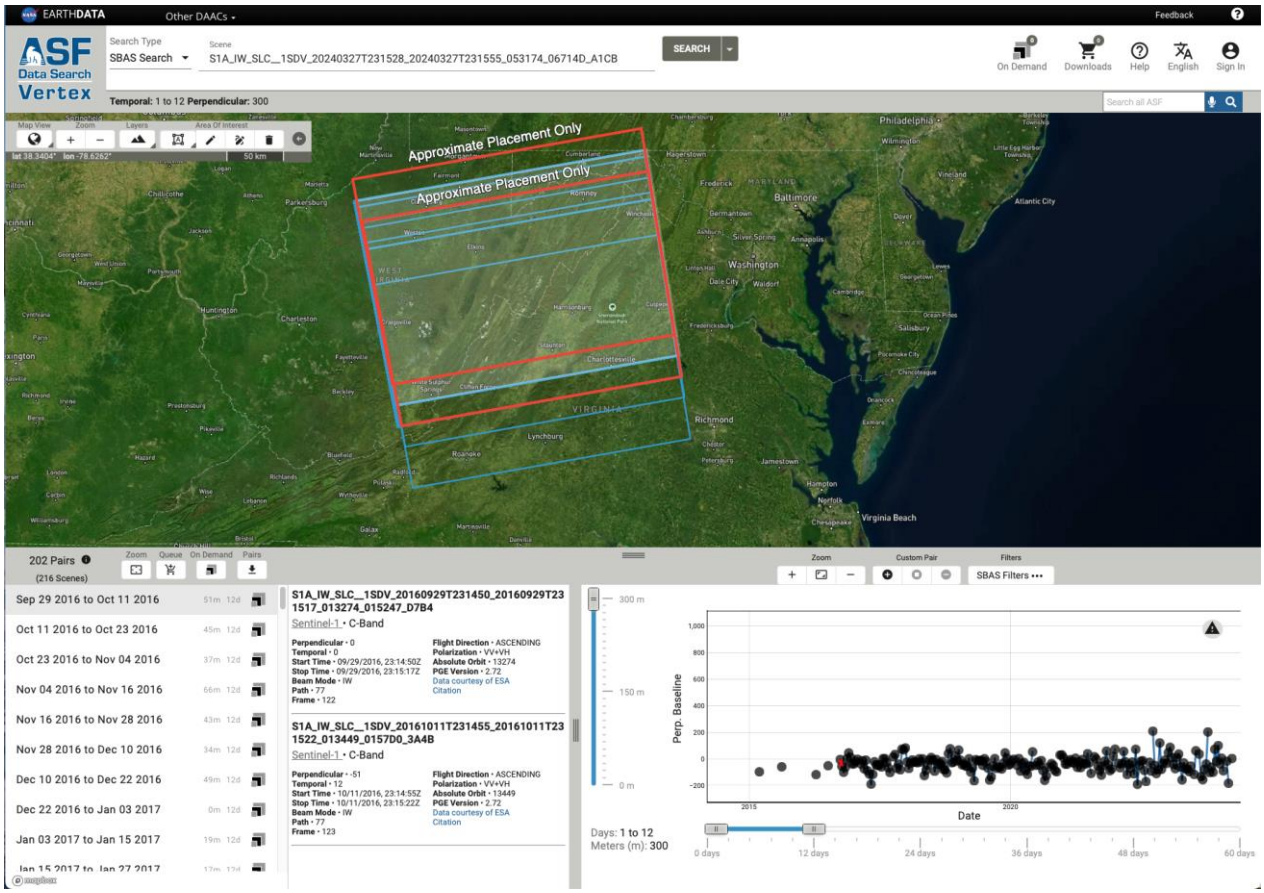

The important MintPy output (a 2.5MB file: velocity.h5) file will have been created and now must be interpreted. This is not a commonly encountered file type in the geotechnical industry, but using python or 'R' tools it can be opened easily and required plotting and mapping performed. Additional notebooks and scripts are being published frequently so that most processing can be performed with a minimum of programming effort. At this point, mapping of results is best accomplished using GIS software. QGIS tends to be the platform of choice, although this user prefers GRASS GIS [9].

Future

After a 30-year slow start, InSAR can now move into the mainstream of ground deformation monitoring. Space agencies around the world are flying SAR missions - USA (shuttle - now retired), EU, China, Japan etc. The biggest and potentially the best will be the NISAR mission scheduled to launch in February 2025. This is a joint project between NASA and ISPO (the Indian space agency) and will create L-band (24 cm) and S band (9 cm) data at a resolution of 3-10 m. The L-band data will be valuable as it has better penetration of vegetation. The repeat cycle will be 12 days. Data will be 'free and open'.

Figure 5 -- NISAR Mission (2025) SAR Satellite with 40 ft Diameter Radar Antenna

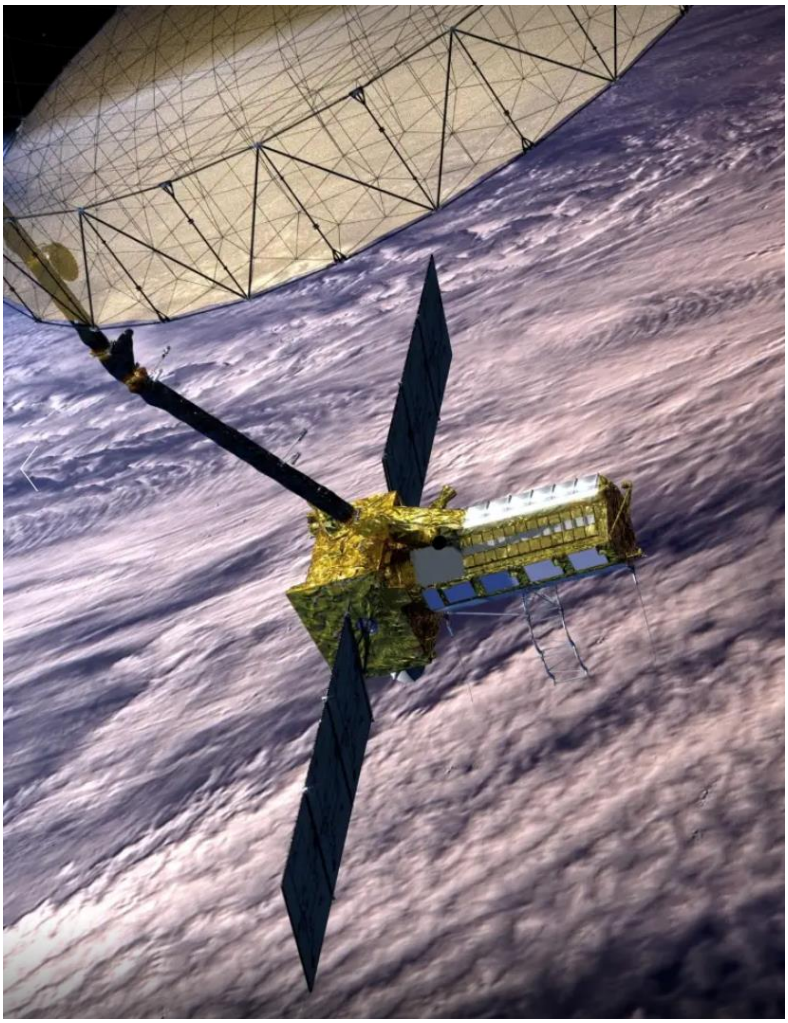

Present workflows for data processing are much improved over those of the past but there is clearly room for improvement by the user community. Software can currently be used to order granules or interferograms on a pre-determined schedule automatically. Interpretation of deformation maps on a pixel-by-pixel basis through machine learning seems well within reach. If the future for InSAR is uncertain, it is only because the imagination and creativity of an active user community has not yet been put to work. The tools are all in place - or will be shortly.

Conclusion

InSAR is an amazing tool for detecting and quantifying slow moving ground deformations at very low cost, and it has not yet realized the potential for use in geotechnical engineering that seems possible. This paper is intended to provide encouragement to others to take a step into the unknown and give it a try and, hopefully, it will be effective in accomplishing that.

As a general note - using InSAR does require some appreciation for 'Big Data' wrangling. This is Very Big Data. A basic comfort level with simple 'unix' commands is helpful. Some knowledge of python or other object-oriented programming language will be useful and of course if the user is fluent with Docker, Conda, Jupyter notebooks, GIS and python it will be a breeze! But all this is free; the data are free too - it doesn't get much better than that.

References

[1] Ferretti,A., Monti-Guarnieri,A., Prati,C., Rocca,F., Massonnet, D. *InSAR Principles: Guidelines for SAR Interferometry Processing and Interpretation (TM-19, February 2007)* ESA Publications

[2] Wikipedia contributors. (2024, September 9). Interferometric synthetic-aperture radar. In *Wikipedia, The Free Encyclopedia*. Retrieved 21:22, September 15, 2024, from https://en.wikipedia.org/w/index.php?title=Interferometric_synthetic-aperture_radar&oldid=1244764082

[3] Colesanti, C., and Wasowski, J. *Investigating landslides with space-borne Synthetic Aperture Radar (SAR) interferometry.* Engineering Geology, Elsvier, 2006

[4] Vervoort, A., *Impact of the Hydrogeological Conditions on the Calculated Surface Uplift above Abandoned and Flooded Coal Mines.* Geosciences, MDPI, 2022

[5] ASF *2024: InSAR Processing and Analysis (ISCE+)* course material may be found at https://github.com/parosen/Geo-SInC/tree/main/EarthScope2024

[6] ASF Vertex SAR distribution portal - https://search.asf.alaska.edu/#/

[7] Github - code repository - http://github.com

[8] Yunjun, Z., Fattahi, H., and Amelung, F. (2019), Small baseline InSAR time series analysis: Unwrapping error correction and noise reduction, *Computers & Geosciences, 133*, 104331. [data | notebook] https://mintpy.readthedocs.io/en/latest/

[9] GRASS Development Team, 2024. Geographic Resources Analysis Support System (GRASS) Software, Version 8.4. Open Source Geospatial Foundation. https://grass.osgeo.org

Case Study: UNDERWATER RETROGRESSIVE SLOPE FAILURE: OBSERVATION AND ANALYSIS

Alex C. Cordogan[1], Abedalqader Idries[2], and Timothy D. Stark[3], F.ASCE, D.GE

ABSTRACT

This paper presents analysis of an underwater retrogressive slope stability failure caused by concurrent construction of a wharf access causeway and dredging near the end of the causeway for the wharf structure. A cross-section was developed along the causeway and analyzed to simulate the retrogressive slope failure using limit equilibrium. The compound failure surface for the inverse stability analysis of each of the five retrogressive slide masses is in agreement with observations before, during, and after the failure. Soil stratigraphy is discussed and the mobilized undrained strength of the seabed clay underlying the causeway fill was estimated using an inverse analysis of the five slide masses. The inverse analysis shows that concurrent dredging and causeway construction reduced the factor of safety (FoS) of the causeway underwater slope, which eventually initiated the retrogressive failure. The stability analyses show that causeway construction contributed to the reduction of the FoS but dredging triggered the first slope failure, which started the retrogressive failure. Nevertheless, had dredging not occurred, a slope failure would still have occurred if causeway construction had extended another 5 m from where the first slope failure occurred.

Keywords: Underwater slope failure, retrogressive failure, undrained shear strength, slope stability, causeway construction, dredging, displacement method

[1] Geotechnical Engineer at Shannon & Wilson Inc. St. Louis, MO 63146. E-mail: Alex.Cordogan@shanwil.com
[2] Geotechnical Engineer at Langan Engineering and Environmental Services, inc., Austin, TX 787059. (Corresponding author). E-mail: aidries2@illinois.edu (aidries@langan.com)
[3] Professor of Civil and Environmental Engineering, Univ. of Illinois at Urbana-Champaign, IL 61801. E-mail: tstark@illinois.edu

INTRODUCTION

Historical submarine landslides are common and can be larger than onshore landslides (Zhang et al., 2021; Saxov and Nieuwenhuis, 2012; Bjerrum, 1971; and Terzaghi, 1956). Smaller submarine landslides that are comparable to onshore landslides are also common (Cornforth, 2005). Both massive and small submarine landslides usually occur with a low tide due to drawdown of the buttressing water (Cornforth, 2005; Bjerrum, 1971; and Terzaghi, 1956). Most of the underwater slope failures are triggered by a manmade fill and/or dredging at the toe of the fill. After the initial slope failure occurs, it can trigger additional failures due to removing lateral support from the toe leading to a retrogressive slope failure that ranges in length of tens of meters as in the case study presented herein and that of Conrnforth (2005), to kilometers in length as those presented in Zhang et al. (2021), Saxov and Nieuwenhuis (2012), Bjerrum (1971) and Terzaghi (1956).

In recent years there have been significant advances in the analysis of submarine landslides. For example, Puzrin et al. (2017) propose a detailed mechanism for submarine spreading failures that use retrogressive shear band propagation (SBP) with active block failures in the stable zone of a slope assuming the weak zone to propagate parallel to the slope surface in normally to slightly overconsolidated deposits. Their research emphasizes the impact of removal of the downslope material, resulting in decreased support, which in turn leads to a retrogressive or uphill propagation of the shear band. Presenting analytical solutions using energy balance, Puzrin et al. (2017) formulated criteria based on the critical depth of the sliding surface and the critical drop of the failed seabed level. Zhang et al. (2021) studied the mechanisms of upslope failures in submarine landslides including the shear band movement in the weak layer and slab failure(s) in the sliding layer using a large deformation numerical model.

Zhang et al. (2021) conclude the limit equilibrium method is applicable to the analysis of retrogressive failure with repeated rotational slides but cannot describe translational retrogressive (spreading) failure. Therefore, the Limit Equilibrium Method (LEM) is used for the analysis of the translational retrogressive failure described herein. This case study is an attempt to use the LEM for a simplified analysis of an underwater translational retrogressive slope failure.

The focus of this paper is a deep-water port with a wharf structure and access causeway that was to be constructed for a mining project. About a month after construction of the causeway started, dredging began for the sheetpile cells or cofferdams for the wharf structure at the eventual termination point of the causeway. Nine days after dredging began, the causeway that would connect the shore to the planned wharf structure failed and disappeared below the sea level. Tension cracks were observed in the causeway shortly before the retrogressive failure initiated. The wharf was to be constructed using four cylindrical steel sheetpile cells connected to one another by sheetpile arches, as shown in **Figure 1**.

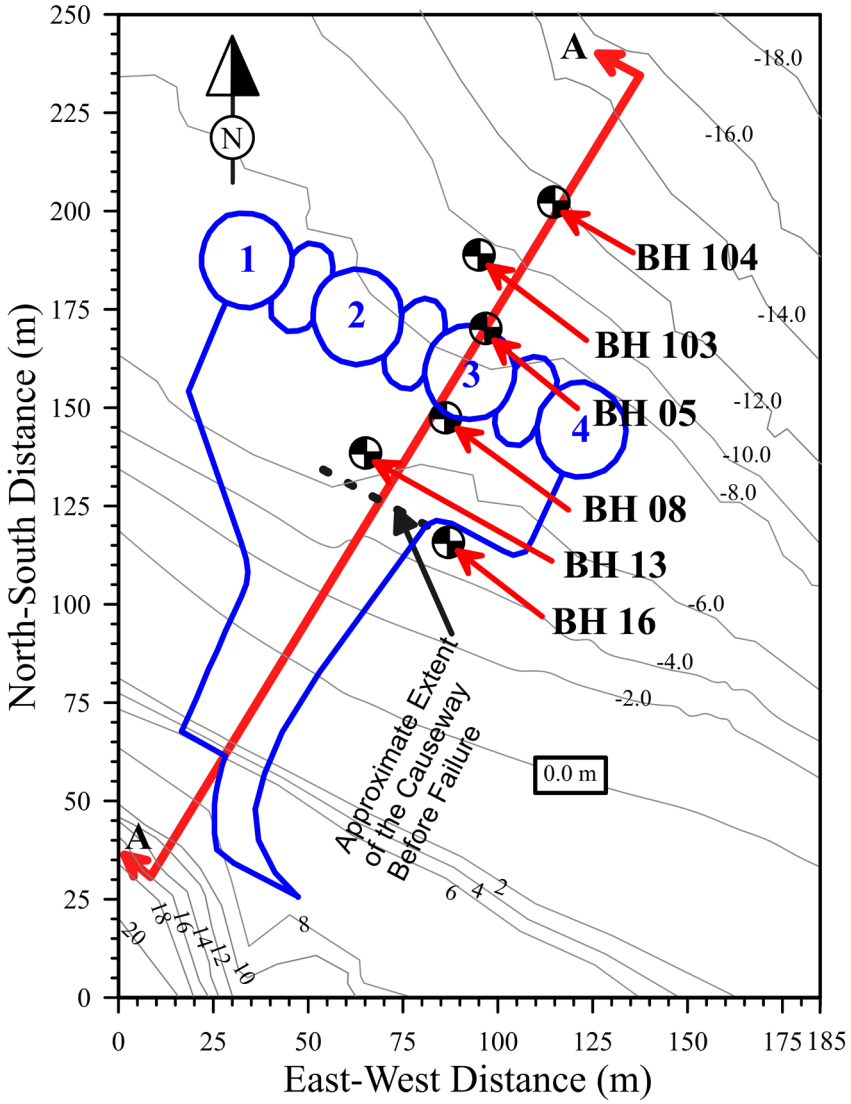

Figure 1. **Plan view of causeway (see blue outline from shoreline) before dredging, sheetpile cells for wharf structure, and borings used to create cross-section A-A'.**

The proposed sheetpile cells were designed to have a diameter of about 24.0 m and were to be backfilled with granular material. The planned causeway was approximately 125 m in length and varied in width from 25.0 m near the shore (southern extent) to 100.0 m near the wharf (northern extent) as shown in **Figure 1**. The high-water line (HWL) is at elevation +5.60 m and the low-water line (LWL) is at elevation +0.20 m, which means there is a tidal fluctuation of about 5.4 m.

The zero-elevation shown in **Figure 1** represents the LWL. The planned ground surface of the causeway was to be located at an elevation of +9.0 m, which is about 3.4 m above the HWL and 8.8 m above the LWL. The slopes on each side of this rockfill causeway were to be inclined at 1.5H:1.0V. The first 60 m length of the causeway was to be situated between the HWL (elevation +5.60 m) and the LWL (elevation +0.20 m), which is referred to as the intertidal zone. The rockfill causeway would have a thickness of about 5 m at the shore and a maximum thickness of about 23 m at the sheetpile cells.

Based on the dimensions of the causeway above, the total volume of fill material required for the causeway and proposed wharf structure is approximately 194,000 m^3. At the time of the failure, it was estimated that about 16,000 m^3 of rockfill had been placed for the causeway and the total slide mass was approximately 34,000 m^3. The causeway was constructed with rock blasted from the rock slope just upslope of the shoreline. The area around the base of the sheetpile cells was being dredged to remove what was thought to be soft sediments so that the sheetpile cells would be founded on rock. At failure, dredging reached a depth of 16 m, but more importantly the dredging that occurred on the day before and the day of the failure was in close proximity to the base of the causeway slope.

COLLAPSE OBSERVATIONS

Figure 2 shows the post-collapse bathymetry survey that indicates the causeway slide mass moved in the northeast direction because of the large amount of material pushed up on the seabed past the alignment of the proposed four sheetpile cells. There are other bulges in the seabed surface, specifically to the southeast of the slide mass, but the smooth nature of the seabed over these bulges

indicates these bulges are not recent and are not related to the causeway failure. In addition, these smoothed bulges are present in prior bathymetric surveys confirming these features were present before the collapse. Unfortunately, no additional information is available about the date or cause of these older bulges in the seabed surface. It is believed these bulges may represent a prior area of material dumping or disposal or a local slope failure.

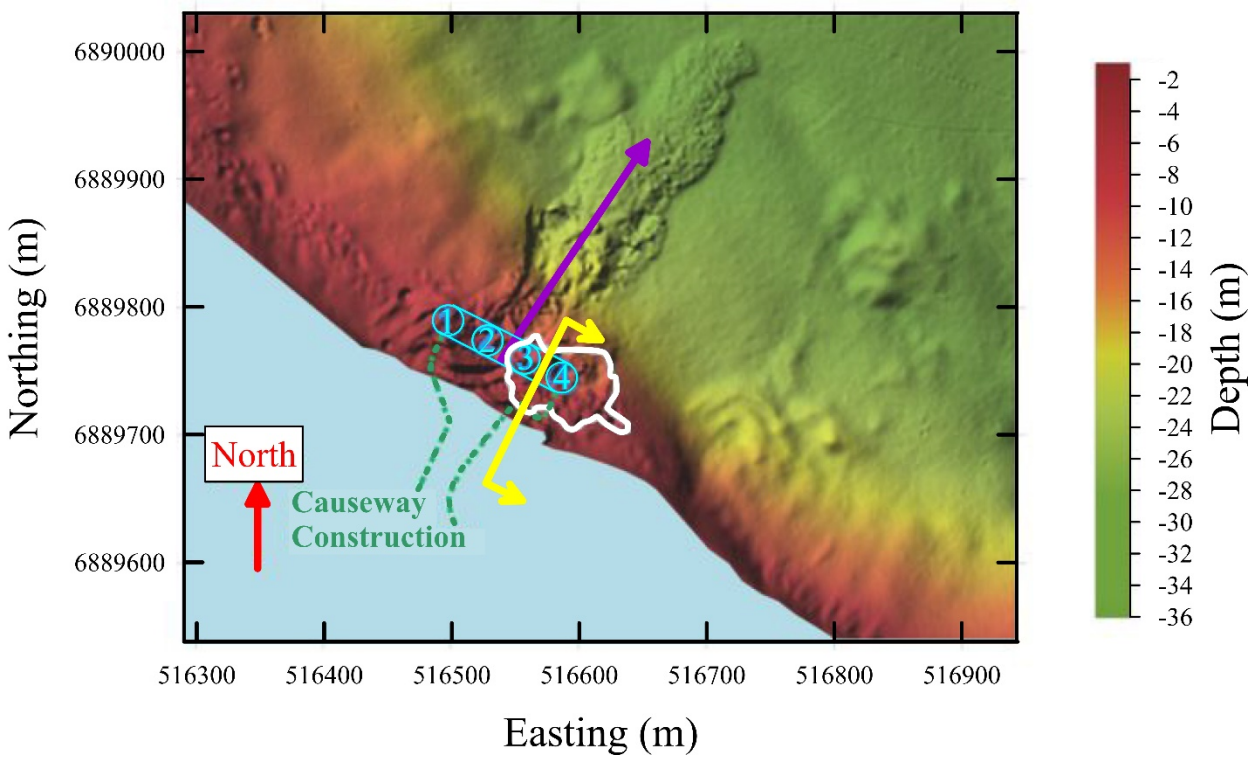

Figure 2. **Results of bathymetric survey after causeway collapse with wharf structure (see blue line), proposed causeway (see green dotted line), and dredged area in last two days (see white line) superimposed.**

Figure 2 also shows the seabed is higher seaward of the proposed sheetpile cells (see purple arrow) and the slot created by the dredging, indicating that causeway material moved past the proposed wharf structure and pushed up or raised the seabed just past the proposed location of sheetpile cells #2 and #3. The area that was dredged in the vicinity of the wharf structure is outlined in **Figure 2**

by the irregular shape (see white outline). The raised seabed past the sheetpile cells likely occurred because the slide mass had to flow through and out of the dredged excavation and northeast of the dredging area. Using the color scale on the right side of **Figure 2**, the area northeast of the dredging area and proposed sheetpile cells rose about 1 to 2 m.

Figure 2 also shows that the dredged area around the proposed location of sheetpile cell #4 and east of the wharf structure did not fill significantly with causeway material, which is likely due to the shallower dredging in this area, a stabilizing stockpile of rockfill on the eastern side of the causeway, and different subsurface conditions. In fact, the shape of the dredged area east of the sheet pile cells has a similar shape before and after the collapse (see white outline in **Figure 2**).

A. Dredging Activities

Figure 2 shows the slide mass moved through a narrow slot in the seabed between the proposed locations of sheetpile cells #2 and #3, at the base of which the highest daily quantity of dredging occurred the day before the collapse. Daily dredging quantities are plotted in **Figure 3**, and based on photographs and reported dredge locations a significant amount of dredging on the day before and day of the failure (July 29, 2011) occurred near sheetpile cell #3 (see **Figure 2**). **Figure 2** also shows dredging was progressing from the proposed location of sheetpile cell #4 towards the proposed location of sheetpile cell #1 (east to west). It can be seen that causeway construction and the failure are also in line with proposed location of sheetpile cell #3.

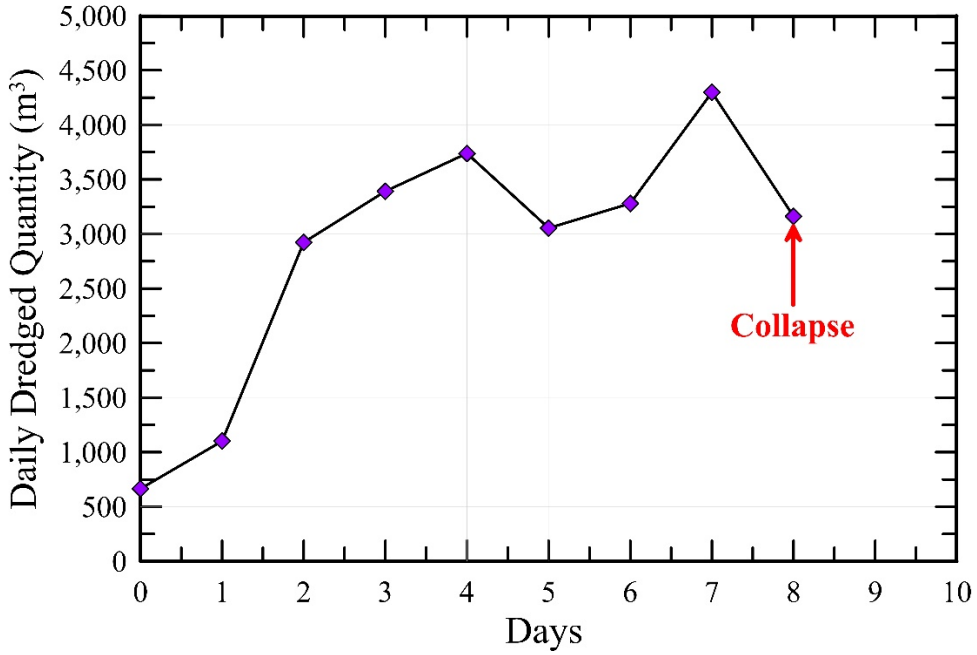

Figure 3. Daily dredging quantities between July 21 and July 29, 2011.

Additionally, on the date of collapse the low tide of +0.2 m occurred at 2:46 pm, which is about 30 minutes after the collapse began at 2:15 pm. Therefore, the collapse developed while the tidal fluctuation exposed an additional 4.4 m of the rockfill causeway. This resulted in a greater driving force on the underlying soils due to the rockfill buoyant unit weight changing to a total or saturated unit weight. Underwater slope failures are common at low tide as reported by Saxov and Nieuwenhuis (2012), Cornforth (2005), Bjerrum (1971), and Terzaghi (1956).

The yellow line on **Figure *2*** shows the location of the cross-section shown in **Figure 4**, which demonstrates the effect of dredging on the seabed two days prior to the collapse (July 27, 2011). Specifically, **Figure 4** shows some of the deepest dredging occurred the day before and day of the collapse between the locations of sheetpile cells #3 and #4 and the slot between the proposed locations of sheetpile cells #2 and #3 through which the slide mass eventually moves. This dredging removed lateral support from the eastern side of the causeway, which reduced the factor

of safety (FoS) for a north-northeasterly moving slide mass by removing some of the three-dimensional resistance the seabed sediments were providing.

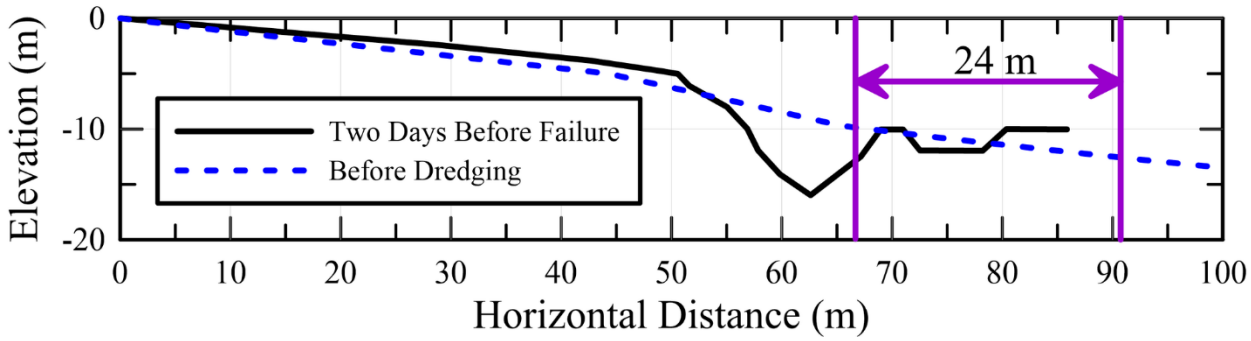

Figure 4. Comparison of bathymetric surveys performed before dredging (see green line) and two days before collapse (see red line) on cross-section shown in Figure 2. The location of the planned cofferdam cells is shown in purple.

These observations indicate dredging undermined the eastern side of the rockfill causeway, i.e. around the proposed location of sheetpile cell #3, which triggered the initial slide mass. Once the collapse was triggered, it retrogressed until it reached the shoreline. Some of the other important observations that can be made from the bathymetric data plotted in **Figure 5** are:

- The deepest dredging two days before collapse occurred near sheetpile cell #3 to elevation -16 m on the landside of the sheetpile cells as shown in **Figure 5**, which is near the toe of the causeway rockfill slope.
- Under and near the proposed location of sheetpile cell #4 in **Figure 5**, dredging occurred to elevation -16 m, but the causeway did not collapse during that dredging because the causeway slope toe was not in close proximity to this excavation. However, when dredging was in close proximity to the applied stresses from the causeway slope, i.e., near the proposed location of sheetpile cells #2 and #3, the collapse occurred.

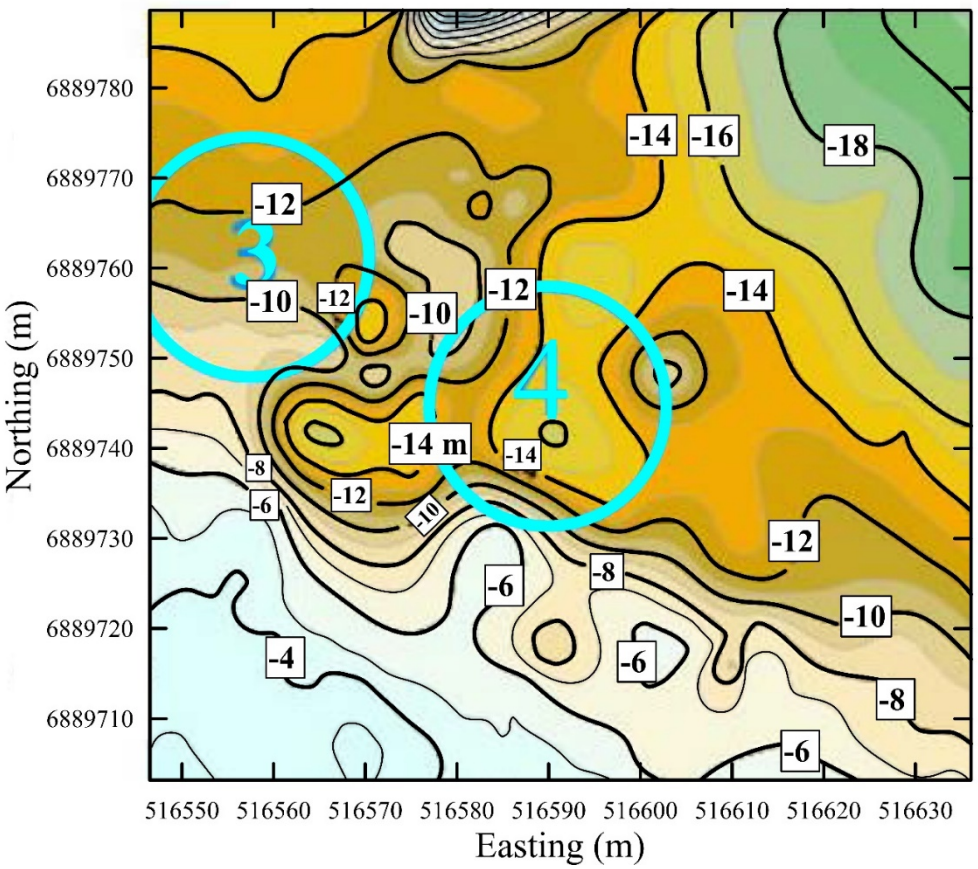

Figure 5. Diagrams showing close-up of bathymetric survey performed two days before collapse near cells #3 and #4.

The causal link between the dredging and causeway filling is also corroborated by the mobilized slide mass damaging two of the vertical pylons or spuds that were stabilizing the dredge barge at the time of collapse (see **Figure 6(a) and (b)**). In other words, the material from the rockfill causeway moved until it was under the dredging equipment during the causeway collapse. This also means the slope toe was near the dredged excavation because the rockfill could move or flow below the dredging equipment (see **Figure 6(b)**).

(a)

(b)

Figure 6. Photographs showing: (a) overview of rockfill causeway and dredging operation and (b) formation of tension cracks near end of causeway and distance to distance to dredging just prior to collapse and stabilizing rockfill on east side (right) of causeway.

In particular, the collapse started around 2:15 pm, but a quantity of 110 m^3 was reported to be dredged at 2:52 pm indicating that further dredging was occurring at the time of failure. In summary, the close proximity of the rockfill causeway to the deepest dredged excavation resulted in the application of significant driving stresses to an unsupported excavation.

STRATIGRAPHY

Initial geotechnical investigations for the project were conducted four years before construction started. No sediment sampling or testing was performed in the area of the wharf construction due to a change in the location of the causeway. Later soil borings (see **Figure 1**) show a layer of sand and gravel overlying a layer of clay, overlying a silty sand on top of granite gneiss bedrock (see **Figure 7**). The seabed clay layer was initially thought to be thin and soft to very soft such that it would be displaced due to the placement of the blasted rock used for the causeway construction. However, the clay layer was not displaced and was present at the time of failure.

The goal of this inverse analysis is to demonstrate the retrogressive failure mechanism, estimate the mobilized undrained shear strength of the marine clay for redesign, and show the extent to which the causeway fill and dredging contributed to the reduction in FoS of the causeway slope until failure was initiated.

The cross section shown in **Figure 7** is based on the five borings shown in **Figure 1**. The piezometric level was estimated in **Figure 7** based on the low tide level, which coincided with the condition at the time of failure. The failure surface was steep through the strong causeway material (see **Figure 8**), with an initial failure mass length of approximately 8 m based on the photograph shown in **Figure 9**.

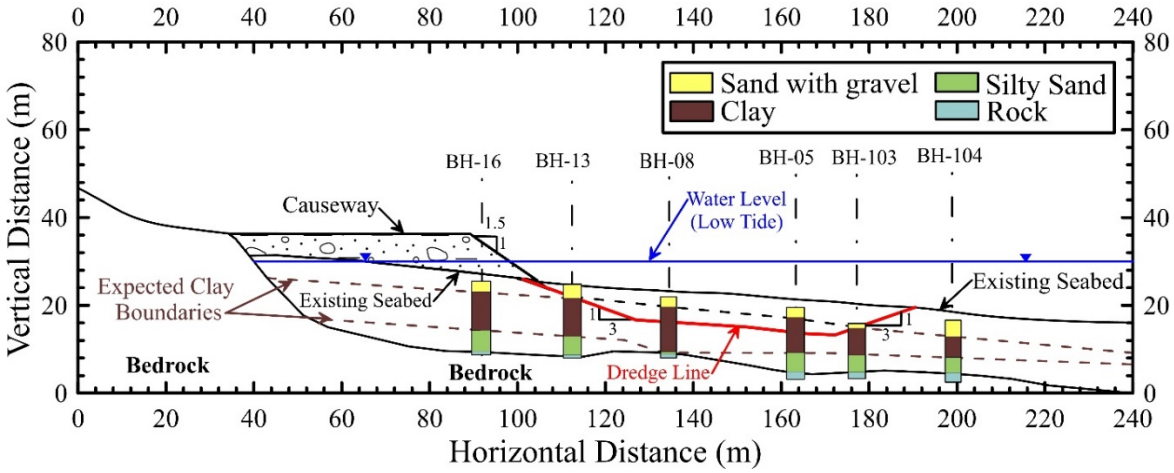

Figure 7. Cross Section at location shown in Figure 1 with soil borings superimposed.

Figure 8. Almost vertical scarp through causeway of the last slide mass near the shore.

Figure 9. **Photograph of slide masses #1 and #2 with the second slide mass developing without large displacement of the first slide mass (Note rockfill fall off the back of the first slide block into the gap between the two masses).**

The following paragraphs discuss the properties of each soil layer in **Figure 7** with a summary of the relevant material properties provided in **Table 1**.

Table 1. **Soil properties for causeway and seabed layers.**

Layer	Rockfill Causeway	Sand with Gravel	Native Clay
Total and Saturated Unit Weight (kN/m^3)	18 and 20	19 (saturated)	17
Undrained Shear Strength, S_u (kPa)	N/A	N/A	22
Drained Friction Angle, ϕ'	40	35	N/A
Plasticity Index (PI) (ASTM D4318)	N/A	N/A	13-19
Plastic Limit (PL) (ASTM D4318)	N/A	N/A	19-20
Liquid Limit (LL) (ASTM D4318)	N/A	N/A	32-39
Clay Size Fraction (CF) (ASTM D7928)	N/A	N/A	40

Note: N/A = Not applicable

Causeway Rockfill

The rockfill causeway is modeled in the stability analyses as a granular soil with a drained or effective stress friction angle (ϕ') of 40° and a total and saturated unit weight of 18 and 20 kN/m^3, respectively. This layer is comprised primarily of blasted boulders, cobbles, and gravel. The friction angle of 40 degrees was estimated from a range of ϕ' for rockfill of 35^0 (loose) to 50^0 (dense) reported by Terzaghi et al. (1996); Barton and Kjærnsli (1981); Leps (1970); and Frossard (2012). Given the short distance of the failure surface through the rockfill, the slope stability model is not particularly sensitive to changes in ϕ' used to model the causeway rockfill. This is further explored in the sensitivity analysis presented below.

Sand with Gravel Layer

The sand with gravel layer is modeled as a granular soil with a drained friction angle of 35° and a saturated unit weight of 19 kN/m^3. This layer is comprised of sand and gravel with occasional cobbles and boulders. This layer is described in boring logs as loose but ranges from very loose to dense. Due to the gravel, cobble and boulder content, this material is better described as a sandy gravel than a sand when estimating ϕ', which is about 35^0 for a loose to very loose sandy gravel (Terzaghi et al., 1996; Yagiz, 2001; and Hamidi et al., 2009).

Clay Layer

Due to the rapid loading of the native clay by the causeway rockfill construction, it was assumed the clay would be undrained so total stress strength parameters were sought (Duncan and Buchignani, 1973) from an inverse stability analysis of the various retrogressive slide blocks using the strength parameters discussed above for the overlying layers.

The first inverse analysis used the first slide mass and the critical translational failure surface with the lowest FoS, which extended about 5 m below the clay-sand interface. This inverse analysis yielded an average undrained strength of 32 kPa. Given the shape of the critical failure surface being a combination of a semi-circle and an almost linear translational part through the clay layer towards the dredged area, this shear strength corresponds to a triaxial compression (TXC) and direct simple shear (DSS) test mode of shear. The TXC mode of shear represents 30% of the failure surface is in clay while the DSS mode of shear represents 70% of the failure surface. Using an undrained strength over preconsolidation pressure ratio (S_u/σ'_p) of 0.33 for the TXC and 0.22 for the DSS mode (Terzaghi et al., 1996), a suitable undrained strength ratio for the clay is 0.253 using a weighted average. The equivalent shear strength for the TXC mode of shear is 41.7 kPa, which corresponds to an unconfined compressive strength (q_u) of 83.4 kPa. Based on this S_u, the clay would be classified as medium stiff with q_u ranging from 53.5 to 107 kPa or S_u=27 to 53.5 kPa as outlined in Table 1.5 in Peck et al. (1974).

Using the undrained strength ratio of 0.33 and $S_{u\text{-}TXC}$ of 41.7 kPa, a preconsolidation pressure of about 126.5 kPa was estimated for the clay layer. Using the effective stress on the clay before construction of the causeway or dredging, the range of overconsolidation ratio (OCR) was calculated to be 2.7 to 4.8 along the top of the clay layer using an initial effective stress of 47.6 to

26.3 kPa, respectively. Thus, the overconsolidation ratio for this clay ranges from 2.7 to 4.8. This range of OCR is typical for glaciolacustrine clay (Drevininkas et al., 2015; Demers and Leroueil, 2011). **Figure 10** shows a photograph of the dredged clay in the disposal barge that was excavated using clam shell equipment. The clay remained in large blocks after excavation indicating the clay was medium to medium stiff, which is in agreement with the mobilized strength.

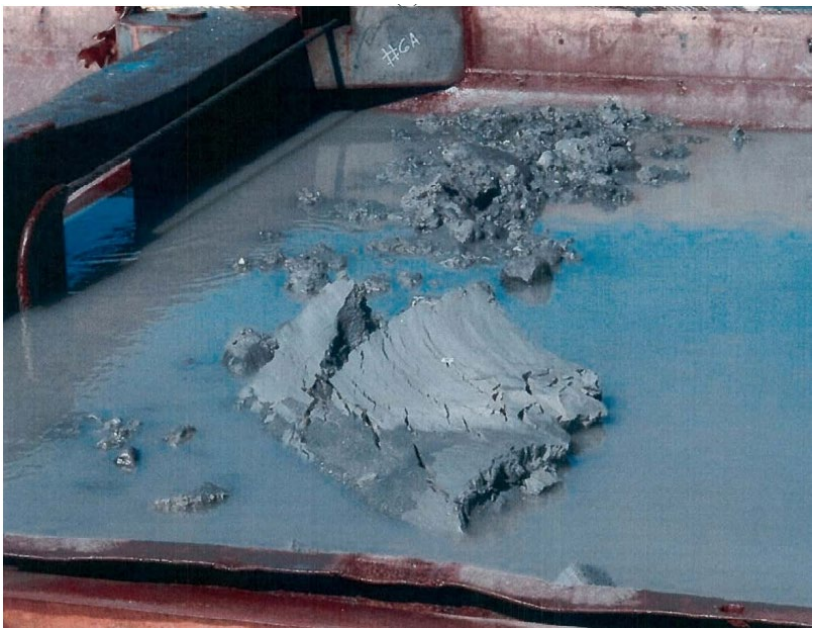

Figure 10. Photograph of dredged clay from wharf area in disposal barge.

Silty Sand and Bedrock

Both of these layers are below the observed failure surface, so the material properties are not relevant to the inverse stability analyses. In addition, the sheet piles for the wharf structure were to be driven into the bedrock.

ANALYSIS RESULTS AND DISCUSSION

The Morgenstern and Price (1965, 1967) stability method as coded in the SLIDE2 software package by RocScience (2022) was used to analyze the retrogressive underwater slope failure. The slope failure only involved the causeway rockfill layer, the natural sand and gravel layer and the clay layer, so only shear strength parameters for these layers impacted the inverse analysis.

For the failure surface of the first slide mass, it is known that the length of the top of the block was about 8 m (see **Figure 9**). Furthermore, the failure was known to be translational as observed in the field and evident from the photographs shown in **Figure 6(b), Figure 8**, and **Figure 9**. Therefore, the critical translational failure surface was searched manually in SLIDE2 until a failure surface with the lowest FoS was located. This critical translational failure surface was considered in the inverse analysis for calculating the mobilized undrained strength of the clay.

An inverse analysis was conducted to estimate the undrained shear strength of the clay, and values of $S_{u\text{-}TXC}$ = 41.7 kPa for the inclined and/or semi-circular part of the failure surface and $S_{u\text{-}DSS}$ = 27.8 kPa for the near horizontal part of the failure surface were obtained for a FoS of near unity (1.00 ± 0.01). This undrained shear strength was used in the analysis of slide masses 2, 3, 4, and 5, as shown in **Figure 11**. The values of ϕ' for the causeway and sand and gravel layers were not varied in the inverse analysis but were varied in the sensitivity analysis presented below.

For the second slide block, the length of the slide block was estimated to be approximately 9 m using the photograph in **Figure 9**. A tension crack was created in the stability model to represent the tension crack/scarp between the first and second slide masses (See **Figure 11(b)**) but was not included in the slope stability model. The appearance of a tension crack is an indication of a post-failure condition of the slope, and therefore, the tension cracks shown in **Figure 11** are only shown

to demonstrate the extent of the previous slide mass. As the clay was sheared during movement of the first slide mass, the undrained strength decreased from the peak undrained strength ($S_{u\text{-}TXC}=0.33*\sigma'_p$ and $S_{u\text{-}DSS}=0.22*\sigma'_p$) to the post-peak undrained strength (i.e., in between the peak and residual undrained strengths depending on the magnitude of shear displacement), where the residual undrained strength is represented as $0.07*\sigma'_{vo}$ as estimated from Stark and Contreras (1996; 1998).

Figure 9 shows that the tension crack at the back of the second mass appeared before the first slide mass moved underwater. Because the tension crack appeared for the second slide mass, the FoS should be near unity for the second slide mass. Therefore, to obtain a FoS of near unity for the second slide mass with the first mass still in place as per photographs, the clay undrained strength under the first slide mass, which is a near horizontal part of the failure surface, was reduced to a strength of $S_{u\text{-}DSS\text{-}PP1}=0.95\ S_{u\text{-}DSS\text{-}Peak}$ = 26.5 kPa, i.e., post-peak #1 (PP1).

The 26.5 kPa undrained shear strength was obtained by inverse analysis of the second slide mass until a FoS of near unity was obtained. Therefore, even though the exact displacement of the first slide mass is not known, it is known that the undrained strength of the first slide mass reduced to a value low enough to trigger movement of the second slide mass, i.e. about 26.5 kPa. Although displacement is required to mobilize a reduced strength of 26.5 kPa, this displacement corresponds to an undrained strength ratio of 0.209, which is greater than the residual undrained strength ratio of 0.07. Therefore, shear displacement of the second slide mass at the onset of movement was less than required to reach the residual undrained strength (Stark and Contreras, 1998).

The analysis procedure described in the last paragraph for the second slide mass was followed for the third, fourth, and fifth slide masses. Based on the slope stability analysis, all blocks remained

adjacent to each other and above the sea level with small movement. Therefore, the residual undrained strength was not mobilized even when the fifth slide mass reached a FoS of near unity. This is reasonable because the construction notes show the entire failure occurred within about two minutes, and therefore, all five-slide mass could have been mobilized before undergoing large movements. Therefore, when analyzing the third slide mass, the first and second slide mass were still in contact with the third slide mass when a tension crack developed between these two slide masses because the first and second slide masses were still above sea level.

The clay under the first and second slide masses mobilized post-peak #2 and #1, but not residual, undrained strengths. As seen in **Figure 11**, the different post-peak strengths for different slide masses are denoted as #1, #2, etc., where the post-peak #2 is lower strength than the post-peak#1 strength. Furthermore, the same post-peak #1 strength that was used in the analysis of the second slide mass of $S_{u\text{-}DSS\text{-}PP1}=0.95*S_{u\text{-}DSS\text{-}Peak}$ = 26.5 kPa was used for the analysis of the third slide mass. Therefore, when analyzing the third slide mass, the only unknown was the post-peak #2 strength which is under the first slide mass and was calculated to be $S_{u\text{-}DSS\text{-}PP2}=0.90*S_{u\text{-}DSS\text{-}Peak}$ = 25 kPa. A similar procedure was used for the fourth and fifth slide masses, where $S_{u\text{-}DSS\text{-}PP3}=0.72*S_{u\text{-}DSS\text{-}Peak}$ = 20 kPa and $S_{u\text{-}DSS\text{-}PP4}=0.40*S_{u\text{-}DSS\text{-}Peak}$ = 11 kPa, as shown in **Table *2***.

The fifth slide mass is the last slide mass to move, and it is located closest to the shore. This left approximately 10% of the natural beach/causeway above sea level after the failure ceased as described by observers and photographs. The mobilized undrained shear strength values for all five slide masses along with their FoS are shown in **Table 2**.

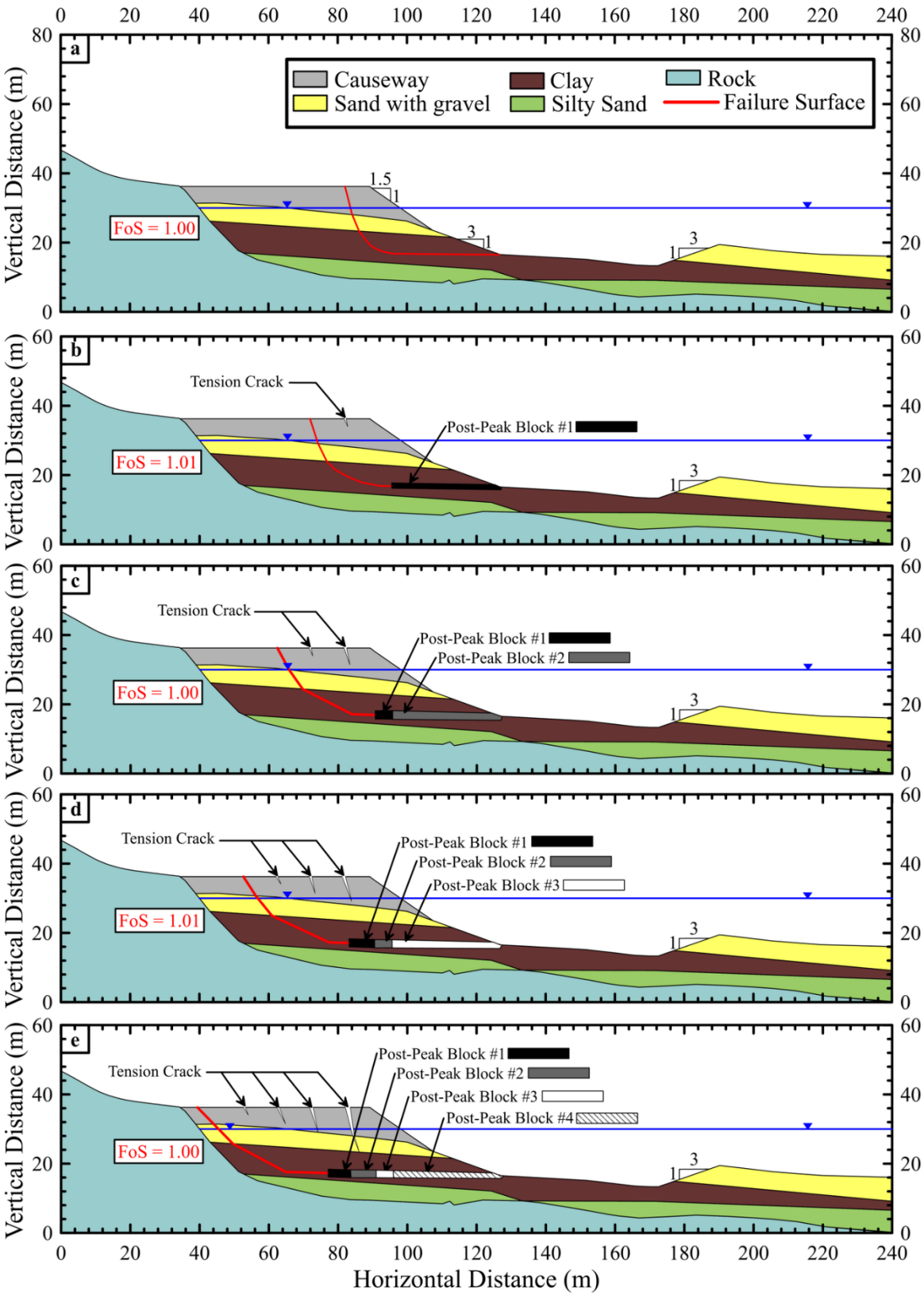

Figure 11. Sequence of retrogressive failure: (a) slide mass 1, (b) slide mass 2, (c) slide mass 3, (d) slide mass 4, and (e) slide mass 5.

Table 2. Clay undrained shear strengths for different slide masses and their FoS.

Slide Mass #	Material	Shear Strength	FoS
For all blocks	Causeway	ϕ'=40°, c'=0 kPa	
For all blocks	Sand and Gravel	ϕ'=35°, c'=0 kPa	
1	Clay TXC Peak	ϕ=0°, S_u = 41.7 kPa (S_u/σ'_p=0.33)	1.01
	Clay DSS Peak	ϕ=0°, S_u = 27.8 kPa (S_u/σ'_p=0.22)	
2	Clay TXC	ϕ=0°, S_u = 41.7 kPa (S_u/σ'_p=0.33)	1.00
	Clay DSS Peak	ϕ=0°, S_u = 27.8 kPa (S_u/σ'_p=0.22)	
	Clay DSS (Post-Peak #1)	ϕ=0°, S_u = 26.5 kPa ($S_{u\text{-}DSS\text{-}PP1}$=0.95 $S_{u\text{-}DSS\text{-}Peak}$)	
3	Clay TXC Peak	ϕ=0°, S_u = 41.7 kPa (S_u/σ'_p=0.33)	1.00
	Clay DSS Peak	ϕ=0°, S_u = 27.8 kPa (S_u/σ'_p=0.22)	
	Clay DSS (Post-Peak #1)	ϕ=0°, S_u = 26.5 kPa ($S_{u\text{-}DSS\text{-}PP1}$=0.95 $S_{u\text{-}DSS\text{-}Peak}$)	
	Clay DSS (Post-Peak #2)	ϕ=0°, S_u = 25 kPa ($S_{u\text{-}DSS\text{-}PP1}$=0.90 $S_{u\text{-}DSS\text{-}Peak}$)	
4	Clay TXC Peak	ϕ=0°, S_u = 41.7 kPa (S_u/σ'_p=0.33)	1.01
	Clay DSS Peak	ϕ=0°, S_u = 27.8 kPa (S_u/σ'_p=0.22)	
	Clay DSS (Post-Peak #1)	ϕ=0°, S_u = 26.5 kPa ($S_{u\text{-}TXC\text{-}PP1}$=0.95 $S_{u\text{-}TXC\text{-}Peak}$)	
	Clay DSS (Post-Peak #2)	ϕ=0°, S_u = 25 kPa ($S_{u\text{-}DSS\text{-}PP1}$=0.9 $S_{u\text{-}DSS\text{-}Peak}$)	
	Clay DSS (Post-Peak #3)	ϕ=0°, S_u = 20 kPa ($S_{u\text{-}DSS\text{-}PP1}$=0.72 $S_{u\text{-}DSS\text{-}Peak}$)	
5	Clay TXC Peak	ϕ=0°, S_u = 41.7 kPa (S_u/σ'_p=0.33)	1.00
	Clay DSS Peak	ϕ=0°, S_u = 27.8 kPa (S_u/σ'_p=0.22)	
	Clay DSS (Post-Peak #1)	ϕ=0°, S_u = 26.5 kPa ($S_{u\text{-}DSS\text{-}PP1}$=0.95 $S_{u\text{-}DSS\text{-}Peak}$)	
	Clay DSS (Post-Peak #2	ϕ=0°, S_u = 25 kPa ($S_{u\text{-}DSS\text{-}PP1}$=0.9 $S_{u\text{-}DSS\text{-}Peak}$)	
	Clay DSS (Post-Peak #3)	ϕ=0°, S_u = 20 kPa ($S_{u\text{-}DSS\text{-}PP1}$=0.72 $S_{u\text{-}DSS\text{-}Peak}$)	
	Clay DSS (Post-Peak #4)	ϕ=0°, S_u = 11 kPa ($S_{u\text{-}DSS\text{-}PP1}$=0.40 $S_{u\text{-}DSS\text{-}Peak}$)	

Figure 11 shows the sequence of the retrogressive failure. The final failure surface matches the observed post-failure bathymetry shown in **Figure 2**. Because there is still uncertainty in the modeled undrained strengths, geometry of the slide masses, and FoS at which slope movement initiated (slopes can start to move at a FoS less than 1.05 (Hussain and Stark, 2011; Silva et al., 2008; Griffiths et al., 2011)), the exact number of slide masses and geometries of the later slide blocks may not exactly model field conditions.

A. Sensitivity Analysis

In all inverse-analyses there is uncertainty in material properties (Idries and Stark, 2024; Idries et al., 2023; Stark and Idries, 2021), so a sensitivity analysis was performed to constrain the mobilized Su of the clay. This was achieved by varying the clay Su with all other soil properties being unchanged except for one property at a time, as shown in **Table *3***. The unit weight of all materials was considered as the selected value (see **Table *1***) $\pm$ 2 kN/m^3. This value was chosen because the unit weight is not expected to vary by more than $\pm$ 2 kN/m^3. For example, the unit weight of concrete is about 23 to 24 kN/m3, and therefore considering the upper limit of the causeway to be at 22 kN/m^3 is reasonable. The same applies to the sand and clay layers and their range agrees with available literature (Leps, 1970; Barton and Kjærnsli, 1981; Terzaghi et al., 1996; Yagiz, 2001; Hamidi et al., 2009; and Frossard, 2012). A similar approach was used for varying the friction angle which was considered as the selected friction angle (see **Table 1**) $\pm$ 5 degrees. This range of friction angles for the causeway fill and native sand is also in agreement with ranges reported in literature (Terzaghi et al., 1996).

Table 3 shows the change in mobilized clay Su ranges from an increase of 7% to a decrease of 10%, which also corresponds to the change in clay Su due to variations in the causeway unit weight. Reducing the unit weight led to a decrease of the Su because this reduction in unit weight leads to a reduction in driving forces along the failure surface, and therefore, a lower mobilized Su. The mobilized Su is most sensitive to the causeway unit weight because most of the causeway is above the water level, and therefore, changing its weight will have a large effect on the driving forces and thus on the mobilized Su. **Table 3** also shows that changing the friction angle of the causeway fill and native sand layer did not lead to a significant change in the mobilized Su for the clay. This is because most of the failure surface is going through the clay layer and not the causeway fill and sand layers, and therefore, it leads to a negligible change in mobilized Su. Nevertheless, the possible percent changes presented in **Table *3*** are within the ranges deemed acceptable in geotechnical practice.

Table 3. Sensitivity analysis results based on uncertainty in material property.

Material	Causeway		Sand		Clay	
Unit Weight (kN/m^3)	18	22	17	21	15	19
Su TXC (kPa)	37.56	44.66	39.65	42.99	40.07	42.99
Su DSS (kPa)	25.00	29.75	26.41	28.63	26.69	28.63
σ'_p (kPa)	113.82	135.34	120.16	130.28	121.43	130.28
% Change	-10%	7%	-5%	3%	-4%	3%
Friction Angle	35	45	30	40		
Su TXC (kPa)	42.16	41.32	42.57	40.91		
Su DSS (kPa)	28.08	27.52	28.36	27.24		
σ'_p (kPa)	127.75	125.22	129.01	123.96		
% Change	1%	-1%	2%	-2%		

FAILURE TRIGGER

Figure 12 shows the effects of causeway construction and dredging activities on the calculated FoS of the causeway. Without causeway construction, the dredging completed at the time of failure would have reduced the FoS from about 5.2 to about four , which is still above a FoS of unity, i.e. failure. With causeway construction completed to approximately 20 m or less from the shoreline, the causeway is not close enough to the dredged excavation for the two activities to interact with each other and for the dredging to reduce the FoS of the causeway slope. Any substantial construction of the causeway slope results in a lower factor of safety than the dredging, hence the dashed lines between 0 and 10m should not be taken to indicate a linear reduction in FoS. Beyond 20 m, dredging of the seabed sediments reduces the FoS by removing the lateral support of the causeway slope.

As shown in **Figure 12**, causeway construction alone without dredging reduced the FoS from about 5.2 to 1.2 when the causeway reached 55 m from the shoreline, which was the extent of the causeway when failure occurred. **Figure 12** also shows that failure could have occurred without dredging had the causeway construction continued for an additional 5 m reaching a total length of 60 m from the shoreline. Nevertheless, **Figure 12** shows that concurrent dredging and causeway rockfilling decreased the FoS to near unity, which initiated the retrogressive failure. Therefore, causeway construction caused a larger reduction in FoS than dredging. However, **Figure 12** shows the trigger of the causeway failure was dredging, and not causeway construction, because dredging reduced the FoS from 1.15 to near unity, triggering the failure.

Alternatively, constructing the causeway after wharf construction was complete would have allowed the causeway rockfilling to start at the bottom of the dredged excavation and progress upward instead of constructing from the shoreline towards the seabed. The rockfill placed in the dredged excavation would have buttressed the causeway slope instead of creating an exposed slope toe near the dredged excavation.

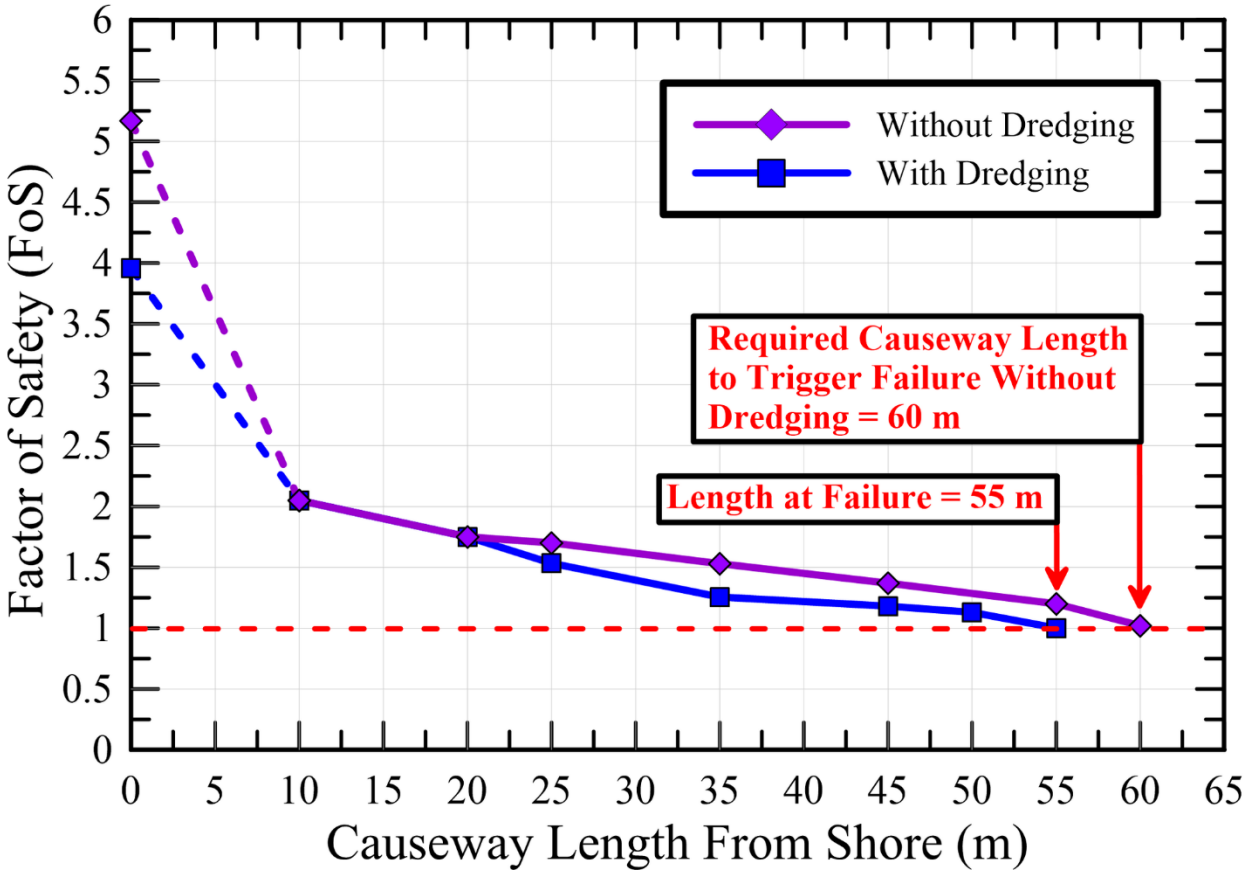

Figure 12. Impact of dredging and causeway rockfilling on FoS as a function of causeway distance from shoreline.

PRACTICAL APPLICATIONS

There are several practical lessons to be learned from the slope failure discussed in this paper. Some may seem self-evident but this failure among others shows that these lessons have not been learned. First, in any slope modification the existing soils in the area of construction should be sampled and tested. Engineers and owners should be cautious of construction methods that make implicit assumptions about soil strength or other characteristics.

Further, planned modifications to a slope that could destabilize it should be thoroughly analyzed, and such analyses should never be restricted to a circular failure surface. If possible, the construction sequence should be modified to reduce the extent to which the slope is destabilized. In this case that would mean constructing the wharf before the causeway.

Finally, construction should be monitored to verify that the proposed methods are working as intended. In this case it was assumed that the rock boulders would displace the clay layer when constructing the causeway. This should have been tested and verified, and the dredged clay coming up in large sheets as seen in **Figure 10** should have made it clear that the clay was not as soft as anticipated.

SUMMARY

This paper presents the analysis of an underwater retrogressive failure due to concurrent causeway construction and dredging activities. Causeway construction contributed the largest reduction in FoS but did not trigger the slope failure because the FoS was still about 1.15 without dredging. Dredging activities near the toe of the causeway slope triggered the failure by reducing lateral

support, and thus reduced the FoS from 1.15 to near unity. The retrogressive failure consists of five slide masses with the second, third, fourth, and fifth masses being triggered by failure of the adjacent seaward slide mass.

This study presents a method of analyzing retrogressive failure using two-dimensional limit equilibrium stability analyses that matches the observed failure sequence. The mobilized undrained shear strength of the native clay underlying the causeway was estimated using an inverse analysis due to a lack of laboratory and field data. Based on the inverse analyses, the causeway should have stopped when it reached about 33 m from the shoreline to ensure a FoS greater than or equal to 1.3 (Stark et al., 2009; Stark et al., 2018; Duncan et al., 2014; Whittlestone and Johnson, 1994; and USACE, 1970). Placement of the remaining portion of the causeway could have been completed after constructing the wharf structure and then placing rockfill behind the sheetpile cells to buttress the causeway. Even though gathering underwater geotechnical data is difficult, it is recommended to perform field tests to evaluate the shear strength of soil layers to perform slope stability analysis. This study shows that even if dredging did not occur, a slope failure probably would have occurred if the causeway construction had extended an additional 5 m further into the sea.

AVAILABILITY

Some or all data, models, or code that support the findings of this study are available from the corresponding author upon reasonable request.

ACKNOWLEDGEMENTS

The contents and views in this paper are those of the individual authors and do not necessarily reflect those of any of the corporations, contractors, agencies, consultants, organizations, owners, and/or contributors to the port development. The second author acknowledges and appreciates the participation of Filippo Massobrio of LANGAN Engineering and Environmental Services, Inc., based in NYC, NY in the initial stages of this case study as they both studied and presented this case study as their CEE 581 course project at the University of Illinois Urbana Champaign.

REFERENCES

ASTM D4318-17. (2017) Standard test methods for liquid limit, plastic limit, and plasticity index of soils. ASTM International, West Conshohocken, PA. www.astm.org. http://dx.doi.org/10.1520/D4318-17

ASTM D7928-21. (2021) Standard Test Method for Particle-Size Distribution (Gradation) of Fine-Grained Soils Using the Sedimentation (Hydrometer) Analysis, ASTM International, West Conshohocken, PA, 2021.

Barton, N., & Kjærnsli, B. (1981). Shear strength of rockfill. Journal of the geotechnical engineering division, 107(7), 873-891.

Bjerrum, L. (1971). Subaqueous slope failures in Norwegian fjords. Norwegian Geotechnical Institute Publ, (88).

Cornforth, D. H. (2005). Landslides in practice. Investigation, analysis, and remedial/preventative options in soils. Page: 529-540.

Demers, D., & Leroueil, S. (2002). Evaluation of preconsolidation pressure and the overconsolidation ratio from piezocone tests of clay deposits in Quebec. *Canadian Geotechnical Journal*, *39*(1), 174-192.

Drevininkas et al. (2015). Geotechnical Characteristics of Barlow-Ojibway Clay in Northern Ontario. GeoQuebec 2015. Ministry of Transportation of Ontario, Toronto, Ontario.

Duncan, J. M., & Buchignani, A. L. (1973). Failure of underwater slope in San Francisco Bay. Journal of the Soil Mechanics and Foundations Division, 99(9), 687-703. Frossard, E., Hu, W., Dano, C., & Hicher, P. Y. (2012). Rockfill shear strength evaluation: a rational method based on size effects. Géotechnique, 62(5), 415-427.

Duncan, J. M., Wright, S. G., & Brandon, T. L. (2014). Soil strength and slope stability. John Wiley & Sons.

Griffiths, D. V., Huang, J., & Fenton, G. A. (2011). Probabilistic infinite slope analysis. Computers and Geotechnics, 38(4), 577-584.

Hamidi, A., Yazdanjou, V., & Salimi, N. (2009). Shear strength characteristics of sand-gravel mixtures. International Journal of Geotechnical Engineering, 3(1), 29-38.

Hussain, M. and Stark, T.D. (2011). “Back-analysis of Preexisting Landslides". *Proceedings of Specialty Conf. GEO-FRONTIERS 2011*, ASCE, Dallas, TX, March, 3659-3668.

Idries, A., and Stark, T. D. (2024). Uncertainty in Drained Fully Softened and Residual Strength Correlations. Journal of Geotechnical and Geoenvironmental Engineering, 150(1), 06023010.

Idries, A., Stark, T. D., Moya, L., & Lin, J. (2023). Case Study: 3D MOBILIZED STRENGTH OF COMPACTED FILL. Canadian Geotechnical Journal, (ja).

Leps, T. M. (1970). Review of shearing strength of rockfill. Journal of the Soil Mechanics and Foundations Division, 96(4), 1159-1170.

Morgenstern, N. R., and Price, V. E. (1965). The analysis of the stability of general slip surfaces. Geotechnique, 15(1), 79-93.Morgenstern, N. R., and Price, V. E. (1967). A numerical method for solving the equations of stability of general slip surfaces. The Computer Journal, 9(4), 388-393.

Peck, R.B., Hanson, W.E., Thornburn, T.H. (1974). *Foundation Engineering, 2nd Edition*. New Jersey: John Wiley & Sons.

Puzrin, A. M., Gray, T. E., & Hill, A. J. (2017). Retrogressive shear band propagation and spreading failure criteria for submarine landslides. Géotechnique, 67(2), 95-105.

Rocscience Inc. (2022). Slide Version 2021 – 2D Slope Stability Analysis. www.rocscience.com, Toronto, Ontario, Canada.

Saxov, S., & Nieuwenhuis, J. K. (2012). Marine slides and other mass movements (Vol. 6). Springer Science & Business Media.

Silva, F., Lambe, T. W., & Marr, W. A. (2008). Probability and risk of slope failure. Journal of geotechnical and geoenvironmental engineering, 134(12), 1691-1699.

Stark, T. D., & Idries, A. (2021). Drained residual shear strength power function coefficients a and b. Geotechnical Testing Journal, 44(6), 1678-1694.

Stark, T. D., & Ruffing, D. G. (2017). Selecting minimum factors of safety for 3D slope stability analyses. In Geo-risk 2017 (pp. 259-266).

Stark, T. D., Choi, H., & Lee, C. (2009). Case study of undrained strength stability analysis for dredged material placement areas. Journal of waterway, port, coastal, and ocean engineering, 135(3), 91-99.

Stark, T. D., Ricciardi, P. J., & Sisk, R. D. (2018). Case study: Vertical drain and stability analyses for a compacted embankment on soft soils. Journal of geotechnical and geoenvironmental engineering, 144(2), 05017007.

Stark, T.D. and Contreras, I.A. (1996). "Constant Volume Ring Shear Apparatus," *Geotechnical Testing Journal*, ASTM, Vol 19, No. 1, March 1996, pp. 3-11.

Stark, T.D. and Contreras, I.A. (1998). "Fourth Avenue Landslide During 1964 Alaskan Earthquake," *Journal of Geotechnical and Geoenvironmental Engineering*, ASCE, Vol. 124, No. 2, February, 1998, pp. 99-109.

Tcrzaghi, K. (1956): Vareties of Submarine Slope Failures. Proceedings of the eighth Texas Conference on Soil Mechanics and Foundation Engineering, 41 pp. Reprint, Harvard Soil Mechanics Series No. 52. Also published as Norwegian Geotechnical Institute Publication 25.

Terzaghi, K., Peck, R. B., & Mesri, G. (1996). *Soil Mechanics in Engineering Practice*. John Wiley & Sons.

U.S. Army Corps of Engineers.1970. "Engineering and design: Stabil-ity of earth and rock-fill dams."Manual EM 1110-2-1902, Dept. of theArmy Corps of Engineers, Washington,

D.C.JOURNAL OF WATERWAY, PORT, COASTAL, AND OCEAN ENGINEERING © ASCE / MAY/JUNE 2009 /99

Whittlestone, A. P., & Johnson, J. D. (1994). Probabilistic risk analysis of slope stability to assess stabilisation measures. In Risk and reliability in ground engineering (pp. 266-276). Thomas Telford Publishing.

Yagiz, S. (2001). Brief note on the influence of shape and percentage of gravel on the shear strength of sand and gravel mixtures. Bulletin of Engineering Geology and the Environment, 60(4), 321-323.

Zhang, W., Klein, B., Randolph, M. F., & Puzrin, A. M. (2021). Upslope failure mechanisms and criteria in submarine landslides: Shear band propagation, slab failure and retrogression. Journal of Geophysical Research: Solid Earth, 126(9), e2021JB022041.

The Effects of Porewater Pressure on Driven Pile Installation in the Ohio Valley

Ben White, P.E.[1] and Bradley Klausing, E.I.T. [2]

Abstract: The geotechnics of a significant portion of the Ohio Valley consist of glacial deposits, often fine-grained soils to deep depths. This area of the country also has a relatively high number of bridge structures, leading to the need for deep foundations in these soils. One of the more common deep foundation elements used in this area are driven piles. Driving piles into the fine-grained soils has presented challenges due to the buildup of excess porewater pressure during driving.

During driven pile installation, resistance is present from both static soil resistance and dynamic soil and water (if applicable) resistance. Analysis of dynamic measurements during pile installation attempts to differentiate the static and dynamic resistances to evaluate the static soil resistance to driving, or the static soil resistance at the time of pile installation. As a pile is installed in saturated soils, water attempts to move away through the soil, however, in fine-grained soils, the water cannot displace, and excess porewater pressure builds. This causes very high dynamic resistance to driving, so while the resistance to driving increases (smaller set per blow, higher blow count), the static pile capacity does not. In addition, the disturbance of the soil from driving reduces the static resistance.

After driving, the excess porewater pressure dissipates and the soil remolds around the pile, providing additional static resistance, a phenomenon called soil set-up. This additional resistance can be quantified by performing monitored restrike testing after an appropriate amount of wait time.

Many projects in the area have taken advantage of additional soil resistance from soil set-up to optimize driven pile lengths. This paper will discuss the mechanisms of soil set-up as well as present case studies where pore-water pressure dissipation after driving had a significant impact on pile driving operations.

[1] Senior Engineer, GRL Engineers, Inc., Cleveland, Ohio. Email: bwhite@grlengineers.com
[2] Staff Engineer, GRL Engineers, Inc., Dayton, Ohio. Email: bklausing@grlengineers.com

Introduction

Driven piles are a primary deep foundation type in the Ohio River Valley. Generally steel pipe piles or H-piles are installed depending on the existing soil conditions. Piles are most often installed through impact driving, and the vast majority use diesel pile hammers in the experience of the author. With the exception of a few cases, the piles installed are generally relatively small, 12 inch to 16 inch diameter pipe piles (mostly closed end) and 10 inch to 14 inch sized H-piles.

The geology in the Ohio River Valley is quite diverse, from shallow bedrock toward Appalachia, to deep glacial deposits which consist of various soil types. This paper is focused on pile driving conditions in deep glacial deposits where installing piles to bedrock is either unnecessary or not possible. Piles in this soil condition are typically installed with the intent of developing resistance primarily from the sides of the shaft interacting with the surrounding soil.

Geotechnical engineers use traditional design methods when considering different pile types and drive lengths to support the required structural loads. Generally, the design methods consider the full geotechnical resistance of the in-situ soils, however the act of pile installation alters the soil structure and, therefore, the soil strength. Installation also increases the porewater pressure, particularly in fine grained soils (both cohesive and non-cohesive).

Morgano, et al. (2008) discuss the use of high-strain dynamic testing to evaluate time dependent changes in soil resistance through testing during initial driving as well as restrike tests after an appropriate amount of waiting time. A loss in soil resistance with time, referred to as relaxation of the soil, is a legitimate concern in some soil conditions, but is rare in cases of piles designed primarily for shaft resistance and in the soil conditions found in the Ohio River Valley, and is not the focus of this paper. Below is a discussion of the phenomenon of soil set-up followed by 3 case studies which provide varying levels of the use of soil set-up to optimize the piling on the respective projects.

Soil Set-up

The resistance encountered during driving of pile installation is comprised of both static resistance and dynamic resistance. Static resistance is due to the soil's resistance to driving. Morgano (2008) states that increased porewater pressure causes a reduction in effective stresses which consequently reduces the soil strength. Conversely, the increased porewater pressure can cause an increase in dynamic resistance during driving.

Figure 1. shows static soil resistance (RX9) and observed blow counts versus depth for a pile driven into saturated soils. The effect of excess porewater pressure is demonstrated graphically by an increasing blow count, yet constant static soil resistance when driving from 35 feet to 55 feet depth. The increasing blow count is due to higher dynamic resistance from excess porewater pressure.

Figure 1: Blow Count and Capacity vs. Depth – A Demonstration of Pore-Water Pressure Effects on soil resistance during driving

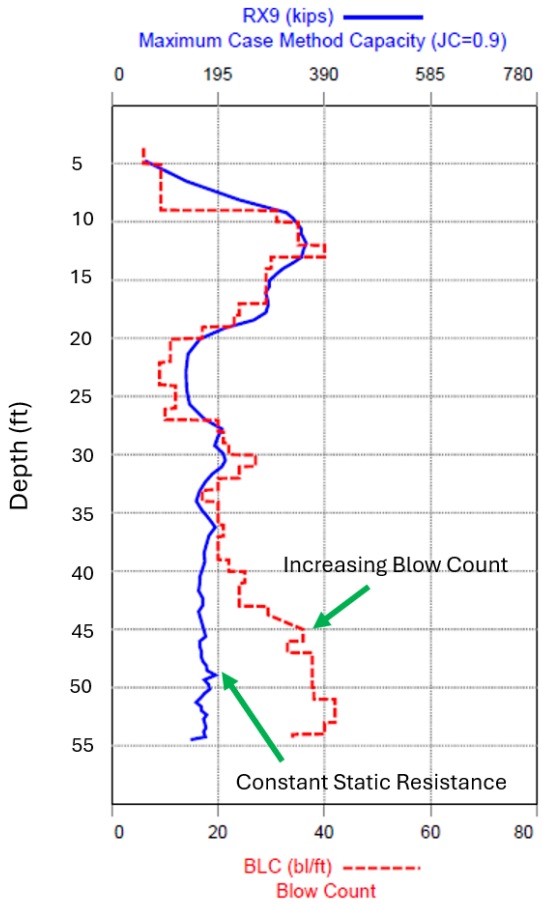

After pile installation, the excess porewater pressure dissipates and static soil resistance (in relation to the soil resistance at the end of installation) increases. This phenomenon is often referred to as soil set-up. In addition to the increased resistance due to excess porewater pressure, Hannigan (2012) discusses how set-up can also be attributed to the closing of an annulus around the pile caused by an oversized boot plate or pile tip reinforcement, the remolding of disturbed soil against the pile, long term soil strength gains (aging effects), or a combination of these effects.

Piles driven into fine-grained soils such as those typically found in the Ohio Valley, often experience soil set-up and see increased soil resistance with time. The extent of soil set-up is largely dependent on soil and pile properties and is also a function of the pile penetration length. A large portion of the soil resistance gain attributed to soil set-up occurs rapidly in the days and weeks after installation, though diminishing returns may continue to be observed in the following months and years.

Piles that do not achieve their target capacity during initial driving testing are often restruck at a later date to evaluate higher resistances that could not be demonstrated during initial driving. Understanding which conditions are favorable for soil set-up can allow engineers to plan for restrikes, achieve higher resistances per pile, and allow for more efficient designs that can save the project time, material, and money. Komurka (2018) demonstrates the utilization of soil set-up resulting in project savings.

Case Studies

Three case studies are presented with various methods of incorporation of soil set-up into the projects. The first demonstrates a situation where the design pile length is simply verified through restrike testing, allowing soil set-up to provide additional resistance after driving. The piles were all installed to a predetermined depth, then a waiting period allowed for soil set-up to occur. The second demonstrates the efforts of the owner to take advantage of soil set-up to reduce the production pile length. Piles were installed at various depths and restrikes were performed to determine the minimum depth necessary provide the required soil resistance. The third is an advanced use of soil set-up to optimize pile length of each installed pile using depth dependent driving criteria. This method uses long term restrikes to establish a soil set-up profile, quantifying the soil set-up versus pile embedment. While the testing program for this method is extensive, the cost savings from pile optimization far exceeded the cost of the testing program.

Case Study #1 – Using soil set-up to confirm design assumptions

The first case study features a design/build project in southern Ohio where HP 12x53 H-piles were utilized as foundations for two bridge structures. The piles were designed to be primarily shaft resistance piles as no competent bearing layer was indicated in the soil boring logs. The intent was to drive the piles until the required target capacity was achieved.

Once pile driving began, dynamic testing results made clear that the soil resistance to driving was often well below the required capacity for the respective substructure locations. Rather than adding additional pile length, the testing company suggested that the piles were installed to the design penetration depth and restrike testing was performed to evaluate pile capacity after soil set-up had occurred. This procedure was followed at 7 of the 8 substructures of the bridges. One location achieved the required capacity at the end of driving, therefore, restrike testing was not necessary.

In some cases, second restrike tests after longer waiting periods were necessary to achieve the required capacities. Some piles were slightly lower than the required capacities at the time of restrike, however, the EOR was sufficiently confident that additional capacity would develop with time, based on the response of other longer term restrikes, and accepted the piles. The results of the testing are summarized in Table 1.

Table 1. Case Study 1 – Bridges #1 (Left) & #2 (Right) - Summary of Total Capacity

Pile No.	Substructure	Target Capacity (kips)	Test Type	Depth (ft)	Total Capacity (kips)
9	Pier 1	264	EOID	50.0	**206**
			9-Day Restrike		**337**
10	Pier 1	264	EOID	50.0	**194**
			9-Day Restrike		**339**
15	Pier 2	264	EOID	65.0	**78**
			7-Day Restrike		**231**
			8-Day Restrike		**242**
24	Pier 2	264	EOID	65.0	**88**
			7-Day Restrike		**240**
			8-Day Restrike		**247**
34	Fwd Abut	304	EOID	75.0	**134**
			6-Day Restrike		**300**
			7-Day Restrike		**313**
45	Fwd Abut	304	EOID	75.0	**105**
			6-Day Restrike		**277**
			7-Day Restrike		**321**
1	Rear Abut	184	EOID	36.0	**217**
4	Rear Abut	184	EOID	37.0	**229**

Pile No.	Substructure	Target Capacity (kips)	Test Type	Depth (ft)	Total Capacity (kips)
38	Fwd Abut	169	EOID	75.0	**112**
			3-Day Restrike		**207**
39	Fwd Abut	169	EOID	75.0	**90**
			3-Day Restrike		**206**
6	Rear Abut	225	EOID	45.0	**97**
			6-Day Restrike		**211**
12	Rear Abut	225	EOID	45.0	**96**
			6-Day Restrike		**130**
19	Pier 1	300	EOID	55.0	**168**
			8-Day Restrike		**288**
22	Pier 1	300	EOID	55.0	**159**
			8-Day Restrike		**318**
29	Pier 2	300	EOID	61.0	**142**
			4-Day Restrike		**305**
32	Pier 2	300	EOID	61.0	**118**
			4-Day Restrike		**252**

Case Study #2 – Using soil set-up to potentially reduce pile length

The second case study involves a traditional Design-Bid-Build project in Southern Ohio. Fourteen-inch diameter, closed end pipe piles were installed to support a highway bridge. The soil boring logs indicated a general subsurface profile consisting of loose to medium dense gravel with sand, underlain by stiff to very stiff silt and clay. For this project, production test piles were installed to pre-determined depths and restrikes were performed prior to installation of the remaining production piles. The owner attempted to reduce the pile length through performing restrikes on piles installed to approximately 75% and 85% of the design pile lengths. In addition to the shorter piles, 2 piles were installed to the design depth for restrike testing similar to Case Study 1. The wait times were 7 to 9 days.

Table 2. Case Study 2 – Dynamic Testing Results of Piles Installed to Various Depths

Pile No.	Location	Target Capacity (kips)	Test Type	Depth (ft)	% of Design Depth	Total Capacity (kips)
1	Rear Abut	390	EOID	62.0	100%	**258**
			9-Day Restrike			**407**
5	Rear Abut	390	EOID	62.0	100%	**262**
			9-Day Restrike			**530**
10	Rear Abut	390	EOID	50.5	85%	**168**
			9-Day Restrike			**204**
15	Rear Abut	390	EOID	47.0	75%	**204**
			9-Day Restrike			**240**
63	Fwd Abut	390	EOID	62.0	100%	**199**
			7-Day Restrike			**410**
71	Fwd Abut	390	EOID	62.0	100%	**234**
			7-Day Restrike			**449**
67	Fwd Abut	390	EOID	50.5	85%	**177**
			7-Day Restrike			**341**
75	Fwd Abut	390	EOID	45.0	75%	**132**
			7-Day Restrike			**281**

In this case, the full design pile length was necessary to achieve the required target capacity of 390 kips. However, had the 75% or 85% depth piles achieved the necessary capacity, the remaining production piles could be installed to shallower depths.

This method provides the opportunity to reduce pile length without significantly affecting the pile driving process. If the shorter piles did not achieve the required capacity, driving continued until they reached the chosen depth. This method of utilizing soil set-up has been effective on projects in the Ohio Valley in various soil types and multiple pile sections.

Case Study #3 – Using soil set-up to develop depth dependent driving criteria

A design/build project to construct a 4,155-foot-long bridge in the northern Ohio area required the use of deep foundations in a river valley well known for providing very little resistance to driving, but very high soil resistance over time. A third bridge at this location was being constructed between two existing bridges. The existing bridges were founded on step taper piles which also had extensive testing in the early 1970's. This was the first site where dynamic measurements were collected, Goble et al, (1973) presented the results of the testing in their publication "Static and Dynamic Tests in the Cuyahoga River Valley". However, the pile type and low pile loads were not economical for the new structure. The design-build team implemented an extensive pile test program which included static load tests and dynamic testing during driving and long term restrikes at 30+ days wait time. The selected piles were 18-inch diameter, closed end pipe piles.

Initial drive testing near the river area, where designers anticipated relying heavily on soil set-up, indicated pile capacities ranging from 234 kips to 502 kips. The target capacity of the piles was determined to be approximately 1,100 kips. Restrike testing was performed at least 30 days after installation and after the piles were filled with concrete. The restrikes were performed using a drop hammer utilizing a 28-ton drop weight as the pile hammer was not large enough to mobilize the full soil resistance of the pile after soil set-up had occurred.

Figure 2: 28-Ton Drop Weight Hammer

Long-term restrikes indicated significant increases in total pile capacity, in some cases up to 5 times as much. Figure 2 presents the magnitudes of the soil resistance at the end of driving and during restrike for each substructure.

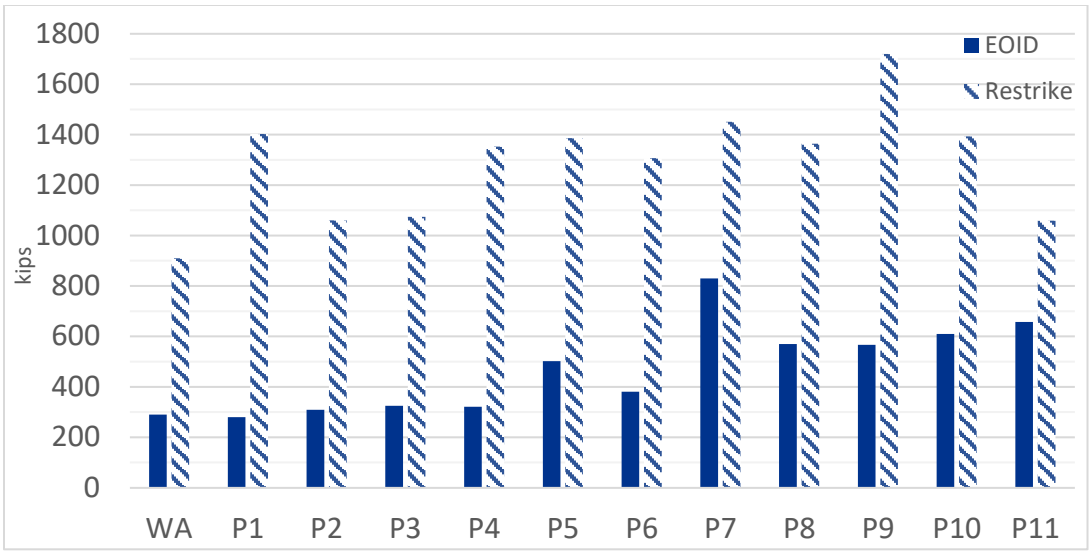

Figure 3: Comparison of End of Drive and Restrike Resistances

Restrike testing had clearly indicated that the project could benefit from the use of soil set-up to achieve the required pile capacities. The design-build used the resistance distribution from end of drive and restrike to develop a curve of resistance provided through soil set-up versus depth, or a set-up profile. Using the soil set-up profile and the determined required pile capacity, a target driving capacity could be determined that decreased with depth. Simply stated, the deeper the pile drives, the greater the soil set-up contribution, therefore, the soil resistance to driving requirement decreases. This is shown graphically in Figure 3 below.

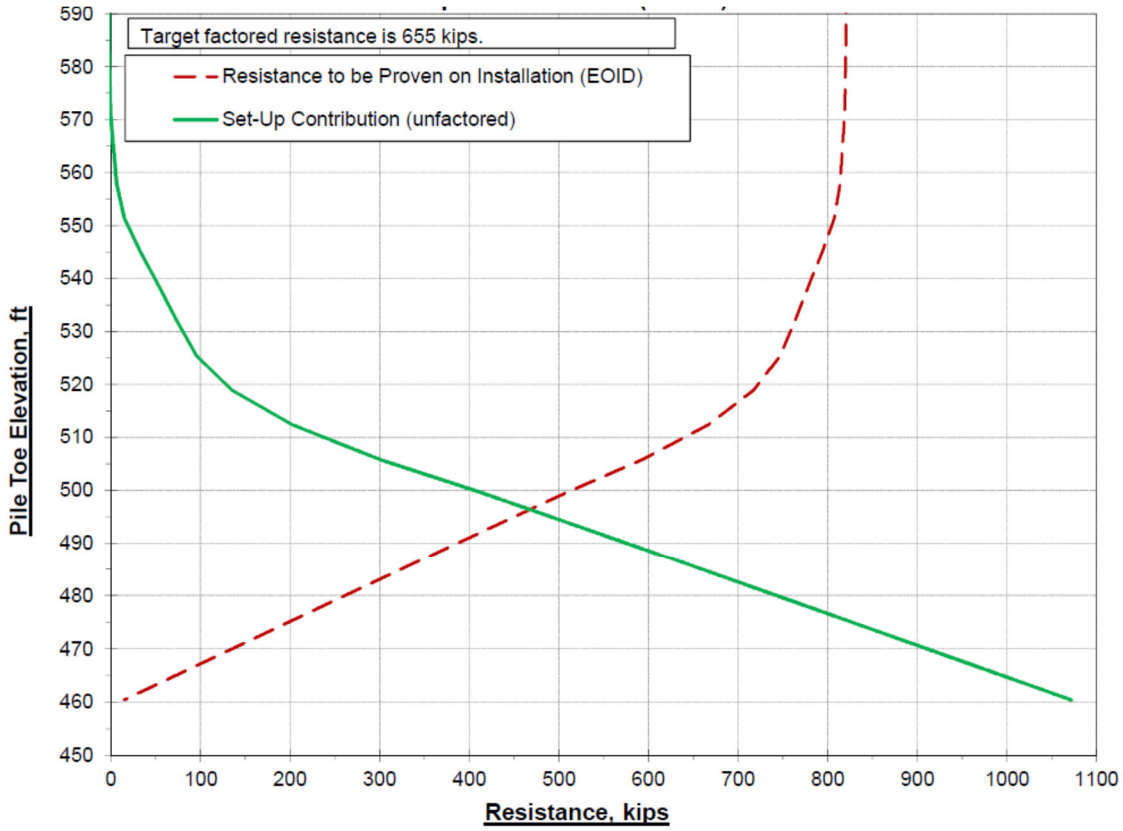

Figure 4: Example of Soil Set-up Profile and Required Soil Resistance vs. Elevation

Production pile driving criteria was established using dynamic testing data collected during production pile installation, as well as the pre-construction test program. Refined Wave Equation Analyses were performed based on the measured production hammer performance and soil resistance profiles. These analyses provided a relationship between observed blow count and soil resistance to driving. That information could then be applied to the already established soil set-up profiles to confirm the pile would achieve the required capacity with the addition of soil set-up. Extensive details of this pile test program can be found in Winter et al. (2019).

While the test program required several months to complete, the savings to the project was substantial and far exceeded the cost of testing.

References

Morgano, M., White, B., Allin, R. (2008). "Dynamic Testing in Sensitive and Difficult Soil Conditions." *Proceedings of the Eighth International Conference on the Application of Stress-Wave Theory to Piles,* pp 135-138.

Hannigan, J., Komurka, V., DiMaggio, J. (2012). "High-Capacity Pipe Piles for the Marquette Interchange Reconstruction" *Geo-Institute Geotechnical Special Publication No. 227*, pp 505-524.

Komerka, Van, E., Theiss, Adam, G., (2018). "Savings from Testing the Driven-Pile Foundation for a High-Rise Building." *Proceedings of the International Foundations Congress and Equipment Expo*.

Goble, George G., Rausche, Frank (1973) "Static and Dynamic Tests in the Cuyahoga River Valley", Case Institute of Technology.

Winter, Charles J., Banik, William. (2019). "Measurement and Use of Pile Set-up in Design and Construction of the I-480 Valley View Bridge." IBC 2019.

Soil and Water: An Appreciation of People, Places, and Experiences

Mark T. Bowers, PhD, PE*

Introduction:

Let me set the stage by quoting Luna B. Leopold. Dr. Leopold was an Emeritus Professor of Geology at the University of California, Berkeley and a former Chief Hydrologist for the U.S. Geological Survey. He was one of the world's leading authorities on river hydraulics and geomorphology. He wrote:

> *Water plays a part in all physical and biological processes. It is essential to the actions that have developed the earth's surface as we now observe it. Mountains are forced up by the collision of the great plates that make up the earth's crust. But mountains on the continental surfaces are gradually worn away by the ubiquitous weathering of their rocks, and the transport of weathered products downhill by the action of water, wind, and gravity. The weathering processes that change hard rock to erodible material incorporate water at every stage. Furthermore, water is the principal agent of movement of the weathered material that makes up the soil and supports vegetation, of the sedimentary rocks formed by the accumulation of the weathering products, and of the channels along which they are carried (Leopold, 1994).*

It is an honor for me to be asked to give the keynote address at this year's Ohio River Valley Soils Seminar. Our general subject is soil and water. I would like to address this through an appreciation of people, places, and experiences that formed my career over the last nearly sixty years.

1964—1968: The Early Formative Years

I will begin by taking you with me to my seventh-grade English classroom in 1964. My teacher had a file of articles from Readers Digest from which we could choose to read. I chose an article about the failure of Vaiont Reservoir in Italy. In the Fall of 1963, the newly completed Vaiont Reservoir formed behind the Vaiont Dam. This concrete double arch dam rose 860 feet from the valley floor. The creation of the reservoir reactivated an ancient landslide mass. The volume of the slide mass involved nearly 350 million cubic yards of material. This volume was about double that of the water impounded behind the dam. It is believed that the slide mass slid into the reservoir in less than 45 seconds, displacing the reservoir into two parts—one part toward the dam and the second upstream of the slide mass. Waves went over the crest of the dam to a height

……..
*Associate Professor Emeritus of Civil Engineering
University of Cincinnati
marktbowers@hotmail.com

of 330 feet. Some 2056 people perished in the ensuing flood. The concrete dam still stands. As a young boy in seventh grade, I was deeply touched by this tragedy and followed many of the studies (for example, see Hendron and Patton, 1986) of the whys and lessons learned from that catastrophe for years.

My stepfather came into my life when I was ten years old. I will henceforth refer to him as my Dad for that is what he became to me. We moved from West Virginia to Arizona in 1961. My dad was a high school graduate and a veteran of World War II. He had learned welding, carpentry, plumbing, and other trades via experience. He loved to read about home and auto repair. He read Popular Mechanics magazine and would replicate the devices and experiments. He helped me with my school projects including a water wheel in 6th grade and a wind direction indicator in 8th grade that had a lighted face like a clockface. Dad was employed as a technician for the U.S. Geological Survey in the Topographic Division hiking to mountain peaks in Arizona, measuring elevations and directions and laying out markers for aerial photography. He later worked for more than a decade for the USGS Hydrologic Division on the Gila River Phreatophyte Project (Culler, 1970). My summers after 7th through 9th grades (1964-1966) were spent in the field checking water-level observation wells, maintaining digital recorders, and recording data from neutron-scattering soil-moisture meters that measured moisture content. My "job" was to convert the data recorded on paper sheets by punching that data into Fortran punch cards. Dad was also part of a study on soil permeability as a function of ped size. The experiment involved a 4-foot diameter steel test cell about five-feet deep (a lysimeter). How I envied the summer interns from the University of Arizona and Arizona State University who could work on such projects.

In 1964 Dad took me on my first overnight camping trip to observe the start-up of a test well on the floodplain of the Gila River near Bylas, Arizona. This experience became a science report in my 7th grade science class.

I was thrilled to help Dad as the USGS Hydrologic Division conducted sedimentation studies in 1966 of the San Carlos Reservoir behind Coolidge Dam (Kipple, 1977). I was a flagman on shore, using flags to keep the boat in-line with a marker on the opposite shore. The lead engineer rewarded my efforts by giving me a rock and mineral collection consisting of some thirty approximately 2-inch-sized specimens. I still have that set in my continued collection.

As a junior-high student I wrote to a number of State Geological Survey offices throughout the western United States about my interest in geology and soil studies and was thrilled to receive large envelopes filled with reports, brochures, and maps.

In 8th grade we were bused to a nearby copper mine and toured the surface facilities. Then some of us were given the opportunity to descend 600 feet down a shaft to some of the underground workings. It was not a place to go if you feared the dark or were claustrophobic. In Arizona where I lived the surface is usually hot and dry. In the underground tunnels it was cooler with water seemingly dripping everywhere. I learned about faults, fractures, fissures, leaching efforts, pumping and processing of these copper-laden waters. I learned how, 65 million years ago, these vast deposits of copper ores had been created by hydrothermal intrusions along faults. It was interesting to learn about enrichment through the ages as water flowed

through these deposits. I learned about oxide minerals and sulfide minerals and how different processes were used to extract the copper from the ores.

1969—1976: Deciding on a Major; Listening to My Heart

My home in Arizona was a geological wonderland, a land consisting of mountains of granite and schist, enormous deposits of sedimentary material (the Gila Conglomerate), and of weathered blankets of volcanic material (dacite, perlite, obsidian). I was amazed at the size of the particles in the sedimentary deposits I viewed in roadcuts. What floods had moved these materials?

I started my college years in 1969 at the University of Arizona as a math major. After two years I realized that theoretical math was not for me…I was more of an "applied math" person. I changed my major to Civil Engineering and loved it. I followed the news concerning engineering failures such as the following.

> *1972—Buffalo Creek Dam, a series of three non-engineered embankments of coal mine waste. The reservoirs behind the embankments served as settling basins for wastewater from the mining operations. The uppermost embankment had no spillway or outlet works except for a 2-foot diameter steel overflow pipe. Heavy rains led to overtopping of the uppermost dam which then cascaded down through the other two reservoirs. The two uppermost embankments were built on the soft sediment of the next lowest settling basin. 125 people died. The town of Saunders was destroyed as well as all or parts of 16 other small communities in southeastern West Virginia. 4000 individuals were left homeless.*

The Buffalo Creek disaster hit home as I had lived in West Virginia for my first ten years. Volpe (1979) covers the engineering aspects of the failure while Erikson (1976) covers the social science issues.

In my mid-years of undergraduate study I especially enjoyed fluid mechanics. My class on Geology for Engineers was good, more so because of the assigned readings in the library. My next class in the sequence was to be Soil Mechanics taught by Dr. Ralph Rollins. The seniors said that you would either love that class or hate it. Well, I loved it, every minute of it. Dr. Rollins had his own consulting firm so he brought much "real" data to be used in our assignments. Dr. Rollins had taught Les Youd who had worked for the U.S. Geological Survey and was noted for his work in liquefaction; Hayward Baker who developed a national company in ground control and improvement which was folded into Keller later on; and many others of geotechnical renown. He invited Dr. Kenneth Lee to speak to us (just before Dr. Lee's tragic death in a skiing accident).

Teton Dam failed the month after I completed my junior year.

> *1976—Teton Dam, Idaho; earth dam failed on first filling of the reservoir. A large leak near the right abutment washed away the embankment and caused the dam breach. Investigations by two groups concluded that the failure was caused by a combination of geologic factors and design decisions that did not adequately take these*

factors into account. The primary geologic factor that caused problems was the existence of numerous open joints in the abutment volcanic rocks. The material used for the embankment core, because it was available, was a highly erodible windblown silt. Water was able to seep under the dam at its right abutment and wash it out at that point, causing the disaster. Eleven people died, 16,000+ head of cattle drowned in feed lots and damages exceeded $400 million (see Teton Dam Failure Review Group, 1977).

The Teton Dam was located just 280 miles north of my home in Provo, Utah. For Engineers Week in 1977, four of my classmates and I built a 6-ft x 6 ft model of the Teton Dam and its reservoir. We used aerial photos and contour maps. We constructed the model with a section that could be lifted out representing the dam breach. We used flags to indicate possible causes of the failure. Dr. Rollins was very impressed and asked if he could keep the model.

1977—1984: First Jobs, Graduate Degrees and Filling Some Gaps

I was fortunate to obtain my first engineering job following graduation with Dr. Rollins' firm. I worked for him for four years, starting in the lab, advancing to Lab Manager where I refined my understanding of lab testing, then into the field for site investigations for schools, churches, warehouses, and other structures. I was Resident Engineer overseeing QA/QC on an earth dam we had designed for Utah Power and Light. This embankment was 6600 feet long (in the shape of a horseshoe), with a maximum height of 50 feet out of the ground, and a 35-foot deep cutoff trench over most of that length. The dam was to impound fresh water piped from mountain reservoirs for use in the boilers of a coal-fired power plant. That assignment took a year to complete but what a year for learning. I purchased a copy of the USBR Earth Manual and studied it in my open hours. I realized quite quickly that my understanding of geotechnical engineering was insufficient. I had many questions. I needed to complete a Masters degree which I did while working for Dr. Rollins. To that point in time, some of my favorite courses included Theoretical Soil Mechanics, Earth Dam Design, Open Channel Hydraulics, Foundation Engineering, and Industrial Water Treatment. I worked on other earth dam projects while working for Dr. Rollins including the rehabilitation of an earthen dam in Wyoming for the U.S. Forest Service, a 90-foot-high dam named Browns Draw in northeast Utah, and a 135-foot high dam in southeast Utah named Recapture Creek. The latter design is one of my fondest experiences as an engineer.

Dr. Rollins shared with us pages from journal articles that he had read as part of his lectures and as guides for our homework assignments. His wife told us at a company picnic that Dr. Rollins kept copies of the ASCE Journal of the Soil Mechanics and Foundations Division on his nightstand and that he read faithfully every night. I thought that would be a great habit to emulate.

I learned a great deal about the influence of water as concerns soil behavior. The quote from Cedergren (1989), which follows, was very influential to me in light of the Vaiont landslide, the Buffalo Creek Dam failure, and the Teton Dam failure.

Powerful though the forces of water may be, civil engineers have long known that engineering works involving water can usually be made safe by (1) keeping the water out

of places where it can cause harm or (2) controlling by drainage methods that which does enter.

Cedergren presents Table 1.2 which describes examples of the consequences of uncontrolled seepage.

Category 1—Failures caused by migration of particles to free exits or into coarse openings:

**piping failures of dams, levees, reservoirs*

Category 2—Failures caused by uncontrolled saturation and seepage forces

**failures of dams, drydocks, and retaining walls caused by excessive saturation, seepage forces and uplift pressures.*

**deterioration and failure of pavements from internal flooding*

**uplifting of canal linings after drawdown*

**uplift pressures in trapped water*

**landslides*

My field studies with Dr. Rollins' firm took me into new realms of study, including

Collapsible soils
Expansive soils
Soluble materials (the presence of gypsum in fractured shale, for example)

What was behind these behaviors? What was the common element? Water. How are we to deal with all the differences, the unknowns, and the designs to produce a safe and efficient product? I appreciate the following quote from Karl Terzaghi, the man we recognize as the father of modern soil mechanics.

In the engineering for such works as large foundations, tunnels, cuts, or earth dams, a vast amount of effort and labor goes into securing only roughly approximate values for the physical constants that appear in the equations. Many variables, such as the degree of continuity of important strata or the pressure conditions in the water contained in the soils, remain unknown. Therefore, the results of computations are not more than working hypotheses, subject to confirmation or modification during construction.

In the past, only two methods have been used for coping with the inevitable uncertainties: either to adopt an excessive factor of safety, or else to make assumptions in accordance with general, average experience. The designer who has used the latter procedure has usually not suspected that he was actually taking a chance. Yet, on account of the

widespread use of the method, no year has passed without several major accidents. It is more than mere coincidence that most of the failures have been due to the unanticipated action of water, because the behavior of water depends, more than on anything else, on minor geological details that are unknown.

The first method is wasteful; the second is dangerous. Soil mechanics, as we understand it today [circa 1945], provides a third method which could be called the experimental method. The procedure is as follows: Base the design on whatever information can be secured. Make a detailed inventory of all the possible differences between reality and the assumptions. Then compute, on the basis of the original assumptions, various quantities that can be measured in the field. For instance, if assumptions have been made regarding pressure in the water beneath a structure, compute the pressure at various easily accessible points, measure it, and compute the results with the forecast. Or, if assumptions have been made regarding stress-deformation properties, compute displacements, measure them, and make a similar comparison. On the basis of the results of such measurements, gradually close the gap in knowledge and, if necessary, modify the design during construction. (Karl Terzaghi, in his draft version of the introduction (1945) to Soil Mechanics in Engineering Practice; presented by Ralph Peck in the Ninth Rankine Lecture, Geotechnique, Vol. 19, No. 2, pp. 171-187).

Note what he says at the end of paragraph two in the quote: "It is more than mere coincidence that most of the failures have been due to the unanticipated action of water, because the behavior of water depends, more than on anything else, on minor geological details that are unknown."

In 1981 I moved with my wife and four children to Arizona to work as a Project Civil Engineer for a large copper mining corporation. One of my projects was to develop a plan for a freshwater collection system on the property. This system was to consist of four earth dams about 100-feet high to be built in canyons surrounding our main open pit. Water from monsoon storms would be impounded before flooding the pit. The water would be pumped and treated before other uses in the mine facilities. All of my previous experience had involved cutoff trenches to rock and the use of grout curtains. Having studied the geology of the mine property, I knew we would be considering dams on pervious foundations. I needed help. I asked my manager if I could take a day to research the issue at Arizona State University's library. The ASU campus was 100 miles away. This was 1981, long before the internet and Google. I used the card catalog and found a paper by Arthur Casagrande (1961) entitled "Control of Seepage through Foundations and Abutments of Dams." I also found another paper Casagrande had written (1937) about flow net construction. I had never drawn a flow net in either my BS or MS studies so I was intrigued. The mining corporation also paid for me to attend a week-long course on earth dam design at the University of Missouri—Rolla.

In late 1982 I started my doctoral studies at Arizona State University. I was funded by the Arizona Department of Transportation on a study concerning sediment transport in ephemeral streams. My predecessors in the study had modified the Corps of Engineers computer model HEC-6 to accommodate larger particle sizes. HEC-6 had been developed to consider sediment transport of clays, silts, and fine sands of the Mississippi River. The riverbeds that I was

studying (dry ten months of the year) for the Salt River and the Agua Fria River were armored with rounded cobbles and boulders up to 12 inches in size. Flooding in the Salt River of 200,000 cfs occurred as upstream dams released water to provide storage for storm events. My thoughts went back to my junior-high days when I had contemplated how the Gila Conglomerate had been transported and deposited. I worked on this contract for two years (see Bowers and Ruff, 1983, and Dust et al., 1986). I am still amazed at the power of water to transport large particles.

In my doctoral program I studied under several outstanding professors including Paul Ruff, Dennis Duffy, Lawrence Hansen, and Charles O'Bannon who served as Department Head. During my first semester of doctoral work at Arizona State University, I took a course in seepage—flow through porous media, taught by Dr. Hansen. Dr. O'Bannon was substituting for Dr. Hansen the day we turned in Assignment 1 which involved the drawing of two flow nets for a weir on a pervious foundation. One flow net was drawn for the case of no sheet piling while the second net was similar to the first case but with the addition of some sheet piling at the toe of the weir. Dr. O'Bannon openly critiqued the nets one by one. I learned that he held nothing back. I was rather new to ASU so he didn't really know me. He had chopped up several papers then came to one which seemed to make him stop and look closer. "Bowers," he said out loud. "Who taught you how to draw flow nets?" I told him that I had gone to the library and had found an excellent paper by Arthur Casagrande which included a list of steps and some examples. "Bowers," he continued, "who taught you to test your flow net using circles?" I explained that a correct flow net was to consist of curvilinear squares. I had been taught in geometry that a square was a figure into which a circle could be inscribed that would be tangent to all four sides. From that day on Dr. O'Bannon took an interest in me and gave me support and opportunities to grow, including the teaching of Statics to undergraduates. Only later did I learn that Dr. O'Bannon had studied for his graduate degree at Harvard following the Korean War and that his mentor was…Arthur Casagrande!

In April 1983 the Thistle Landslide occurred in Spanish Fork Canyon, Utah, just fifteen miles from my former home in Orem, Utah. I had passed through Spanish Fork Canyon every week for a year while serving as the Resident Engineer on the construction of Emery Dam. Alan Mayo wrote the following description (1988): "The years 1982 and 1983 were very wet years. An ancient landslide was reactivated and began to move downhill toward the Spanish Fork River. The slide was a mile long and 500 feet wide. Within eight days the 15 million cubic yard slide had created a dam 221 feet high and blocked the river. The highway was destroyed and the railroad was cut off. The lake which formed behind this landslide dam eventually impounded 80,000 acre-feet of water. The lake depth rose to 180 feet in 50 days." The lake was later drained. The highway was rebuilt over the top of Billies Mountain while the railroad built a new line seven miles long and drilled a tunnel 3000 feet long then reconnected to the tracks above the lake. The Thistle landslide was the fifth-largest landslide in recorded US history and the most costly at $200 million. Kaliser and Fleming (1986) wrote an excellent paper on the Thistle landslide dam. See also Sumsion (1983) for a most interesting chronologic and photographic account of the disaster.

Bell (1999) wrote the following about the impact of pore water pressures within a slide mass:

Internal slides are generally caused by an increase in pore water pressures within the slope material which causes a reduction in the effective shear strength. Indeed, it is generally agreed that in most landslides, groundwater constitutes the most important single contributory cause. Therefore, identification of the source and amount of water movement and development of excess pore water pressure is important. An increase in water content also means an increase in the weight of the slope material or its bulk density, which can induce slope failure. Significant volume changes may occur in some materials, notably clays, on wetting and drying out. Not only does this weaken the clay by developing desiccation cracks within it, but the enclosing strata may also be affected adversely. Rises in the levels of water tables because of short-duration, intense rainfall or prolonged rainfall of lower intensity are a major cause of landslides. At times the water table may perch on the failure surface of a landslide. Seepage forces within a granular soil can produce a reduction in strength by reducing the number of contacts between grains. Water can also weaken slope material by causing minerals to alter or by bringing about their solution.

The following quote from Simons et al. (2002) is also enlightening:

Nearly all geotechnical hazards are associated in some way with water. Water in soils and rocks can, through reducing effective stresses, bring about a reduction in strength which may lead to slopes becoming unstable. Changes in groundwater conditions can cause the collapse of subsurface voids that can result in subsidence. Changes in moisture content in certain clay-rich soils can result in swelling and shrinkage leading to structural damage of buildings founded in them. The movement of water through certain rocks and soils can result in weathering at a rate that may result in changes in the mechanical properties during the life of a structure placed on or in them.

My doctoral coursework was demanding both mentally and timewise but has proven to be most valuable in my teaching and research over the last forty years. Those courses included:

Theoretical Soil Mechanics—Consolidation and Settlement
Advanced Fluid Mechanics
Geotechnical Aspects of Earthquake Engineering
Seepage—Flow through Porous Media
Theoretical Soil Mechanics—Shear Strength
Applied Soil Mechanics—Lateral Earth Pressures
Soil Stabilization
Graduate Statistics
Groundwater Hydrology
Geomorphology

Some of these classes were taught using the Socratic method. We were given an extensive list of journal articles and book chapters to read. Our lecture periods were then of the question-and-answer type where the professor would ask a question regarding a topic in the reading and the class members were to respond. For example, the discussion may have started with a basic statement about the construction of an earthen embankment. We know it is built of

borrow which is moisture-conditioned and thoroughly compacted. We test the compacted lifts against specified standards. Yet there are other very important issues to consider. The professor would ask us to then expound or he may have directed the question to a specific student. You had to be ready at all times. We might answer with the following thoughts on the site geology:

What do we know about the foundation rock?
Is there any indication of karstic conditions?
What is the bedding orientation in the basin?
What is the bedding orientation in the abutments?
What is the geologic history of the site?
Is there evidence of any ancient landslides or buried channels?
As concerns the foundation rock, are there fissures, joints? Can they be sealed?
Are the proposed embankment materials subject to erosion or dispersion?
What effect might the impounded waters have on regional seismicity?

Other courses invited questions and discussions about the following topics:

Is there such as thing as "true cohesion"?
What do we understand by the drainage conditions in triaxial testing (UU, CU, and CD)?
How does liquefaction occur?
In which soils is liquefaction expected? We studied the Bootlegger Clay from Alaska which liquefied in the 1964 earthquake and the sandy soils of Niigata Japan, in its 1964 earthquake.
How do pore pressures develop, both positive and negative, and what is their impact on effective stress and thus shear strength with time? Here we studied the failure of a section of the Houston Ship Channel.
Can we develop internal filters and drains that can prevent piping? If so, where can such criteria be found?
How do sinkholes develop?
What is the impact of excessive groundwater pumping?
Here we studied the Phoenix Basin. There the groundwater table has been drawn down over 300 feet. The impact is that, in general, the basin has settled two feet with some areas having subsided over ten feet. This has led to the development of extensive earth fissures throughout the valley. These fissures are miles in length, several feet wide and may reach thirty feet or more in depth.
What is meant by a "collapsible soil"? How can we build on such sites?
What is meant by an "expansive soil"? What construction techniques are available to us?
What is meant by a "dispersive soil"? How can we identify them? Can they be treated?

The questions just continued to multiply. My undergraduate degree was just an introduction to the study of Geotechnical Engineering. The more experienced I became, the more I recognized the need to be a lifelong learner. There is wisdom in requiring that licensed professional engineers have a record of continuing education each license renewal period.

1985—Present: Accepting a Professorship; New Challenges in Research

I began my Assistant Professorship at the University of Cincinnati in January of 1985 and was immediately immersed in a number of interesting research studies of an environmental nature. For many of our cases, the fluid moving into and through a soil is water, but other fluids also move through soils. Some of those may be termed contaminants and include gasoline from leaking underground storage tanks, solvents and cleaning fluids from industrial sites, radioactive plumes from Cold War-age processing plants, and leachates from old landfills and mining locations. These conditions and concerns led me to seventeen years of funded research including five years of research funded by the U.S. Environmental Protection Agency on containment of hazardous wastes and twelve years of research funded by the U.S. Department of Energy on the cleanup of the former Fernald Plant near Ross, Ohio which processed uranium and thorium ores during the Cold War. Working with low-level radioactive waste stretched our imagination. Have you ever tried to roll Atterberg plastic limit threads while wearing two pairs of latex gloves that were in turn duct-taped at the wrists of your Tyvek whole body coveralls? For further details, see Bowers and Lutz (1995).

My partner in the Geotechnical Engineering program for the first fourteen years of my work was Dr. Andrew Bodocsi. He was the Lead Investigator on the USEPA study which was headquartered at the USEPA's Center Hill Facility in Cincinnati. In the past, much waste had simply been dumped into old quarries or unlined dump sites without thought. Leachate was moving from the waste into groundwater with potential human health effects. Some of those wastes were acids, others were bases. There were paint wastes, oil wastes, and chemical contaminants including ethylene glycol (antifreeze), methanol, and others. These waste sites could not simply be excavated and treated. Our idea was to drill through the waste, install new impermeable floors through grouting, then encircle the site with a vertical barrier and cap it until such time as a treatment method was developed. This was the idea behind "containment." We tested various grouts against chosen waste streams. Our grouts included acrylates, acrylamides, microfine cements (three types amended with microsilica, emulsified bitumen, and bentonite, respectively), sodium silicates, and urethanes (see Bodocsi and Bowers, 1991). The courses I had taken in my doctoral program on seepage—flow through porous media, soil stabilization, and groundwater hydrology proved very useful in this research. I had written a term paper on sodium silicate stabilization in my class on Soil Stabilization. I needed that information just two years after I had written that paper.

I am grateful to have had Dr. Bodocsi as my academic and research partner. He continued to be a great sounding block even after he retired from the University of Cincinnati. He asked me probing questions about my research. I appreciated his wisdom. Dr. Bodocsi passed away in 2021, yet I still seek his counsel by asking myself "what would Andy do? How would Andy approach this problem?" While the Socratic method was sometimes nerve racking, it was an effective learning method for me.

In 1987 I was one of about 55 professors from across the United States and Canada who were selected to participate in the first Drilled Shaft Workshop for faculty sponsored by the Association of Drilled Shaft Contractors. This week-long training took place in the mountains outside Denver, Colorado. We sat at assigned tables of four people. At my table were Robert

Holtz, William Kovacs, and…Ralph Peck. We attended classes all day then had evening firesides where we heard from these great geo-engineers. I treasure my breakfasts with Dr. Peck, our walks along the trails, and playing horeshoes with him. He was a man who was down-to-earth, humble, willing to share his knowledge, noble, and a complete gentleman.

I would like to quote a story Ralph Peck gave in his Ninth Rankine lecture (1969). He relates his study of the subsidence of a chemical plant. I have learned much from his telling of this experience.

> *If the governing phenomena are complex, or are not yet appreciated, the engineer may measure the wrong quantities altogether and may come to dangerously incorrect conclusions. The possibility of serious error for this reason was harshly impressed on me more then twenty years ago. In those days, in addition to his regular duties at Harvard, Terzaghi held the title of Lecturer and Research Consultant at the University of Illinois. He conscientiously spent most of a week each semester in Urbana, lecturing and discussing recent developments with students and staff. As part of the routine he took to his hotel with him whatever reports I had written on jobs since his last visit, and the following day always cross-examined me in the greatest detail.*
>
> *On one of these occasions, I had handed him a report on subsidences of a large area occupied by a chemical plant. The site was underlain by a thin surficial deposit of sand with occasional organic inclusions, followed by some 50 ft of soft, normally loaded clay which rested in turn on limestone bedrock. The upper part of the limestone was known to be pervious and in the early 1900s to have contained water at a piezometric level about 20 feet above the present ground surface.*
>
> *Widespread irregular subsidences had occurred at the site over many years. They had provoked little attention until the arrival of a new chief engineer. As he sat in his newly painted office, he observed the appearance and widening of cracks in the walls and set out to investigate their cause.*
>
> *It developed that shortly after 1900 the chemical plant began to derive its basic raw material, sodium chloride, by solution of beds of salt at depths from 800-1100 ft. Water from a nearby river was injected into wells, become saturated and was withdrawn. In some of the older wells, however, no river water was furnished. The outer casings of the brine wells were simply perforated, or had deteriorated, in the pervious upper part of the limestone and the groundwater in the limestone flowed freely into the wells. The piezometric levels in the limestone were accordingly reduced by about 80 ft. I concluded that the reduction in piezometric levels at the base of the clay had induced consolidation of the soft overlying materials. Calculations of settlement on the basis of laboratory values of the compression index of the clays indicates that the ultimate settlements should be of the order of 3-5 ft, values that agreed well with those deduced from the settlement observations. The agreement was so satisfactory that I considered all the observed settlement to be accounted for, and felt confidence in the explanations.*

I still recall vividly the conversation when I called for Terzaghi the morning after he read the report:

[Terzaghi]: "Now, about that report on the subsidence…."
[Peck]: "Yes?"
[Terzaghi]: "I think you have missed the boat…." He paused. "It is obvious that the settlement is in the bedrock."
[Peck]: "But that is impossible. The bedrock is too thick," I protested.
[Terzaghi]: "How do you know it is impossible? You didn't establish any reference points at the surface of the bedrock, did you?"
[Peck]: "No, but the general magnitudes of the observed settlements agreed with the computed ones."
[Terzaghi]: "Didn't you notice that the real pattern of differential settlement is much more abrupt and erratic than the computed one?"
[Peck]: "Yes, but I think this difference is caused by the presence of erratic, compressible organic deposits near the ground surface."
[Terzaghi]: "What is the evidence? You have forced the evidence to fit your preconceived notions," he accused.

Indeed, I had, as I gradually and painfully learned. Together, Terzaghi and I embarked on an excursion, to last more than a decade, into the use of the observational method, this time not in soil mechanics but in engineering geology. Eventually the study demonstrated conclusively that subsidence of the rock strata was taking place above solution cavities, and it was found necessary to develop new brine fields not located beneath the plant areas. Had my original conclusion been believed, it is quite likely that a serious accident, such as a surface sinkhole, might have occurred with possible destruction of life and property.

Terzaghi in his broad experience had encountered similar situations before; I had not. My observational programme was inadequate to disclose a phenomenon I did not even suspect. Yet my lack of experience was not the only reason for failure: I had also failed to examine all the available evidence with an open mind.

Careful attention to detail of observations intended to support my working hypothesis might have thrown doubt on its validity. Essentially, however, preoccupation with the wrong phenomenon succeeded in creating a blind spot with respect to the significant one. The user of the observational method must constantly be aware of this possibility.

Conclusion:

I am grateful for the many classmates, professors, colleagues, and others who have influenced my career. They were fine examples. They patiently schooled me, worked with me, carefully chastised me, and led the way by their humble character and their mastery of sound principles. Soil and water—studying them has been as manna to my soul. I still have much to learn.

Thank you for your kind attention.

References and Select Bibliography:

Bell, Fred G. (1999), Geological Hazards—Their Assessment, Avoidance and Mitigation, Taylor and Francis.

Bodocsi, Andrew and Mark T. Bowers (1991), "Permeability of Acrylate-, Urethane-, and Sillicate-Grouted Sands with Chemicals," Journal of Geotechnical Engineering, Vol. 117, No. 8, August, ASCE, pp. 127-1244.

Bowers, Mark T. and Dale A. Lutz (1995), "Geotechnical Characterization of the Waste Pit Material for the Fernald Environment Management Project," Proceedings of the 26th Ohio River Valley Soils Seminar, Clarksville, Indiana, October 20, 1995.

Bowers, M.T. and P.F. Ruff (1983), "An Evaluation of Computer Models to Predict the Erosion and Deposition of Sediment for Selected Streams in Arizona," a report prepared for the Arizona Department of Transportation and the Arizona Transportation Research Center.

Casagrande, Arthur (1937), "Seepage through Dams," Journal of the New England Water Works Association, Vol. 51, No. 2, June 1937, pp. 131-172. (Reprinted in Contributions to Soil Mechanics—1925-1940, Boston Society of Civil Engineers, 1940, pp. 295-336.)

Casagrande, Arthur (1961), "Control of Seepage through Foundations and Abutments of Dams," the First Rankine Lecture, Geotechnique, Vol. 11, No. 3, September 1961, pp. 161-181.

Cedergren, Harry R. (1989), Seepage, Drainage, and Flow Nets, Third Edition, John Wiley and Sons, Inc.

Culler, R.C. et al. (1970), "Objectives, Methods, and Environment—Gila River Phreatophyte Project, Graham County, Arizona," United States Geological Survey Professional Paper 655-A, U.S. Government Printing Office, Washington, D.C.

Dust, D.W., M.T. Bowers, and P.F. Ruff (1986), "Application of HEC-6 to Ephemeral Rivers of Arizona," a report prepared for the Arizona Department of Transportation.

Erikson, Kai T. (1976), Everything in Its Path—Destruction of Community in the Buffalo Creek Flood, Simon and Schuster, New York.

Hendron Jr., A.J., and F.D. Patton, "A Geotechnical Analysis of the Behavior of the Vaiont Slide," Civil Engineering Practice, Volume 1, Number 2, Fall 1986.

Kaliser, B.N. and R.W. Fleming (1986), "The 1983 Landslide Dam at Thistle, Utah," in Landslide Dams—Processes, Risk, and Mitigation, Geotechnical Special Publication No. 3, ASCE, edited by Robert L. Schuster.

Kipple, Frank P. (1977), "The Hydrologic History of the San Carlos Reservoir, Arizona, 1929-1971, with Particular Reference to Evapotranspiration and Sedimentation," United States Geological Survey Professional Paper 655-N, U.S. Government Printing Office, Washington, D.C.

Leopold, Luna B. (1994), A View of the River, Harvard University Press, Cambridge, Massachusetts.

Mayo, Alan L. (1988). This description about the Thistle landslide was paraphrased from a narrative for a slide set purchased from GeoPhoto Publishing Company. Mr. Mayo was a member of the Geology Department at Brigham Young University.

Peck, Ralph (1969), "Advantages and Limitations of the Observational Method in Applied Soil Mechanics," Ninth Rankine Lecture, Geotechnique. Vol. 19, No. 2, June 1969, pp. 171-187.

Simons, Noel, Bruce Menzies and Marcus Matthews (2002), A Short Course in Geotechnical Site Investigation, Thomas Telford Limited, London.

Sumsion, Oneita Burnside (1983), Thistle—Focus on Disaster, Art City Publishing Company, Springville, Utah.

Terzaghi, Karl (circa 1945). This quote is from Terzaghi's draft version of the Introduction to Soil Mechanics in Engineering Practice. This quote was presented by Ralph Peck in his Rankine Lecture (1969) which may be found in Geotechnique, Vol. 19, No. 2, June 1969, pp. 171-187.

Teton Dam Failure Review Group (1977), Failure of Teton Dam—A Report of Findings, U.S. Department of the Interior.

Volpe, Richard L. (1979)," Engineering Aspects of the 1972 Buffalo Creek Dam Failure," Chapter 24 in Stability in Coal Mining, Proceedings of the first International Symposium on Stability in Coal Mining, Vancouver, 1978, Miller Freeman Publications, San Francisco.

On-line References:

Excellent synopses of dam incidents and failures are available on-line from the Association of State Dam Safety Officials (ASDSO) in their "Lessons Learned Case Studies." For example:

Buffalo Creek Dam, see damfailures/case-study/buffalo-creek-dam-west-virginia-1972/

Teton Dam, see damfailures.org/case-study/teton-dam-idaho-1976/

Vajont Dam, see damfailures.org/case-study/vajont-dam-italy-1963/

From PFMs to PZ Readings: Considerations for a Dam Seepage Modification

Kyle Blakley, P.E., M. ASCE[1]

Abstract: Wet areas have been observed along the downstream toe of the Clear Fork Reservoir Dam since at least 1979. The reservoir and dam are operated and maintained by the City of Mansfield, Ohio for water supply. To supplement the water supply, the City also relies on a network of groundwater wells, including one well screened in the native alluvial soils directly below the dam embankment. The City of Mansfield worked with Stantec to design a modification addressing the observed wet areas. Initial assessments included review of historical data, performing subsurface exploration, conducting seepage and slope stability analyses, and evaluating 15 identified potential failure modes (PFMs) associated with seepage. Stantec developed a seepage model to evaluate exit gradients and uplift pressures at the dam toe. Erratic piezometer (PZ) readings were observed, indicating up to five feet of fluctuation over periods as short as 15 minutes. The piezometer readings were compared to available groundwater well pumping records, which indicated a direct correlation. Stantec worked with the City to discontinue pumping from the groundwater wells nearest to the project area for approximately one month. Stantec monitored the piezometers to evaluate the pressure increases as conditions stabilized without well pumping. The design seepage model was validated by comparing predicted pressures with the stabilized field piezometer readings. Analyses indicated exit gradient factors of safety were below standard criteria at the dam toe in the areas of observed seepage. To address the risk-driving PFMs and the deficiencies identified through the engineering analyses, a graded filter toe berm was designed. The toe berm design considered the seepage PFMs and the impact of the groundwater well network. Construction of the modification was completed in October 2023. The nearest groundwater supply well was operated continuously during construction to lower the groundwater table and aid in constructability. The project is an example of how risk assessment of dams can be scaled down from a full PFM Analysis to focus on specific, targeted issues that have been observed. It also shows the importance of considering nearby infrastructure (groundwater wells) to design and construct an appropriate dam safety solution.

[1] Principal, Stantec Consulting Services Inc., Indianapolis, IN. Email: kyle.blakley@stantec.com

Introduction

Clear Fork Reservoir is located in Richland and Morrow counties in Ohio, approximately 7 miles southwest of Mansfield, Ohio. The reservoir was designed to be the primary source of water for the City of Mansfield. The reservoir is retained by an earthfill embankment dam located at the southeast end of the reservoir. The construction of the dam and appurtenant structures was completed in 1949. Clear Fork Reservoir Dam is a Class I High Hazard dam due to the storage capacity and potential loss of life and/or property in the event of dam failure. Fig. 1 shows an overview of the study area with pertinent dam features labeled.

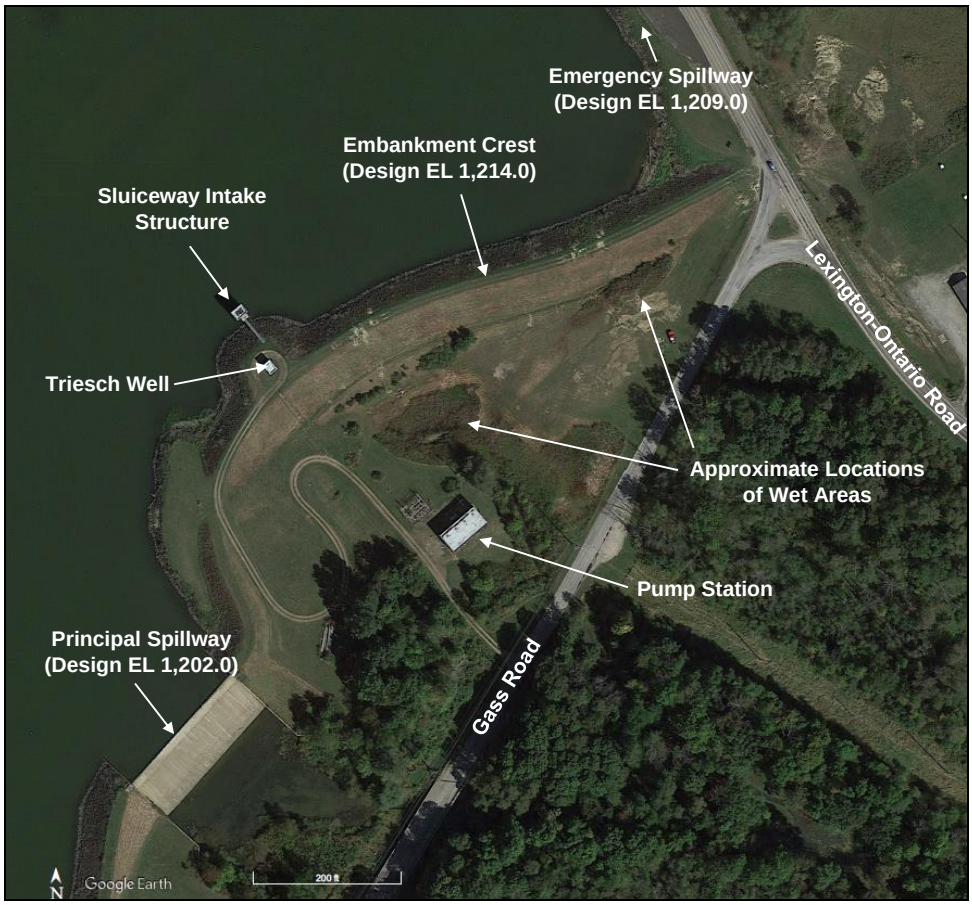

Fig. 1. Overview of Study Area (from GoogleEarth, August 2018)

The Phase I United States Army Corps of Engineers (USACE) Inspection in 1979 (Benedict et al. 1979) and subsequent Ohio Department of Natural Resources (ODNR) inspections in 2000, 2005, 2010, and 2015, recorded observations of two distinct wet areas at the toe of the dam near the left abutment. Several historical explorations were conducted to evaluate the wet areas including those completed in 1982, 1983, and 2017. The reports from those explorations indicated the wet areas were likely due to underseepage in the alluvial deposits below the dam within the original Clear Fork channel, but that the seepage did not adversely affect the slope stability of the dam. The 1982 and 1983 reports recommended further study, and the 2017 report recommended improvements to the dam to meet USACE criteria for allowable exit gradients at the toe.

The City of Mansfield worked with Stantec to design a modification addressing the observed wet areas. Initial assessments included review of historical data, performing subsurface exploration, conducting seepage and slope stability analyses, and evaluating 15 identified potential failure modes (PFMs) associated with seepage. To address the risk-driving PFMs and the deficiencies identified through the engineering analyses, a graded filter toe berm was designed. Construction of the modification was completed in October 2023. The project included several types of analyses and multiple phases of evaluation, design, and construction. This paper focuses on the seepage modeling, PFMs, and the unique piezometric conditions considered to design and construct a dam safety solution for the City.

Clear Fork Reservoir Dam

The earthfill embankment dam is approximately 3,400 feet long at the crest with a maximum height of about 44 feet. The design crest elevation is 1,214.0 feet. The upstream slopes of the dam are typically 3:1 (horizontal to vertical) and the downstream slopes are typically 2:1. A 10-foot-wide berm is located on the downstream side at mid-slope.

A one-foot-thick gravel blanket drain at the toe of the dam was shown on the design drawings but several historical studies as well as the most recent exploration concluded that the blanket drain had not been installed or was no longer functional.

The sluiceway conduit consists of a 30-inch diameter cast iron pipe located within a 6- by 6.5-foot reinforced concrete tunnel beneath the embankment. The sluiceway runs from the reinforced concrete intake tower to an access at the downstream toe of the embankment. A 24-inch diameter suction from the sluiceway main feeds the pump station to the water treatment plant. The concrete tunnel includes five rectangular anti-seepage collars (1-foot thick by 16-feet wide by 15-feet, 1-inch tall) on 24-foot centers. The anti-seepage collars are generally located on the upstream half of the concrete tunnel.

A groundwater well (called “Triesch Well”) is housed at the crest of the dam. The well predates the dam and was extended vertically through the embankment during construction. It feeds water through a 14-inch cast iron main to the water treatment plant (City of Mansfield 2010).

Seepage Evaluation

Stantec reviewed available historical data and performed additional explorations and analyses to advance toward design of a dam modification. Stantec conducted site visits, exploration, laboratory testing, and performed seepage, slope stability, and internal erosion analyses to develop a comprehensive understanding of the site conditions and potential remediation options. Potential failure modes (PFMs) were considered, and site piezometric data was studied in detail to develop an adequate design.

Site Visits

Stantec representatives visited the project site to make observations pertinent to the seepage, stability, and internal erosion assessment. Those observations are summarized below, and Fig. 2 shows their approximate locations.

- Two large wet areas, with cattails and overgrown vegetation were observed near the toe of the dam.

- Surface water was observed flowing down the hillside to the wet toe area. After review of existing documents, it appeared that the water was coming from the Triesch Well discharge pipe. This was later confirmed and repaired by the City during a separate project.

- Patches of woody vegetation were noted along the embankment toe and downstream bench between the sluiceway pipe and the left abutment. This vegetation was later removed by the City.

- Artesian conditions were observed in the two piezometers located at the toe. Extensions were added to these riser pipes, and subsequent piezometer readings indicated water levels at or just below the ground surface.

Fig. 2. Approximate Locations of Site Visit Observations (from GoogleEarth, August 2018)

Material Characterization and Analyzed Cross Sections

Available project records, boring logs, and laboratory test data from Stantec's and historical explorations were used to interpret and assign embankment and foundation material parameters for use in design analyses. The key materials represented in analyses are identified in Table 1. Bedrock is deep and did not influence the analyses. Two specific cross sections were selected and developed to model the dam along sections where wet areas were observed. The section locations are shown on Fig. 3.

Fig. 4 and Fig. 5 show the cross sections developed near Station 23+50 and Station 27+00, respectively. Various explorations of the study area had attempted to locate the gravel blanket drain and determine whether it was originally placed during construction. Conclusions were consistent that the gravel blanket drain had not been constructed or was not functional. Because of the uncertainty of its construction and apparent lack of effectiveness, the gravel blanket drain was not modeled in the analyzed cross sections.

Table 1. Identification of Materials

Material Name	General Description
Embankment Fill	Brown lean clay with sand and varying amounts of gravel, medium stiff to very stiff
Foundation Clays	Brown and gray lean clay or silty clay with sand, medium stiff to very stiff
Foundation Sands	Gray silty sand, loose to medium dense
Foundation Sands and Gravels	Brown and gray silty gravel with sand, medium dense to very dense
Rip Rap	Stone rip rap placed on the upstream slope of the embankment

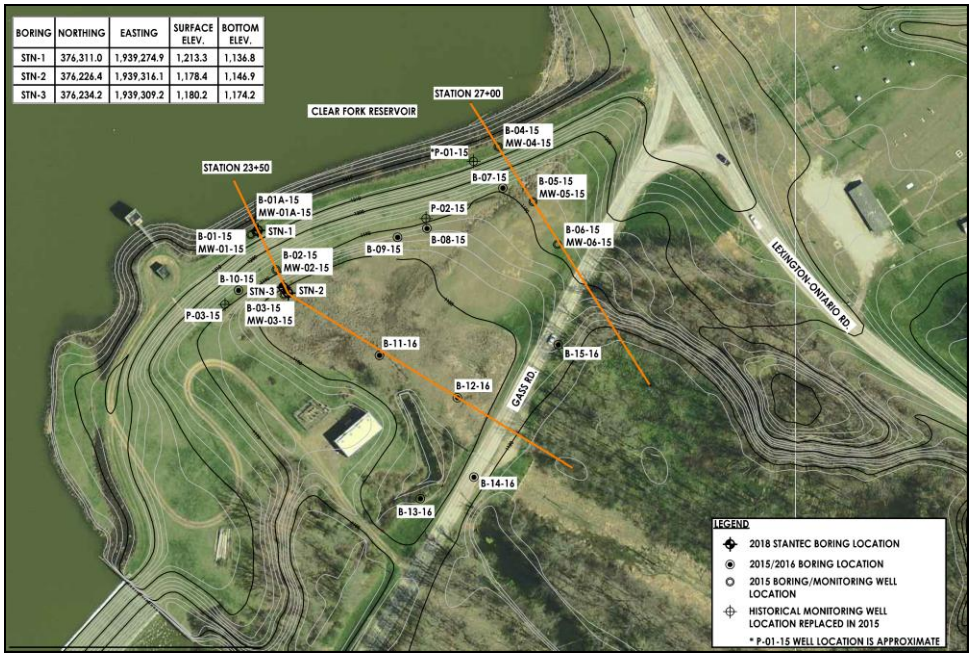

Fig. 3. Boring, Instrument, and Cross Section Location Site Plan

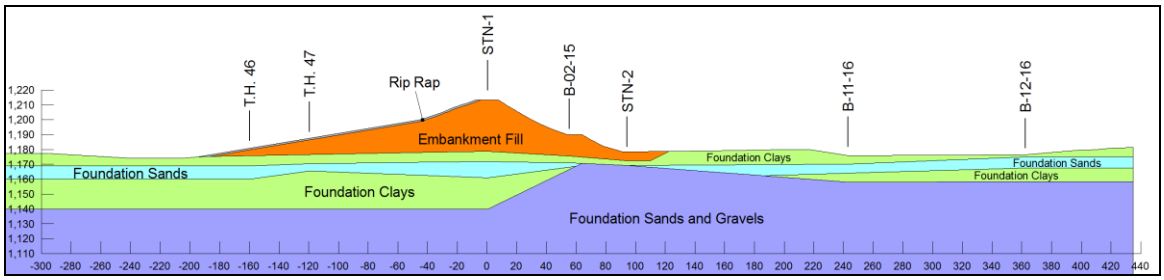

Fig. 4. Station 23+50 Cross Section

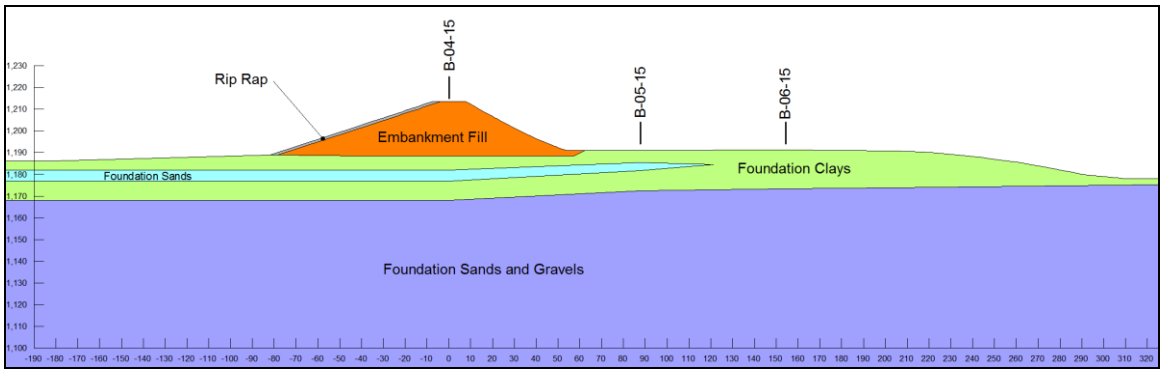

Fig. 5. Station 27+00 Cross Section

Site Instrumentation and Data Trends

Ten open standpipe piezometers/monitoring wells have been installed in the study area, as shown in Fig. 3. One is screened in Foundation Clays, three are screened in the Foundation Sands, and six are screened in the Foundation Sands and Gravels. The instruments were sounded during a site visit and MW-01-15 was blocked approximately 11 feet above the expected bottom depth. Readings from MW-01-15 were considered suspect for this study. Details regarding the ten instruments in the study area are provided in Table 2.

Table 2. Study Area Instrumentation

Instrument ID	Ground Surface Elevation (ft)	Screened Elevations	Screened Material
MW-01-15[(1)]	1,213.5	1,144.0 - 1,154.0	Foundation Clays
MW-01A-15	1,213.5	1,159.7 - 1,169.7	Foundation Sands
MW-02-15	1,190.1	1,159.1 - 1,169.1	Foundation Sands and Gravels
MW-03-15	1,178.6	1,159.6 - 1,169.6	Foundation Sands and Gravels
MW-04-15	1,213.5	1,157.3 - 1,167.3	Foundation Sands and Gravels
MW-05-15	1,191.0	1,179.0 - 1,184.0	Foundation Sands
MW-06-15	1,191.3	1,162.3 - 1,172.3	Foundation Sands and Gravels
P-01-15	1,213.8	1,178.8 - 1,183.8	Foundation Sands
P-02-15	1,190.5	1,177.5 - 1,180.5	Foundation Sands and Gravels
P-03-15	1,190.1	1,180.1 - 1,183.1	Foundation Sands and Gravels

[(1)] Measured bottom of screen elevation was 1,155.6 feet.

Stantec took three sets of readings for this project in the spring and summer of 2018. The City of Mansfield provided spreadsheets with readings of MW-01-15 through MW-06-15 taken with automated data loggers from September to November 2015 and October 2016 to May 2017. Several instruments exhibited significant fluctuations in relatively short periods of time. The City of Mansfield also provided ground water supply well pumping records from September and October 2015. The Triesch Well (below the embankment in the study area) had a significant influence on piezometric levels, and, to a lesser extent, the Wiles and Brumenshenkle Wells also impacted readings. Fig. 6 shows the location of the groundwater wells in relation to the study area, and Fig. 7 shows an example of the influence of the groundwater well pumping on piezometric levels in MW-03-15.

Instruments screened in the Foundation Sands and Gravels are hydraulically connected to the pumping of the Triesch Well. The magnitude of influence on the total head within the instruments depended on the proximity to the Triesch Well and the duration of pumping. The instruments near Station 23+50 exhibited greater total head fluctuations during pumping compared to those instruments near Station 27+00. During one day of pumping on September 19, 2015, MW-02-15 and MW-03-15 experienced approximately six feet of drawdown while MW-04-15 and MW-06-15 saw approximately three feet drawdown.

Fig. 6. Groundwater Wells in Vicinity of Study Area (from OEPA 2013)

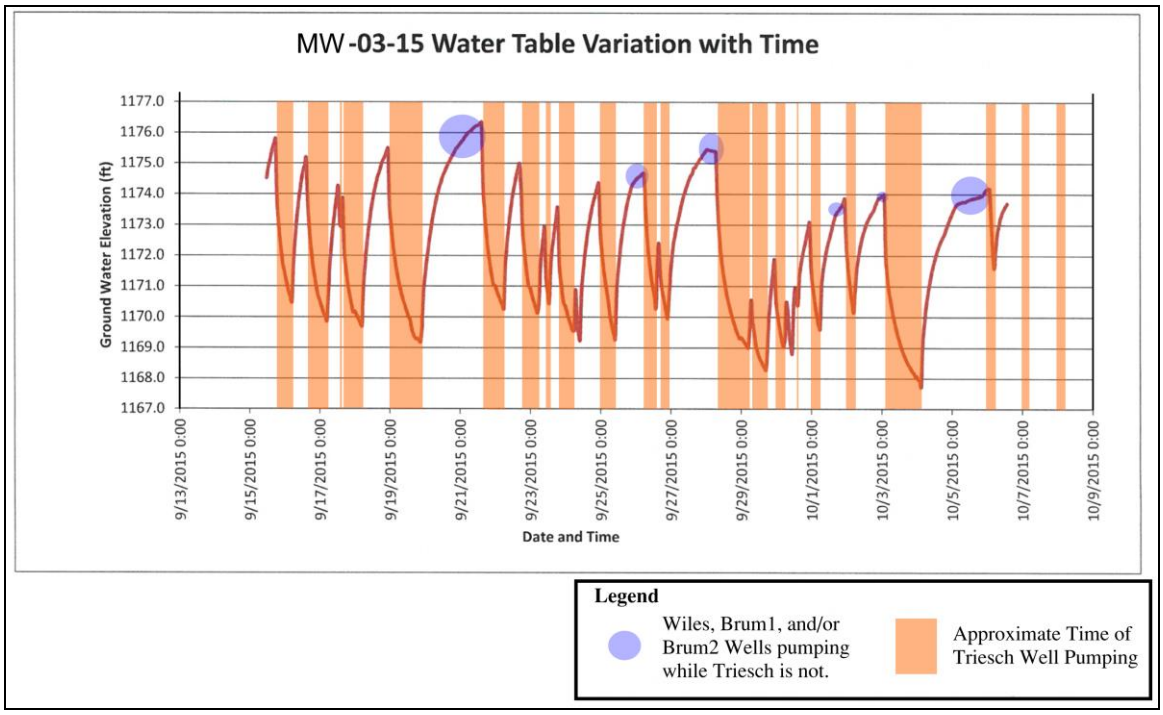

Fig. 7. Piezometric Levels in MW-03-15 with Groundwater Well Pumping

Instruments screened in the other foundation materials near station 23+50 generally exhibited a delayed response to Triesch Well pumping. However, MW-05-15 (screened in the Foundation Sands) near station 27+00 did not respond to the groundwater well pumping, or lags enough to appear unrelated.

Other than P-03-15, MW-03-15, and MW-05-15, the instruments indicated a correlation with headwater; as headwater generally increased, so did the instrument reading. Because of the influence of the Triesch Well pump on most instruments onsite, it was difficult to define the correlation to headwater. However, looking at the general shape of the headwater vs. time and the instrument reading vs. time plots, a general trend with headwater can be seen.

These trends are generally consistent with expectations:

- As the reservoir rises and falls, the groundwater pressures in the permeable foundation soils beneath the dam also fluctuate.

- Near the toe of the dam, the groundwater pressures are generally controlled by conditions downstream of the dam and are less affected by changes in pool.

- On top of these trends, pressures in the foundation are affected by short-term pumping of the aquifer. This influence decreases with distance from the wells, and in less permeable foundation deposits.

Analyses to Support Evaluation

Stantec conducted seepage, slope stability, and internal erosion analyses as part of the evaluation. We also developed potential failure modes due to seepage and internal erosion. The sections below focus on the influence of the piezometer readings on the seepage model, key findings from internal erosion analysis, and how those analyses influenced the assessment of potential failure modes.

Seepage

Seepage analyses were conducted using Seep/W by GeoStudio. Field data were used to validate the seepage models by adjusting material properties in an attempt to "match" selected instrument readings. The models included nodes at the horizontal and vertical locations of the piezometer screens along the cross section. The total head computed at these nodes was then a prediction of the piezometer readings for a given pool condition.

The comparison is illustrated graphically by plotting the predicted total head reading versus the field reading, for each piezometer at a selected pool elevation. A perfect match between the field data and model predictions would be indicated by points falling on the predicted=measured line. Seepage conditions within a dam are sensitive to variations within the embankment zones, relative values of hydraulic conductivity and anisotropy, three-dimensional seepage paths, and a myriad of other details that cannot be precisely known or modeled. An adequately "validated" seepage model is not expected to be a perfect match, and may predict piezometer levels that are several feet different than the field measurements.

Piezometer readings obtained by Stantec on April 18, 2018, were used for initial seepage model validation. The readings on this date were generally higher than what was recorded in the available 2015-2017 data. However, as described above, instruments screened in the Foundation Sands and Gravels are hydraulically connected to the Triesch Well, and readings fluctuate accordingly. Pumping of the well appears to keep water levels in the aquifer under the dam below the steady-state, maximum pressures, which was potentially the case for the April 2018 field readings.

During the detailed design phase of the project, Stantec installed electronic pressure transducers in the existing monitoring wells on March 24, 2020, to collect data while the groundwater wells were not operating. The groundwater wells were shut down from April 10 until mid-May, and water level readings were recorded on 15-minute intervals through May 11, 2020. After reviewing approximately one month of data after the groundwater wells were out of service, the piezometric levels generally stabilized at slightly higher elevations than observed when the wells were operated as normal. The stabilized levels indicated by the data were a maximum of 1.6 feet higher than the field readings obtained in April 2018 that were initially used to validate the seepage model. An example of the data collected at MW-03-15 is shown in Fig. 8.

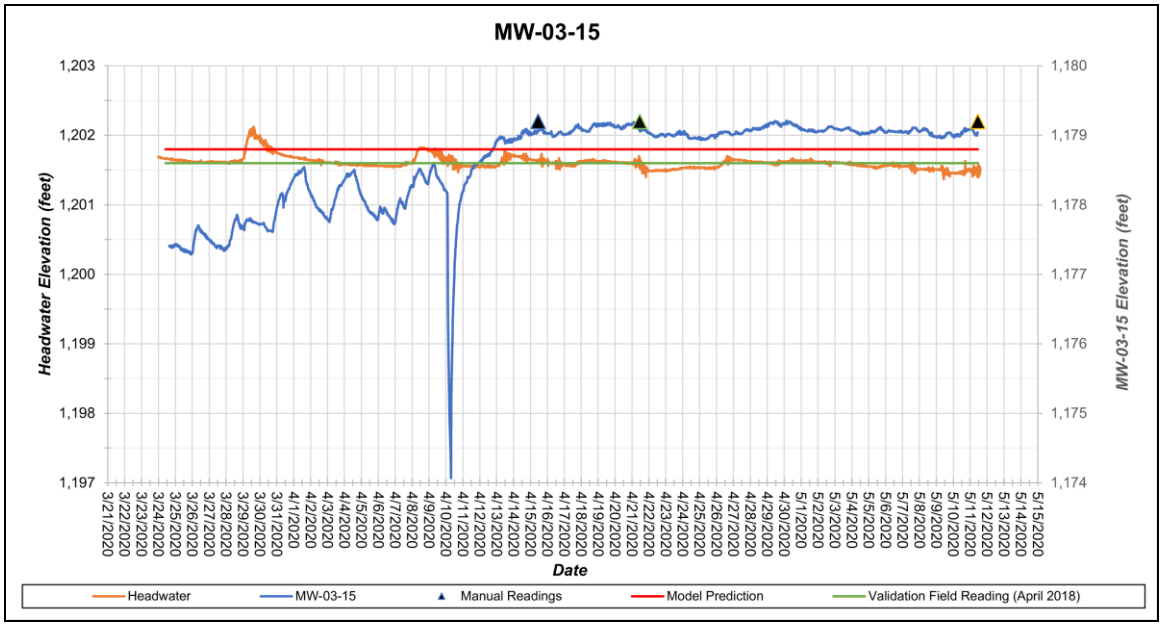

Fig. 8. Monitoring in MW-03-15 During Groundwater Well Shut Down

Fig. 9 is a plot comparing the model predictions to the stabilized field readings during the groundwater well outage. The stabilized readings were within an average of 2 feet of the total head predicted by the validated seepage models, and were judged to be an acceptable representation of the piezometric conditions at the project site.

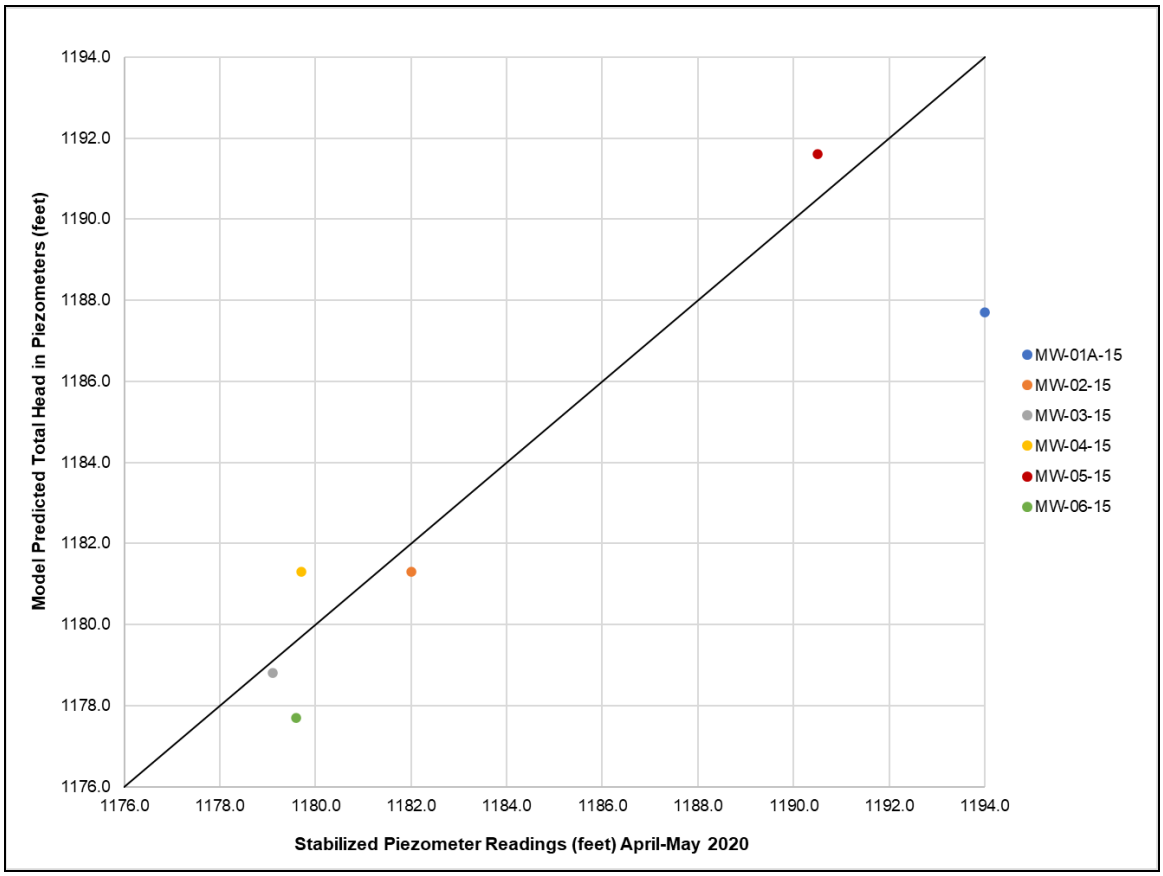

Fig. 9. Predicted Total Head Values Compared to Stabilized Piezometer Readings

Internal Erosion

To evaluate internal erosion susceptibility of the dam, Stantec reviewed site piezometers and data trends, internal seepage gradients, exit seepage gradients (factor of safety against piping), filter compatibility, and soil erodibility. Key conclusions from the internal erosion assessment are discussed below.

- Wet surface conditions and artesian piezometric pressures were observed at the toe of the dam in the study area.

- The gravel blanket drain does not appear to function as designed.

- Seepage through the Foundation Clays into the granular foundation soils is adequately filtered, such that significant erosion of the native clays into the sandy foundation layers is not expected.

- Pumping of the Triesch Well strongly influences the piezometric conditions in the study area.

- The high upward exit gradients below the ground surface near the toe could initiate potential failure modes, especially during periods with flood reservoir levels.

- The soil erodibility assessment indicated that soils within the study area are characterized with intermediate to least resistance to backward erosion piping, and moderately to highly erodible considering concentrated leak erosion. The susceptibility to erosion could allow the progression of potential failure modes after initiation.

Potential Failure Modes Due to Internal Erosion

Potential Failure Modes (PFMs) are mechanisms that could initiate, progress, and ultimately result in an uncontrolled release of the reservoir. Identified PFMs are hypothetical and do not necessarily represent known, active failure mechanisms at the dam site. However, development of PFMs does provide a basis for assessing the application of potential modifications to address risk-driving conditions at a dam. Only PFMs associated with seepage and internal soil erosion through the embankment, foundation, and left abutment were evaluated for this study.

The PFM evaluation here represented a scaled version of risk assessment to target specific observations, rather than a robust PFM Analysis workshop typically associated with dam risk analyses. The PFMs were assigned to one of the categories defined in Table 3. Fifteen PFMs were identified, defined, and evaluated. The identified PFMs were associated with seepage through the embankment and foundation, with the Triesch Well, and with the sluiceway conduit. Results of the seepage, slope stability, and internal erosion analyses were used to discuss factors that may make the PFMs more or less likely. Assignment of PFM categories also considered the desire for access to and maintenance of the historically wet areas near the toe.

Table 3. PFM Category Descriptions

Category	Description
1	Recommend Remediation
2	Warrants Continued Monitoring
3	No Evidence the PFM is Active
4	Insignificant Risk to the Dam

Three PFMs that were assigned to Category 1 were addressed by the design project that followed the seepage evaluation. Summaries of those PFMs are below.

1. PFM 1: Heave and/or sand boils at the toe initiate backward erosion piping of the Foundation Sands and/or Foundation Sands and Gravels.

   Wet areas have historically been observed at the toe of the dam, making it difficult to control brush and maintain the area. Although normal pool factors of safety against piping were found to be acceptable, flood pool factors of safety were below recommended criteria. If an elevated pool is retained for a significant period, or if the Triesch Well pump goes out of service, hydraulic pressures at the dam toe could increase and drop the piping factors of safety below criteria. Sand boils could then initiate backward erosion piping. Soils at the site were found to have susceptibility to internal erosion, allowing progression of the backward erosion piping, and could eventually lead to a failure. Because of the observed conditions, analysis results, and desired maintenance of the area, the PFM required remediation.

2. PFM 2: Backward erosion piping occurs through the left abutment soils or embankment/abutment contact.

   A wet area has been historically observed at the bottom of the left abutment groin, and the analyses showed that gradients are generally higher toward the left abutment. Conditions through the left abutment are like those through the foundation, and similar mechanisms could develop as those described in PFM 1. PFM 2 considers the potential for seepage flows at the dam toe or in the groin or

abutment above the toe. Because of the observed conditions, analysis results, and desired maintenance of the area, the PFM required remediation.

3. PFM 3: Lateral seepage through the embankment exits on the downstream face and causes sloughing.

   The seepage models predicted that flows would exit the sloping, downstream face of the dam. The exit point is near the toe for normal pool levels, and is higher on the embankment face during a steady-state flood pool. Lateral seepage flows like these can erode the surficial soils and cause progressive sloughing of the embankment face. These conditions can be monitored and repaired but, during a critical flood pool event, it may not be practical to repair sloughing failures. Hence, this PFM required remediation.

Design of Graded Filter Toe Berm

Remediation concepts for Clear Fork Reservoir Dam were focused on addressing on the three Category 1 PFMs described above, based on the dam's identified susceptibility to potential internal erosion due to piping and soil erodibility. The concepts also considered that the toe and left abutment areas were too wet to maintain effectively. Concepts consisted of a graded filter toe berm, a trench drain along the toe of the dam, and a line of relief wells along the toe of the dam. A graded filter berm was recommended to improve drainage of the wet areas, increase resistance to uplift, provide a filtered exit for seepage, and allow for maintenance access.

Filter Berm Extents

The width of the filter berm ranged up to approximately 270 feet, measured from the toe of the graded filter berm to the intersection with the dam. The graded filter toe berm followed a baseline alignment approximately 15 feet downstream from the existing toe of the dam, with the final grade on a varying slope along the baseline that mimicked the existing grade. The top surface of the filter berm was designed to slope at a two to three percent grade from upstream to downstream, until reaching the ditch near the downstream extent of the berm. The berm maintained a thicker profile for approximately 50 feet as measured between the existing toe of the dam and a 3H:1V slope down to a lower profile berm that extended over the historical stream channel location.

In some areas, the berm terminated at the top of a drainage ditch, designed to collect seepage and surface water from the berm and direct it toward the remaining wetland area. The ditch elevation varies, but it is generally designed as a trapezoidal shape, with 5H:1V side slopes and two-foot bottom width. Overall, the berm extends for approximately 572 feet along the existing toe of the dam.

Filter Berm Composition

The placement and gradation of the aggregate was designed as a reverse-graded filter in accordance with the empirical methodology in EM 1110-2-2300 (USACE 2004), to assist in seepage control and to resist uplift pressures at the toe. The filter berm was designed to generally consist of the following layers, from subgrade to finished grade:

- One to three feet of Fine Aggregate - ODOT Fine Aggregate for Mortar or Grout – Natural (ODOT 703.03)
- Structural Soil Fill - thickness varies.
- Six inches of topsoil to reach the design finish grade.

Layer thicknesses varied depending on the total planned thickness of the berm. The Fine Aggregate met filter compatibility criteria with the Embankment Fill and the Foundation Clays subgrade soils. The Fine Aggregate was required to be comprised of natural material and not consist of crushed limestone. Limestone materials have the potential to become cemented over time when exposed to wet conditions. Cementation of the sand layer would reduce the effectiveness of the filter berm. The Fine Aggregate layer also provided grading back toward the finer structural soil fill that comprised the top layer of the toe berm.

The Fine Aggregate was specified to be placed without using vibration to densify the materials, so that it would be placed in a state that allowed for water flow through the material for filtering purposes. The structural fill was specified to be comprised of fine-grained soil compacted to at least 95% of the maximum dry density, with a moisture content that ranges from 0 to +4 percentage points above optimum.

Upon completion of filter berm construction, the topsoil surface was to be vegetated to provide a surface suitable for dam safety maintenance and observations. A general cross section and plan view extents of the graded filter toe berm are shown in Fig. 10 and Fig. 11.

Toe Berm Drainage Pipes

A six-inch PVC pipe network embedded in the graded filter toe berm was designed to provide a means for observing and measuring seepage water flow from the area. The pipe network included four outlets into the designed ditch near the downstream extent of the graded filter toe berm that serve as points to monitor flows. The pipes were designed for placement in a shallow trench within the subgrade so that they would be within the lowest areas of the berm to collect seepage water. The shallow trench included layers of

Fine Aggregate and Coarse Aggregate (ODOT No. 7 Coarse Aggregate, ODOT 703.01) around the pipe to provide filtering of the native soil, and the pipe perforation size was designed to limit particle infiltration of the surrounding Coarse Aggregate. Cleanouts with sweeping elbows were included to allow for jetting, and the pipes were designed to allow for periodic camera inspections at the end of construction and at other times as needed.

Drainage Ditch

The drainage ditch at the toe of the graded filter berm was sized to convey the 10-year storm peak and checked against overtopping during the 50-year storm peak to direct flows to the existing ditch. Based on the analysis, a trapezoidal ditch with minimum depth of 1.5 feet was recommended, with sides slopes of 5H:1V and 2-foot bottom width. The ditch was proposed to be lined with open-cell, articulating concrete block along its length for erosion risk reduction and establishment of vegetation for additional stability.

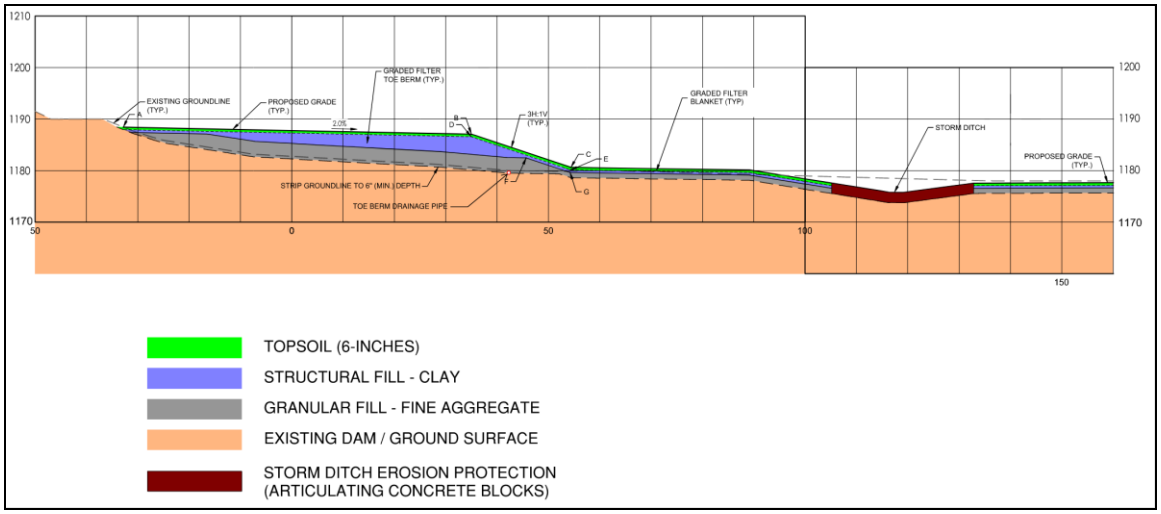

Fig. 10. Graded Filter Toe Berm – General Cross Section

Fig. 11. Graded Filter Toe Berm – Plan View Extents

Construction

General

The City of Mansfield selected Shook Construction as the general contractor to manage the construction of the dam modifications. The City and the general contractor selected Trucco Construction as the contractor to complete the project. Stantec was retained to provide engineering and oversight during construction, as well as to provide the as-built records to the City upon completion. ODNR Dam Safety was also a partner and was consistently involved with construction meetings, oversight, and coordination during construction.

Construction began with clearing, grubbing, and silt fence installation on July 24, 2023. Final punch list items were completed on October 18, 2023. The Triesch Well was operated continuously during construction to lower the groundwater table and aid in constructability.

The City, general contractor, contractor, and Stantec collaborated prior to and during construction on potential design changes that would bring value and improve function of the constructed toe berm. Two changes were made prior to construction to add value for the City.

1. The specified Fine Aggregate proved difficult to source in the required quantity, making it a large expense for the project. The contractor suggested alternate materials, but the gradation of the specified Fine Aggregate was required for filter compatibility with the existing subgrade soils. As a value to the project and through coordination with ODNR Dam Safety, the thickness of the Fine Aggregate within the graded filter toe berm was reduced from 3-feet maximum thickness to 2-feet maximum thickness. The minimum 1-foot thickness requirement remained.

2. Although a standard ODOT gradation, the specified Coarse Aggregate was also not readily available from local quarries. The contractor recommended that the coarse aggregate material be changed from ODOT No. 7 coarse aggregate to ODOT No. 8 coarse aggregate. Stantec reviewed the filter compatibility of the No. 8 aggregate with the Fine Aggregate and the toe berm drainage pipe perforations, and approved the change.

Construction Summary

Construction activities for the Clear Fork Reservoir Dam Modification consisted of seven major tasks:

1. Clearing and grubbing,
2. Subgrade preparation (with geogrid stabilization as needed),
3. Installation of toe berm drainage system,
4. Graded filter toe berm construction,
5. Articulating concrete block (ACB) storm ditch construction,
6. Surface protections for instrumentation and toe berm drainage pipe cleanouts, and
7. Final grading and seeding.

The contractor used earthwork equipment that was equipped with GPS capabilities and input the design CAD surfaces for use in placing the toe berm drainage pipes and filter berm materials to proposed grades.

The contractor began installation of toe berm drainage system, including 6-inch perforated schedule 80 PVC toe berm drainage pipe, 6-inch solid schedule 80 PVC toe berm cleanout pipes, and pipe fittings. The methods for installation of the toe berm drainage pipes were coordinated with ODNR Dam Safety for review and approval. The contractor dug the toe berm drainage pipe trenches using a custom excavator bucket to develop the sloped sides of the trench. Then, using a laser level and portable rover to monitor elevations, filter sand was placed on the bottom of the trenches. The contractor then used a custom trench box to maintain separation of the Fine and Coarse Aggregates around the installed toe berm drainage pipe segments. Solid toe berm cleanout pipes were used to construct the cleanout risers vertically from the toe berm drainage pipe alignments.

Undercutting and geogrid subgrade stabilization was needed in two locations. During installation of the toe berm drainage system, a proof roll was conducted on an observed wet area near the left abutment. Thirteen inches of rutting was observed after three passes of a dozer. In addition to the subgrade stabilization, a bleeder trench was excavated to tie the wet area into the toe berm drainage system to direct the seepage water away from the toe of the dam. The area was undercut by approximately 12 inches, then geogrid was placed over the affected area. The second location that needed the undercut and subgrade

stabilization was located toward the west end of the project area. This area showed 8- to 12-inches of deflection during a proof roll.

Following construction of the toe berm drainage system and subgrade stabilization, the contractor began the construction of the graded filter toe berm. The subgrade elevation was recorded, then Fine Aggregate was placed in 8- to 10-inch lifts.

Approved structural fill was imported and placed above the finished areas of Fine Aggregate. Structural fill was placed in 6” loose lifts and compacted with a sheepsfoot roller. A handheld GPS system was used to monitor the structural fill placement elevations across the project area.

Following completion of structural fill placement, topsoil stockpiled from the initial clearing of the site was placed to bring the toe berm to final design grades.

After substantial completion of the graded filter toe berm, the ACB storm ditch and anchor trenches were excavated. The ACB mats were lowered in place using a spreader beam attached to an excavator. These mats were tied back into the anchor trenches and the anchor trenches filled with concrete.

After completion of the ACB storm ditch, final spreading and grading of topsoil was completed. Surface protections for the toe berm drainage pipe cleanouts and piezometer extensions were installed. A final video inspection of the toe berm drainage pipe system was completed to verify it was free of debris, and a final punch list site walkdown was conducted. A list of minor repair or completion items was developed and addressed. The site was then seeded and mulched to promote growth of new grass across the project area.

An overview of the final constructed condition is shown in Fig. 12.

Fig. 12. Completed Construction of the Graded Filter Toe Berm

Conclusions

The City of Mansfield worked with Stantec to address dam safety seepage concerns at the toe of Clear Fork Reservoir Dam. A targeted approach to risk informed decision making was used by reviewing historical records, conducting site visits, and performing detailed seepage, stability, and internal erosion analyses. Although it was known that a project to address the wet areas at the toe was needed, it was important to complete the background analyses so that PFMs contributing to the conditions could be considered. Focusing the assessment on PFMs related to seepage avoided the cost of conducting a full PFM Analysis workshop and subsequent steps of full risk assessments. This process allowed the City to choose a design project that addressed the risk-driving PFMs at the project site. Through that targeted risk assessment, we were able to identify the contribution of the Triesch Well to the hydraulic pressure conditions in the project area, and perform the necessary studies to design a toe berm sized to maintain safe conditions if the well were to go out of service. It also allowed for an understanding of how continuous use of the well during construction could help the contractor perform their work effectively. The completed graded filter toe berm was able to address the key PFMs by providing a filtered exit for seepage at the toe of the dam and near the left abutment, increasing factors of safety against piping in the historically wet area, and filter potential seepage exits on the lower portions of the downstream face of the embankment. The City is now able to access the toe area of the dam for maintenance, and can monitor seepage flows from the toe berm drainage pipe network. The project addressed the seepage conditions that had been observed for over 40 years.

References

Benedict, Bowman, Craig, and Moos (1979). "Phase I Inspection Report." National Program of Inspection of Non-Federal Dams. Clear Fork Reservoir Dam. August.

City of Mansfield (2010). "Operation, Maintenance and Inspection Manual, Clear Fork Reservoir Dam." March.

The Jennings-Lawrence Co. (1946a). "Specifications Contract and Contract Bond for Clear Fork Dam. Mansfield Water Works." Contractor: Roger J. Au.

The Jennings-Lawrence Co. (1946b). "Plans and Details of Clear Fork Dam. Mansfield Water Works." Revised November 1949.

Ohio Department of Natural Resources (2000). "Dam Safety Inspection Report." Clear Fork Reservoir Dam. Inspection Date: February 15.

Ohio Department of Natural Resources (2005). "Dam Safety Inspection Report." Clear Fork Reservoir Dam. Inspection Date: June 17.

Ohio Department of Natural Resources (2010). "Dam Safety Inspection Report." Clear Fork Reservoir Dam. Inspection Date: September 30.

Ohio Department of Natural Resources (2015). "Dam Safety Inspection Report." Clear Fork Reservoir Dam. Inspection Date: November 12.

Ohio Department of Transportation (ODOT). (2019). "Construction and Material Specifications." January 1.

Ohio Environmental Protection Agency (OEPA) (2013). "Drinking Water Source Assessment for the City of Mansfield's Wellfields, Public Water System ID #OH7002914." Prepared by Division of Surface Water, Division of Drinking and Ground Waters, Northwest Division. February.

U.S. Bureau of Reclamation and U.S. Army Corps of Engineers (2015). "Best Practices in Dam and Levee Safety Risk Analysis, Chapter IV-4. Internal Erosion Risks for Embankments and Foundations." Version 4, July.

Bifurcation and Repurposing of a Lime Sludge Lagoon

Daniel Woeste, P.E., M. ASCE[1] and David Mueller, P.E., M. ASCE[2]

Abstract: Geosyntec Consultants, Inc. (Geosyntec), as a subcontractor to Fluor-BWXT Portsmouth LLC (FBP), is providing engineering services for the design, permitting, and construction of an on-site waste disposal facility (OSWDF) and associated waste disposition support facilities for the decontamination and decommissioning (D&D) of the United States Department of Energy's (DOE's) Portsmouth Gaseous Diffusion Plant in Pike County, Ohio. Richard Goettle Inc. (Goettle) was contracted by FBP to construct a 400-foot-long anchored wall designed by Geosyntec for construction of a sedimentation and detention pond. The pond (Pond 1) was proposed to manage stormwater runoff from the nonimpacted areas of the OSWDF. However, the location originally planned for Pond 1 had to be abandoned because of geological site constraints and concerns about its proximity to a pervious sandstone layer encountered at grade. The north branch of an existing lime sludge lagoon was selected as the location for the replacement sedimentation and detention pond (Pond 1B). Construction of Pond 1B at this location required structural and hydraulic bifurcation of the north branch of the lime sludge lagoon. Geosyntec's design of Pond 1B included excavation, management, and removal of lime, filter berm and earthen baffle construction, outfall structures, and a permanent, anchored combined soldier pile and sheet pile lagging wall to achieve the structural and hydraulic bifurcation. Goettle developed shop drawings and constructed the anchored wall. Changes to the proposed earthwork by the general contractor prior to and during construction required close coordination between Geosyntec and Goettle to redesign and revise construction plans accordingly. Namely, the elimination of an earthen causeway along the wall alignment required a shift to barge-based construction, and the removal of a support buttress behind the wall required a unique tieback anchor installation and testing approach. This paper summarizes Geosyntec and Goettle's involvement in this project and highlights the importance of strong communication between designers and contractors to collaboratively solve challenges that arise during construction.

Introduction

The Portsmouth Gaseous Diffusion Plant in Pike County, Ohio, which operated from 1954 to 2001, was one of the three large gaseous diffusion plants in the United States that were constructed to produce enriched uranium to support the country's nuclear weapons program (**Figure 1**). Following the Cold War, the facility shifted to producing enriched uranium used by commercial nuclear reactors. Enrichment operations were ceased at the site in 2001. Environmental cleanup of the site began in 1989 under the Department of Energy's (DOE's) Office of Environmental Management. Decontamination and decommissioning (D&D) activities at the site began in 2011 and are ongoing in cooperation

[1] Senior Engineer, Geosyntec Consultants Inc., Cincinnati, Ohio. Email: dwoeste@geosyntec.com.
[2] Project Manager, Richard Goettle Inc., Cincinnati, Ohio. Email: dmueller@goettle.com.

with the United States Environmental Protection Agency and the Ohio Environmental Protection Agency.

Geosyntec Consultants, Inc. (Geosyntec), as a subcontractor to Fluor-BWXT Portsmouth LLC (FBP), is providing engineering services for the design, permitting, and construction of an on-site waste disposal facility (OSWDF) and associated waste disposition support facilities, including a sedimentation and detention pond. Richard Goettle Inc. (Goettle) was contracted by FBP to construct an anchored wall that was designed by Geosyntec as part of a proposed sedimentation and detention pond.

Background

The OSWDF is situated on the northern end of the federally owned site and is designed to contain low-level radioactive and hazardous impacted material resulting from the D&D activities. When completed, the OSWDF will have 12 cells and approximately 5.7 million cubic yards of capacity. To help manage stormwater runoff from the nonimpacted areas around the OSWDF, a sedimentation and detention pond (Pond 1) was originally planned to be located adjacent to the OSWDF. However, further site investigation revealed the presence of a pervious sandstone layer at grade in the originally planned location for Pond 1.

Fig. 1. Aerial View of the Portsmouth Gaseous Diffusion Plant Site.

This sandstone layer, termed the “680 sandstone” for the elevation at which it is located, presented a potential subsurface pathway for off-site transportation of water within Pond 1. To eliminate this potential, the Pond 1 location was abandoned, and the north branch of a nearby existing lime sludge lagoon was selected for the new sedimentation and detention pond (Pond 1B) below the 680 sandstone. Construction of Pond 1B at this location required the installation of a 400-foot-long wall to provide structural and hydraulic bifurcation of the north branch of the lime sludge lagoon (one of several on-site used to settle lime sludge from a water-softening process over the decades of site operations).

Geosyntec evaluated a range of options to achieve this goal, including a cofferdam, stacked geotextile tubes, an earthen dam, and a structural cutoff wall. Ultimately, FBP decided to move forward with a permanent, combined soldier pile and sheet pile lagging wall (i.e., king pile wall) to provide the required separation between the proposed Pond 1B and the existing lime sludge lagoon.

Subsurface Conditions

The subsurface material at the site generally consists of 30 to 40 feet of unconsolidated Quaternary clastic sediments (such as sand, silt, and clay) overlying Paleozoic bedrock. In stratigraphic order, bedrock is overlain by fluvial Gallia sand and gravel and by the lacustrine Minford clay and silt of the Teays Formation (**Figure 2**). The erosion and subsequent fill of the Portsmouth River Valley during the Pleistocene epoch played a primary role in controlling the shallow geologic units beneath the site. A portion of the ancestral Portsmouth River Valley underlies the plant (Fluor-BWXT Portsmouth LLC 2014).

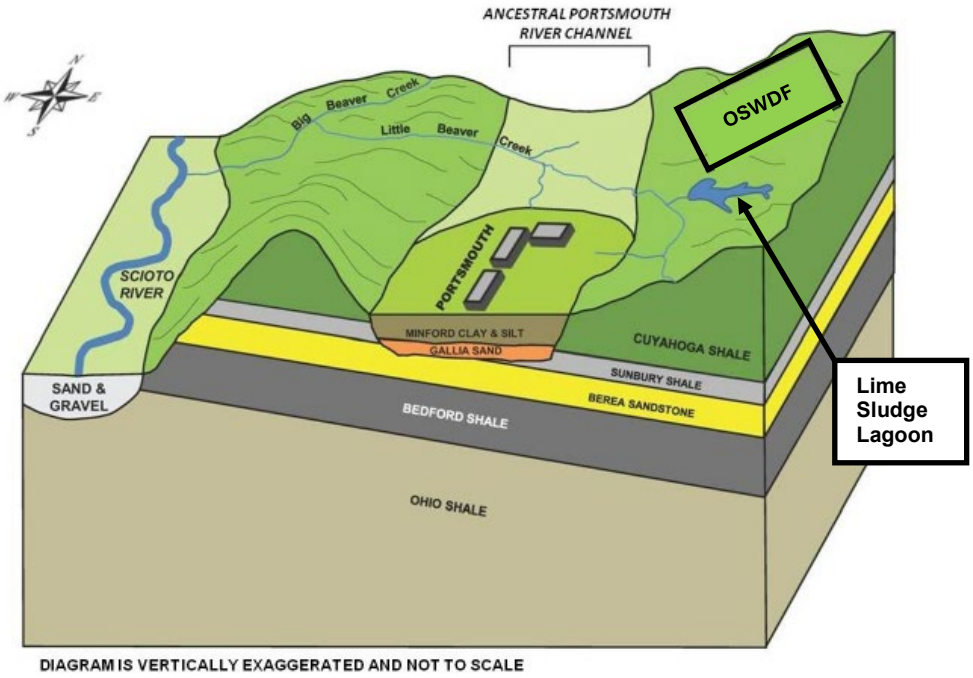

Fig. 2. Generalized Site Geology.

Extensive subsurface investigations were previously conducted across most of the site as part of the remedial investigation and feasibility studies. However, few data were available within and around the lime sludge lagoon. Geosyntec planned and conducted a subsurface investigation to identify the depth of lime sludge along the proposed wall alignment and confirm the underlying subsurface stratigraphy. An amphibious drill rig was used to advance six standard penetration test boreholes along the proposed wall alignment and collect samples for laboratory testing. The generalized subsurface stratigraphy along the wall alignment included a very soft lime sludge, overlying medium-to-hard lean clay, overlying weathered Cuyahoga Shale, overlying Sunbury Shale. The boreholes were intentionally terminated before encountering the Berea Sandstone, a confined aquifer with artesian pressure that underlies the Sunbury Shale and is the uppermost regional aquifer system.

Design Analysis

The DOE design criteria required that the OSWDF remain effective for 1,000 years, to the extent reasonably achievable, and in any case for at least 200 years. Given Pond 1B's role as a support facility for the OSWDF, a minimum design life of 100 years was originally selected for the pond design. However, following design completion and prior to the start of construction, the design life was reduced to 30 years based on new information about the long-term plan for the lime sludge lagoon behind the wall.

The wall was designed with consideration for temporary, long-term, and seismic loading conditions. The temporary construction loading condition controlled the design and included a 20-foot exposed height with a 15-foot hydrostatic water differential. The design also included placing a structural fill buttress on top of the lime behind the wall to prevent excessive backward deflection of the wall during tieback anchor testing. The bottom of the soldier piles and tieback anchors were required to maintain at least 5 feet of vertical clearance from the Berea Sandstone to minimize the potential for creating a hydraulic connection with the formation. This constraint pushed the limits of what was possible at this site for the expected loading conditions.

For wall stability, tieback anchors spaced at 11.4 feet on center with a design load of 130 kips per anchor were required. The permanent anchors were specified with Class I corrosion protection and included permanent steel casing to bedrock. The permanent steel casing was selected to provide protection of the anchor length extending through the open water column behind the wall. Tieback anchor bond lengths in the Sunbury Shale were designed using an ultimate transfer load of 50 pounds per square inch and a factor of safety of 2.0, and the design assumed that the top of the anchor bond zone started at least 5 feet into the shale.

A reinforced concrete capping beam was designed to be installed at the top of the wall to provide (i) long-term protection of the tieback anchor heads, tie points, and soldier pile and sheet pile tops and (ii) redundancy in the load transfer mechanism from sheet pile infill members to the soldier piles. However, after the wall's design life was reduced and Goettle provided constructability input, the concrete capping beam was replaced with a steel beam that would achieve acceptable goals and could be more easily installed over the water.

Corrosion protection was incorporated into the design using sacrificial steel. The amount of sacrificial steel was calculated by accounting for differences in corrosion potential associated with different zones (e.g., atmospheric, splash, tidal, submerged). A worst-case corrosion rate of 0.11 millimeters per year was selected based on a total corrosion loss of 4.3 mm over the originally planned 100-year design life (European Committee for Standardization 1997). The decision to reduce the design life was made after soldier piles had been procured, so changes to the corrosion rate could not be incorporated into the design.

Construction

FBP issued a request for bids for this project in June 2021. The design drawings at the time of the bid showed the wall installed through an earthen causeway that would be constructed by others before Goettle's mobilization. The planned wall was designed as a conventional king pile wall consisting of W27×194 soldier piles with two pairs of NZ-14 sheet piles between adjacent soldier piles. Sheet pile interlocks filled with joint sealant would be welded to the soldier pile flanges to create the watertight wall that FBP was seeking. Anchors would be installed though prefabricated sleeves in the soldier piles. Finally, a concrete cap would be installed over the full wall length.

Change Happens

At the preconstruction meeting between FBP, Geosyntec, and Goettle in mid-August 2021, FBP notified the parties that the earthen causeway was no longer going to be installed and the wall would need to be installed utilizing barges. This change made it difficult to achieve the construction tolerances required for a conventional king pile wall. Geosyntec and Goettle therefore worked together to develop a new approach that would meet the design intent while keeping the wall economical and constructable.

The revised design utilized the same soldier pile and sheet pile components. However, instead of installing the sheet piles between the soldier piles, the sheet piles would be threaded to each other and installed immediately behind the soldier piles, with the face of the sheets directly abutting the flange of the soldier piles (**Figure 3**). Additionally, instead of installing a concrete capping beam to tie the system together, the decision was made based on constructability considerations to use a steel cap beam. The reduced design life assured that the team that they could eliminate the extra anchor head protection afforded by the concrete capping beam and instead go with the more easily constructable steel beam.

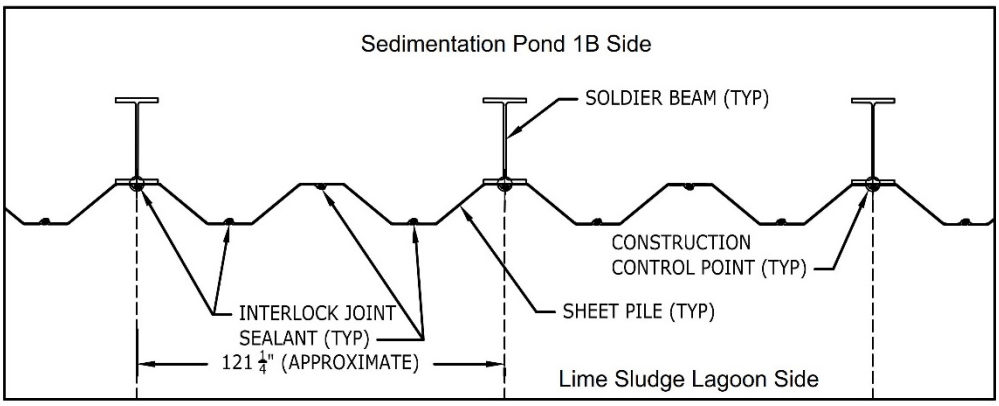

Fig. 3. Revised Wall Configuration for Barge-Based Construction.

Construction Begins

Goettle's mobilization began in early September 2021. Goettle designed and installed a temporary dock that was sized to allow equipment to drive off the dock and directly onto

the barges. Soldier pile installation began in mid-September. Temporary casing was vibrated through the overburden materials and seated into the Sunbury Shale before the soldier piles were drilled. The casing was held in place using a project-specific template designed and constructed by Goettle. Goettle elected to use an excavator-mounted CZM brand drill that allowed for ample reach and had enough torque to drill the required rock sockets. After the shaft was drilled, the soldier pile was set into the shaft and clamped to the template. A crane and concrete bucket were used to tremie-pour concrete into the shaft, and then the casing was removed.

After soldier piles were installed, Goettle installed the steel cap beam, which provided a secondary benefit as a sheet pile driving template. Next, the sheet piles with shop-applied interlock sealant were installed with a vibratory hammer. After the sheet piles were installed to the required elevation or until they encountered refusal, they were welded to the cap beam.

During installation of the sheet piles, the general contractor and FBP initiated discussions with Geosyntec about eliminating the structural fill buttress originally proposed to be installed behind the wall. Constructing the buttress with the barge-based approach would be challenging, so Geosyntec was asked to further evaluate whether the wall could withstand the loads during tieback anchor testing without the buttress. A three-dimensional Plaxis model was developed to evaluate the geotechnical and structural response of the wall (**Figure 4**). The analysis considered various tieback anchor loading scenarios,

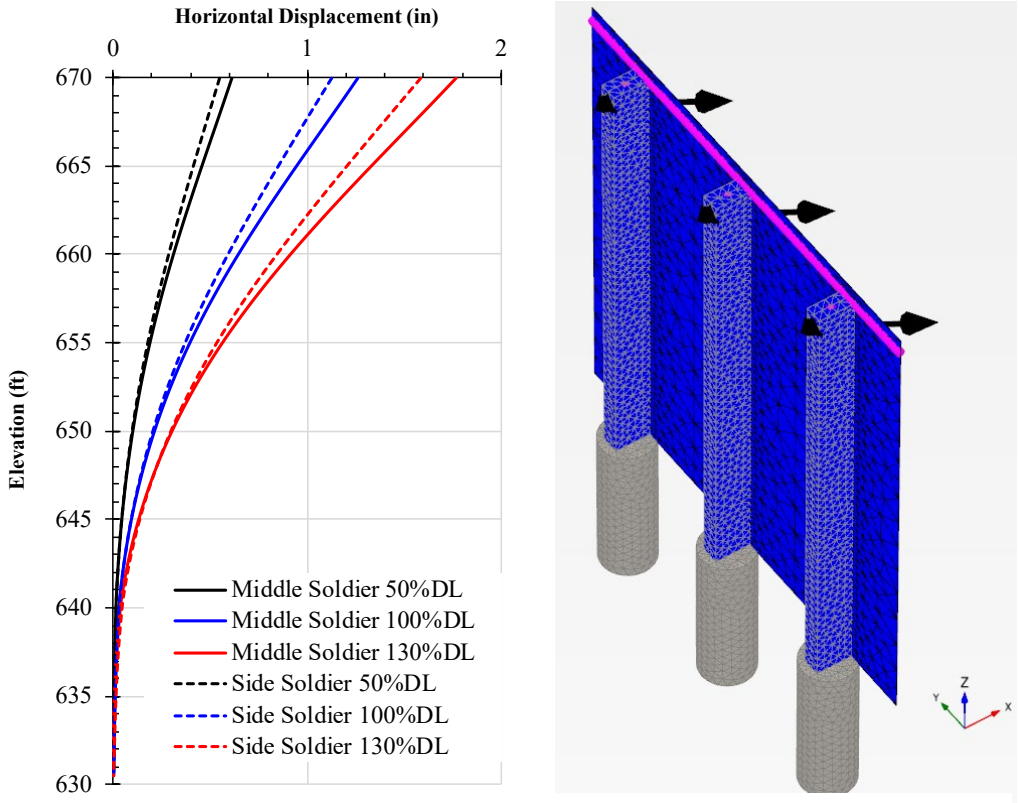

Fig. 4. Plaxis Analysis of Tieback Anchor Testing Sequence.

including one in which the adjacent tieback anchors are locked off and the middle anchor is stressed to the maximum test load. The analysis results verified that the wall had sufficient structural capacity to withstand the loading and that approximately 2 inches of backward deflection could occur during tieback anchor testing. Given the amount of backward deflection, and to avoid having the bearing plate contact the top of the permanent casing which would result in a bootstrap effect during testing, it was recommended that a 2.5-inch-thick shim pipe be welded between the anchor sleeve and back of the bearing plate to provide space for the expected movement.

The tieback anchors were installed by advancing permanent casing through the overburden materials and seating it into the Sunbury Shale (**Figure 5a**). After each anchor was drilled to the required length, the tendon was installed and tremie-grouted. Three of the 29 tieback anchors were performance-tested and the remaining anchors were proof-tested in accordance with the Post-Tensioning Institute *Recommendations for Prestressed Rock and Soil Anchors* (Post-Tensioning Institute 2014). The lime sludge in front of the wall was not competent enough to support a conventional independent reference rail for the dial indicator (typically a tripod). Instead, the dial indicator was mounted to the stressing ram, and a site level with a 0.03125-inch graduated ruler was used to measure the amount of backward wall deflection, which generally ranged between 1 and 1.5 inches. The backward deflection was resolved along the anchor angle and subtracted from the gross elongation measured by the dial indicator to get the net anchor elongation. All 29 anchors passed the testing criteria.

(a) (b)

Fig. 5. (a) Tieback Anchor Installation and (b) Excavation and Buttress Construction.

Excavation and Wall Leakage

Following anchor testing and acceptance, the general contractor began removing ponded water and excavating lime sludge in front of the wall (**Figure 5b**). The work was performed with long-reach excavators and involved mixing the soft lime sludge with the underlying native soils to make it easier to manage. As excavation progressed, multiple points of water leakage were identified through the sheet pile interlocks and through the tieback anchor penetrations.

As previously noted, the sheet piles were delivered to the site with pre-applied sealant in the interlocks. The selected sealant uses a natural resin as its base and is marketed to have several advantages over hydrophilic swelling sealants, such as its ability to remain flexible and adapt to wall movement, its ability to reduce interlock friction during driving, its immediate usability (does not require "activation"), and its environmental friendliness. The exact cause of the wall leakage could not be determined, but it is suspected that unexpected difficult driving conditions at some locations led to the interlocks heating due to friction during driving. This heat might have caused the sealant to liquify and migrate out of the interlocks, leaving sections of the sheet piles without the proper amount of sealant.

Multiple methods were used to attempt to mitigate the water leakage at the interlocks, including welding, plugging with crushed cinders, and using bentonite. Welding was used to seal the interlocks where the leakage rate was relatively slow. At other locations where leakage was too significant to weld directly, steel channels were welded around the face of the interlocks, packed with bentonite, and capped shut (**Figure 6a**). On the back of the wall, the tieback anchor penetrations were sealed with a caulk-like product (**Figure 6b**) and then topped with a rubber pipe boot (**Figure 6c**).

(a) (b) (c)

Fig. 6. (a) Steel Channel with Bentonite to Plug Leakage Through Sheet Pile Interlock, (b) Sealant Around Tieback Casing, (c) and Rubber Boot Around Tieback Casing.

Lessons Learned

The completed wall and sedimentation and detention Pond 1B (**Figure 7**) was put into operation in June 2022. The following are some of the lessons learned and takeaways from this project:

- It is the designer's responsibility throughout the design process to communicate how site constraints (perceived and real) and changes to loading conditions will impact the design and construction.
- Unique site constraints might require that more advanced tools (e.g., finite element modeling) be used for the design.
- Water-based construction operations require careful construction sequencing and thoughtful site setup and staging.
- The degree of sheet pile watertightness can depend (in part) on the type of interlock joint sealant and the driving conditions encountered during installation. Difficult driving conditions might reduce the effectiveness of some interlock joint sealants and can cause damage to the interlocks that further results in water leakage.
- A modified king pile wall, wherein sheet piles are installed immediately behind the primary load-bearing elements (e.g., soldier piles), can meet the design intent as long as sheet piles are installed to be in intimate contact with the primary load-bearing element for their full depth.
- Depending on the installation method and level of support behind the anchors, unique installation and testing methods might be required to prevent a bootstrap effect for tieback anchors with permanent casing.
- Open lines of communication between the owner, designer, and contractor are key to collaboratively solving challenges that arise during construction, and they result in more efficient and effective solutions.

Fig. 7. Completed Sedimentation and Detention Pond 1B.

Acknowledgements

The authors would like to acknowledge their client, Fluor-BWXT Portsmouth LLC, for the opportunity to work on this project and for their contributions to the design and efforts throughout construction.

References

European Committee for Standardization. (1997). "Part 5: Piling." In *Eurocode 3: Design of steel structures* (pp. 150–154). European Prestandard ENV 1993-5.

Fluor-BWXT Portsmouth LLC. (2014). *Remedial Investigation and Feasibility Study Report For The Site-Wide Waste Disposition Evaluation Project At The Portsmouth Gaseous Diffusion Plant, Piketon, Ohio*. United States Department of Energy. DOE/PPPO/03-0246&D3.

Post-Tensioning Institute. (2014). *Recommendations for Prestressed Rock and Soil Anchors*. PTI DC35.1-14.

Near-Surface Geophysical Methods for Subsurface Characterization Across River Channels

Presented By:

John M. Schneider, PG

Senior Geophysicist/Service Line Leader (S&ME Cincinnati, OH)

Amber K. Lacy

Associate Geophysicist III (S&ME Cincinnati, OH)

Co-Authored By:

Adam Gostic, PG

Geophysicist I (S&ME Cincinnati, OH)

54th Annual Ohio River Valley Soils Seminar

Cincinnati, Ohio

November 13, 2024

Outline

- INTRODUCTION – *Surveying River Crossings with Geophysics*
- GEOPHYSICS – *Brief Overview*
- CASE STUDIES – *Survey Study & Geophysical Method(s):*

1. **U.S. 231 Over Doe Creek: Indiana**
   - Karst Analysis
   - Electrical Resistivity Tomography (ERT)
2. **Line 223, Twelve-Mile Creek: North Carolina**
   - Horizontal Directional Drilling (HDD) Study
   - Electrical Resistivity Tomography (ERT)
   - 2D Multi-Channel Analysis of Surface Wave (2D MASW)
3. **Line 467, Crooked Creek and Rocky River: North Carolina**
   - Horizontal Directional Drilling (HDD) Study
   - Electrical Resistivity Tomography (ERT)
   - 2D Multi-Channel Analysis of Surface Wave (2D MASW)
4. **C367 Pipeline, East Fork Little Miami River: Ohio**
   - Horizontal Directional Drilling (HDD) Study
   - Electrical Resistivity Tomography (ERT)
   - Frequency Domain Electromagnetic (FDEM)
   - 1D Multi-Channel Analysis of Surface Wave/Microtremor Array Method (1D MASW/MAM)
5. **Creston Bridge, Little Kanawha River: West Virginia**
   - Bridge Replacement Study
   - Electrical Resistivity Tomography (ERT)

Surveying River Crossings with Geophysics

In the geotechnical community, river crossings are somewhat inevitable and generally have terrain and environmental challenges, to name a few. A drilling barge is usually used to collect geotechnical information within larger river systems. However, hundreds of thousands of narrow and shallow tributaries within the Ohio River basin cannot be reached with a drilling barge or conventional drilling units. It's within these scenarios that various geophysical methods have the propensity to assist the geotechnical program.

Conditions that May Hinder Drilling within or near a River System:

1. Environmental regulations (i.e., protected wildlife, water contamination, etc.).
2. Steeply-sided riverbanks.
3. River channel size.
4. Expense (both time and fees) using a barge system or platform drill rig.

Surveying River Crossings with Geophysics

S&ME employees are conducting amphibious drilling operations on two different scales: a smaller barge platform on the left and, to the right, a river barge setup.

Surveying River Crossings with Geophysics

Ohio River Basin Watershed

Most geophysical methods can generally be conducted in streams with a flow/discharge rate of less than 200.00 CFS.

Geophysics Basics

Geophysical methods measure contrasting physical properties of materials to assist in the characterization of the subsurface.

ASTM D6429-99 (2011) "Standard Guide for Selecting Surface Geophysical Methods"

Geophysical Method	Measured Physical Properties
Seismic Refraction and Reflection	Elastic Material Properties and Density (Wave Velocity)
Surface Wave Seismic	Elastic Material Properties and Density (Wave Velocity)
Electromagnetics (EM)	Electrical Conductivity
Magnetics	Magnetic Susceptibility
Ground Penetrating Radar (GPR)	Dielectric Permittivity (Electromagnetic Properties)
Spontaneous Potential (SP)	Natural Ground Potentials
Electrical Resistivity Tomography (ERT)	Resistivity (Inverse of Conductivity)
Induced Polarization (IP)	Chargeability
Microgravity	Density
Wireline	Various Geophysical and Optical Properties

**Bold geophysical methods are presented in this presentation*

Geophysics Basics: Surface Wave

Near-surface seismic wave brief analysis: A hammer strikes a rock, and the rock is now stressed (force/area), which is followed by a strain (change in shape), and the rock returns to its original state (shape). This can be summed up with a single term, elasticity.

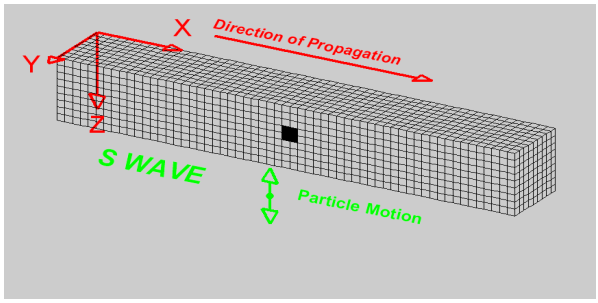

Shear Waves (V_s, Secondary, or S-wave)

- Shear Wave = Body Wave
- Particle motion is perpendicular to the propagation direction
- The velocity of an S-wave is slower than compression waves, or primary waves (P-wave)
- S-waves cannot propagate through liquids of very low viscosity!

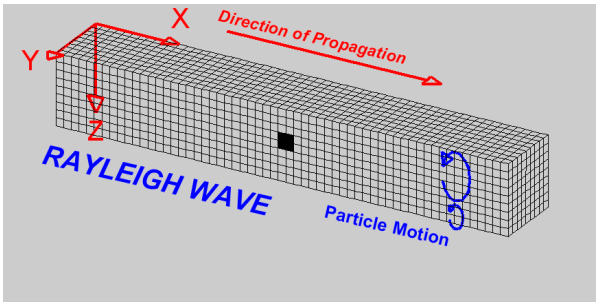

Rayleigh Waves

- Rayleigh Wave = Surface Wave
- The velocity is about 10% slower than that of a Shear Wave velocity through the same material
- Exhibit dispersion, meaning, that velocity is not constant but varies with wavelength.

In both examples, velocity depends on the traveled material's elastic properties.

Animation by Larry Braile (https://web.ics.purdue.edu/~braile/edumod/waves/Swave.htm)

Geophysics Basics: Surface Wave to Model

Multi-Channel Analysis of Surface Waves (MASW) consists of recording different frequency surface waves generated from an active energy source traveling across a linear array.

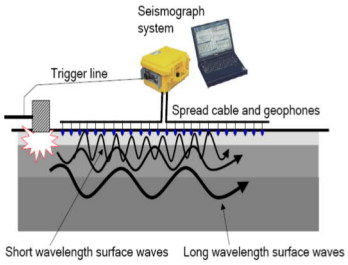

Shot Gather

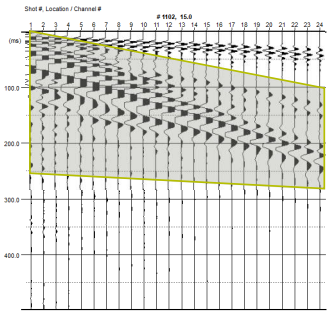

Dispersion Spectra

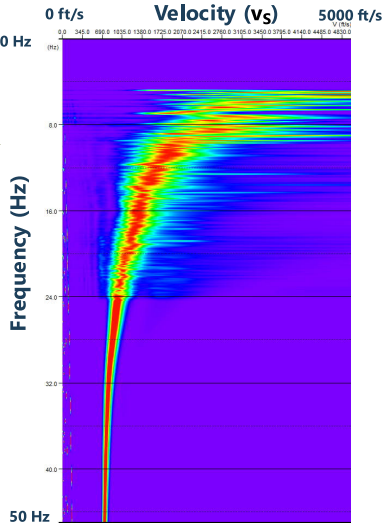

Example Applications

- Estimate depth to top of bedrock
- Identify low-velocity zones (landslides, slumps, etc.)
- Karst exploration
- Landfill delineation

Reference: Gostic, Adam, Saving Money with Surface Wave Testing, 2024 S&ME Technical Conference

Geophysics Basics: Surface Wave to Model

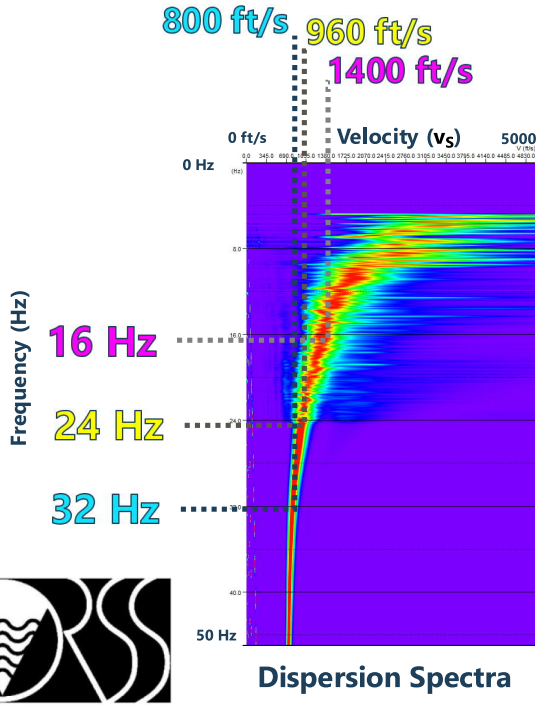

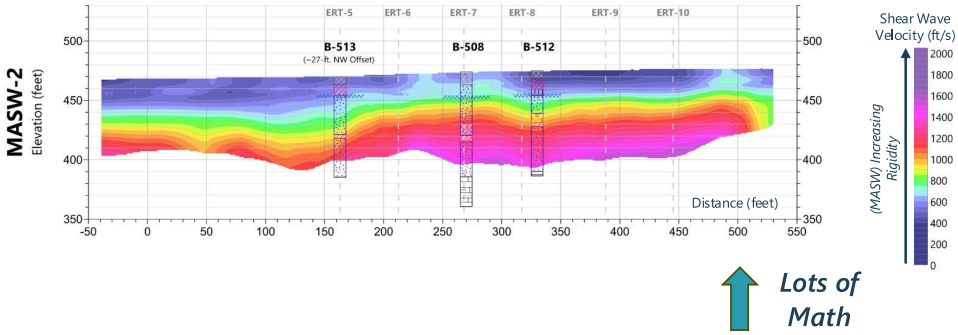

Lots of Math

Velocity	Frequency		Wavelength		Depth
800 ft/s	32.0 Hz		25.0 ft		12.0 ft
960 ft/s	24.0 Hz	$V = f\lambda$	40.0 ft	$Depth = 1/2\lambda$	20.0 ft
1400 ft/s	16.0 Hz		87.5 ft		88.0 ft

Reference: Gostic, Adam, Saving Money with Surface Wave Testing, 2024 S&ME Technical Conference

Geophysics Basics: Electromagnetic

Frequency Domain Electromagnetics (FDEM) is used to measure the electrical conductivity of subsurface soil, rock, and ground water.

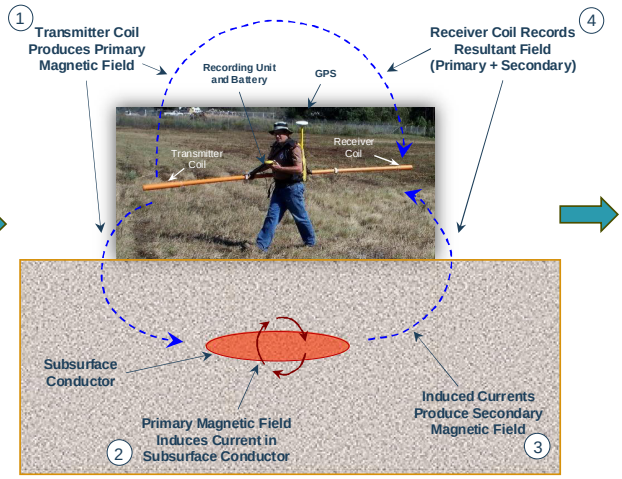

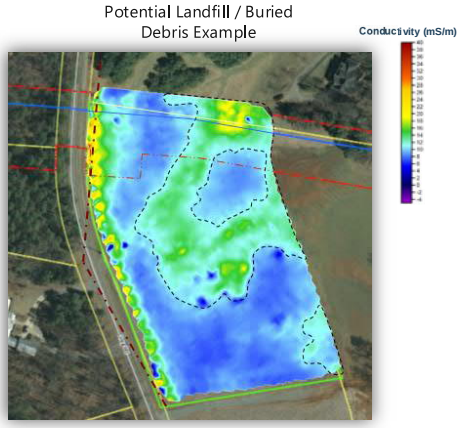

Example Applications

- Delineate buried debris and landfill material
- Locate buried metallic objects (e.g., underground storage tanks, utilities, etc.)
- Map anomalous subsurface zones (e.g., stump pits, contamination plumes, etc.)
- Identify lateral soil/bedrock conductivity changes (e.g., sand/clay lenses, agriculture, etc.)
- Archaeology (e.g., unmarked graves)

Geophysics Basics: ERT

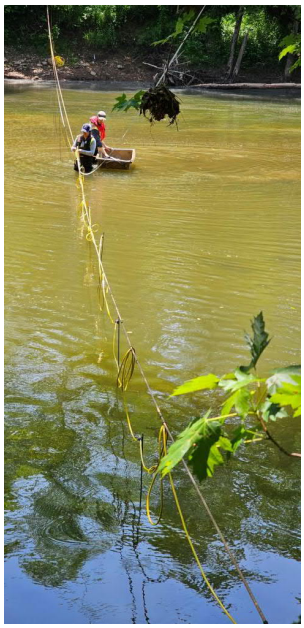

Electrical Resistivity Tomography is a measure of how strongly a material opposes the flow of an electrical current (DC).

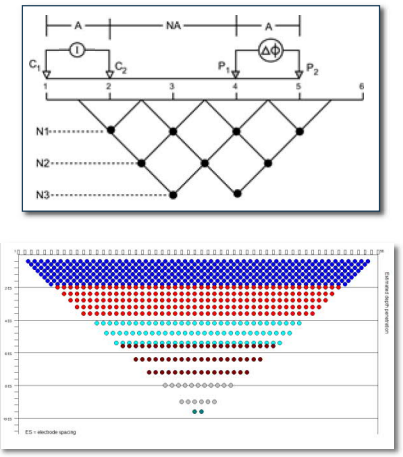

Example Applications

- Depth and topography of bedrock
- Delineating karst features (e.g., cavities, slots, solution features, etc.)
- Locating clay layers and/or sand and gravel deposits
- Mapping zones that have potential for concentrated groundwater flow (e.g., seepage paths in dams and levees, etc.)

Geophysics Basics: ERT

Apparent resistivity values for each point are plotted, inverted through modeling and contoured to create a 2D pseudosection

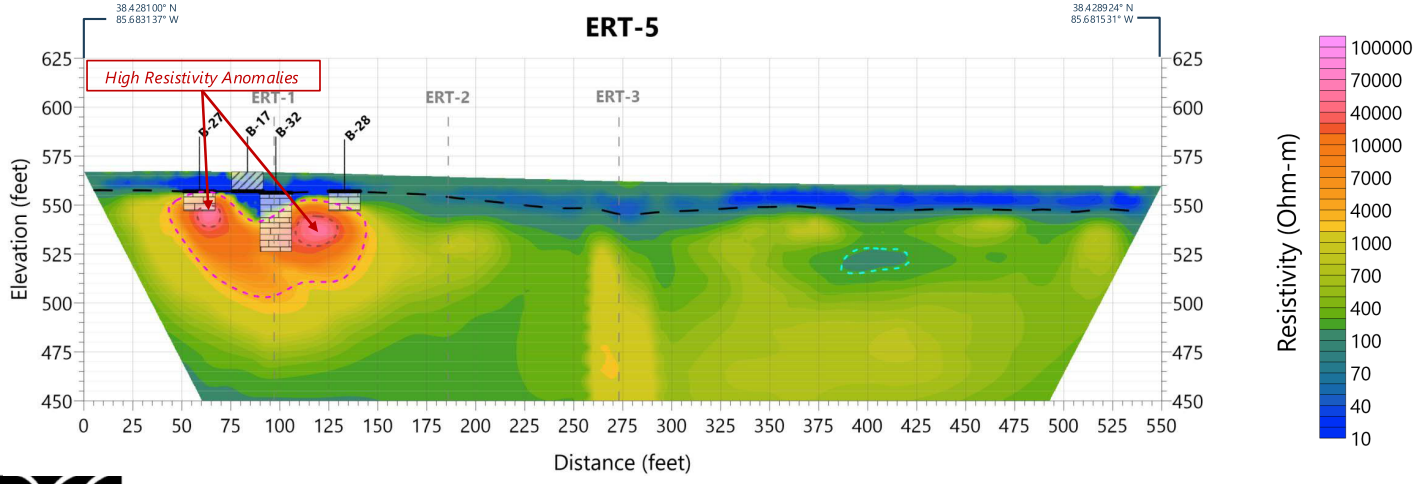

What are the benefits?

Incorporating geophysics into a geotechnical program has the capability of improving the accuracy of the subsurface model; either prior to a drilling program, in support of a site that has already been drilled, or within areas where accessibility is limited for drilling (i.e., river system).

Minimally Invasive

- Ideal for populated and sensitive areas (e.g., environmental, archaeological, etc.)
- Can reduce or eliminate invasive tests

Efficient

- Evaluation of large areas in a relatively short time
  - Approximately 2,000 linear feet of ERT per 10-hour timeframe
  - Up to 3,000 linear feet of 2D MASW per 10-hour timeframe
- Can Be Cost Effective

Comprehensive

- Combining geophysical method(s) and ground truth data, which is generally more invasive, typically leads to a higher confidence in the developed subsurface model.

Case Study 1:

U.S. 231 Over Doe Creek: Indiana

Project Study Type: Karst analysis for Bridge Replacement

Methodology: Electrical Resistivity Tomography (ERT) and Two-Dimensional Multi-channel Analysis of Surface Waves (2D MASW)

Principles of Karst

The term Karst is applied to the topography of a region that is underlain by limestone, dolomite, gypsum, or other rocks which can be affected by dissolution. Karst topography is characterized by surface depressions into which water is channeled and diverted into underground passageways and caverns.

Four Conditions Necessary for Karst Terrain Development:

1. Soluble rock at or near the surface
2. Dense rock with zones of weakness (i.e., highly jointed, thin-bedded, etc.)
3. Located in entrenched valleys below uplands
4. Region of moderate to abundant rainfall

NOTE: Geologic timeframe must be considered with karst development conditions

Ohio River Valley Karst Region

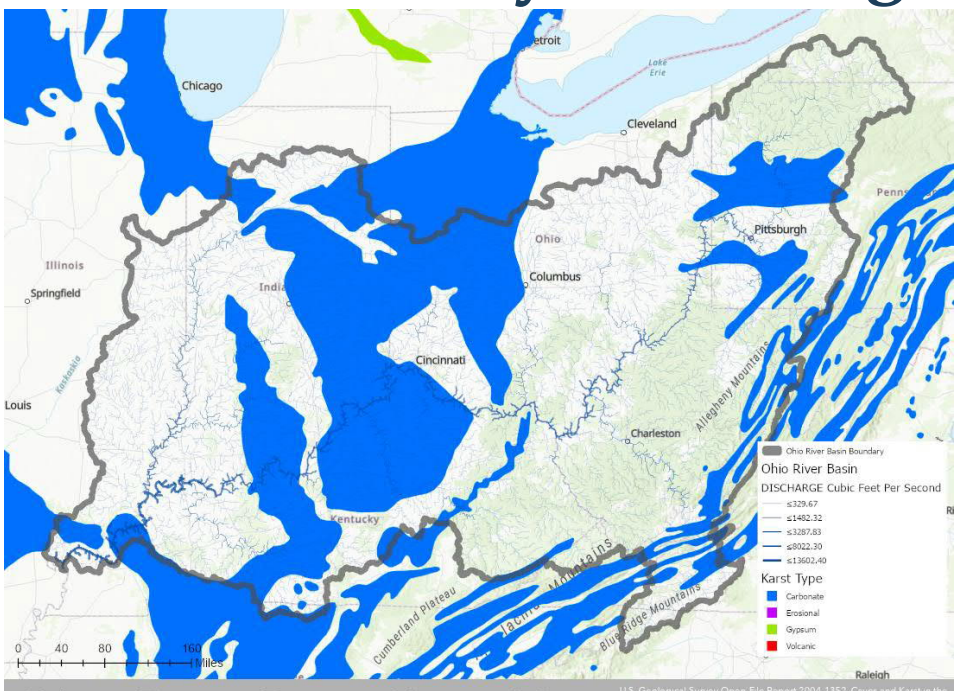

Karst Feature Illustrations

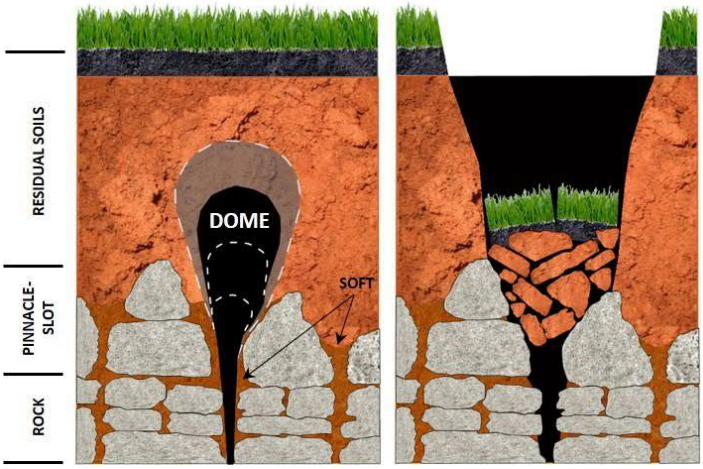

Hon, K. D. & Cox, J. B., (2016). Multi-Method Geophysical Exploration of the McMinn County Airport. *Fast Times,* 21(3), 10. (modified from Sowers, 1996)

Case Study 1

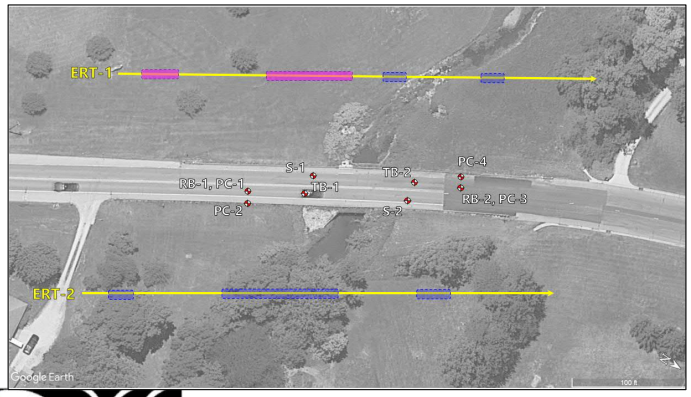

Approximate Location of ERT Anomaly (Type I)

Approximate Location of ERT Anomaly (Type II)

Primary Goals of the Geophysical Survey

- ERT – Karst features, depth to rock, and general subsurface information

Case Study 1

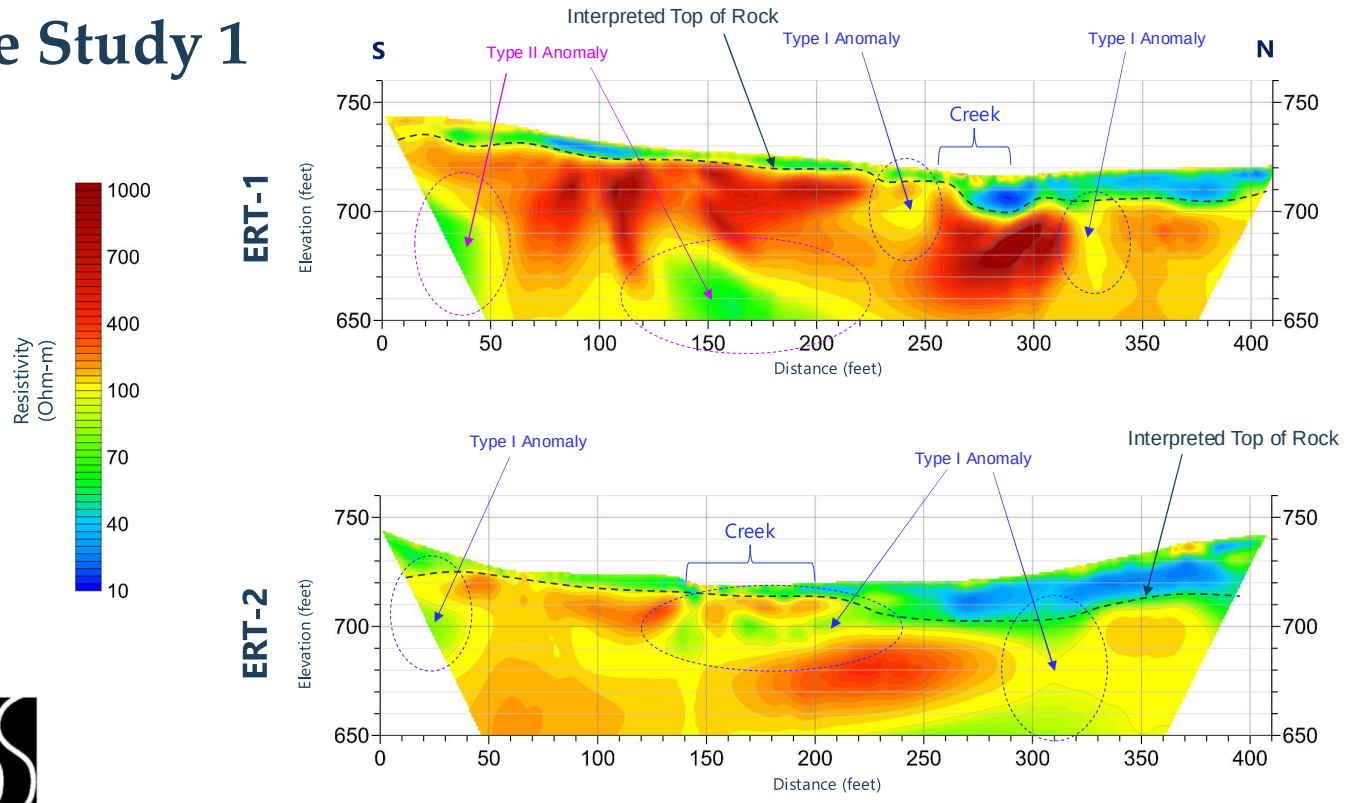

Case Study 2:

Line 223, Twelve-Mile Creek: North Carolina

Project Study Type: Horizontal Directional Drilling (HDD)

Methodology: Electrical Resistivity Tomography (ERT) and Two-Dimensional Multi-channel Analysis of Surface Waves (2D MASW).

Case Study 2

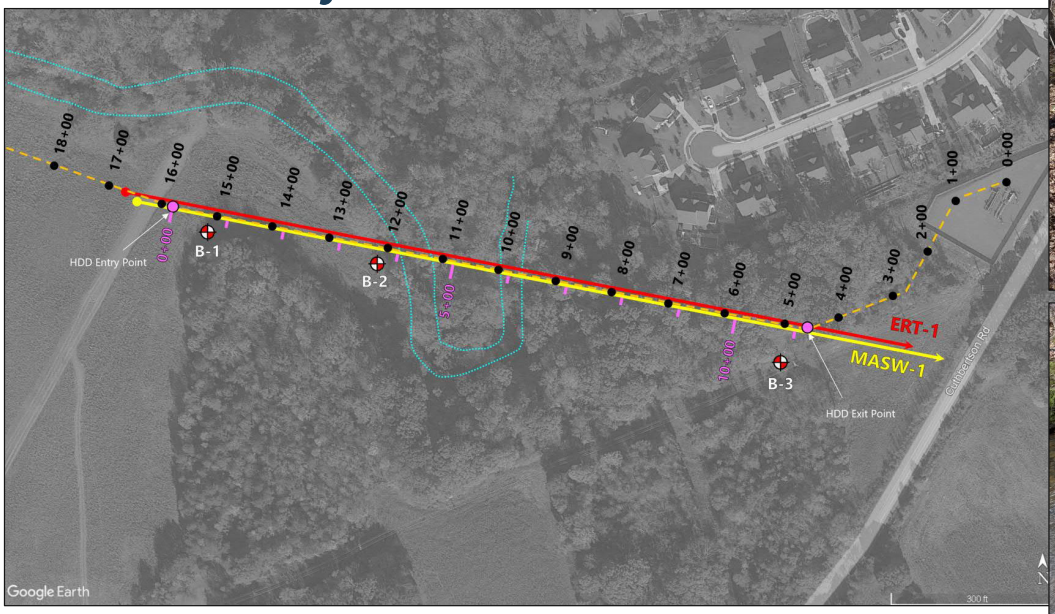

Primary Goals of the Geophysical Survey

- ERT – Depth to rock and general subsurface information
- 2D MASW – Depth of rock and material rigidity

Case Study 2

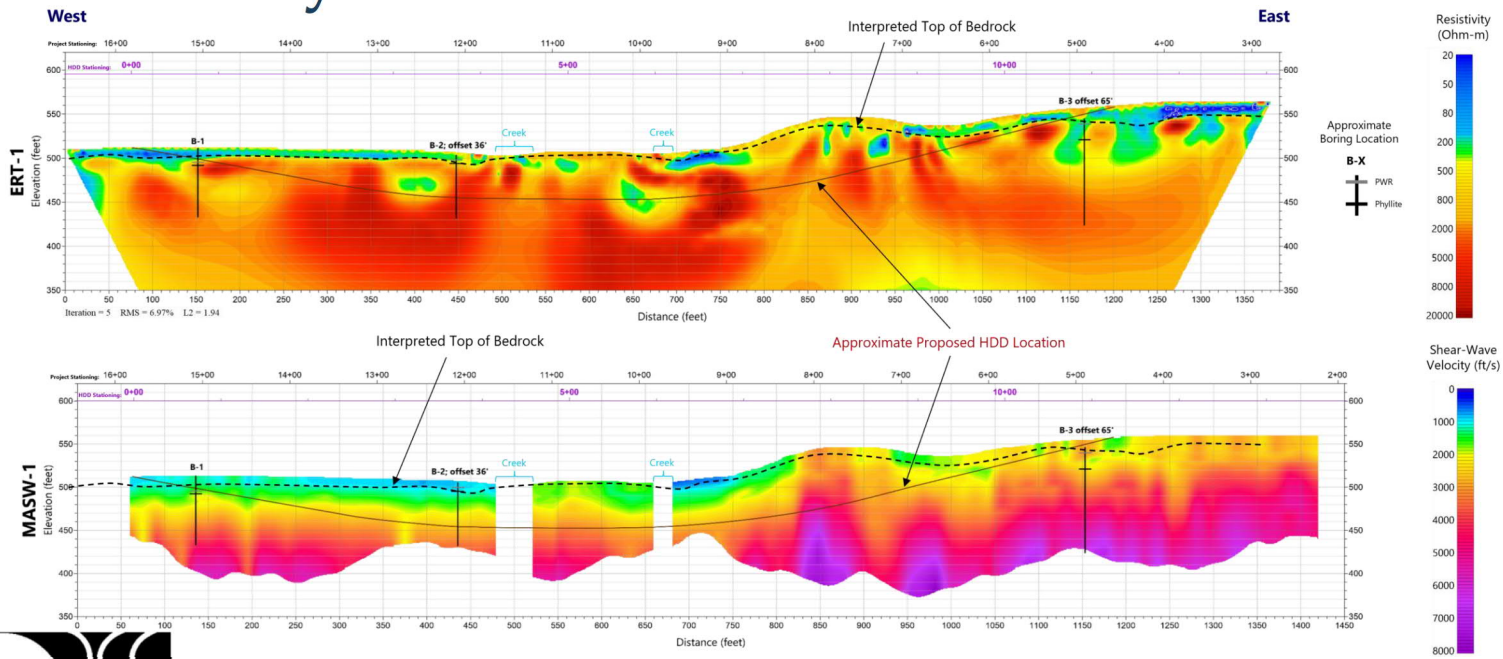

Case Study 2

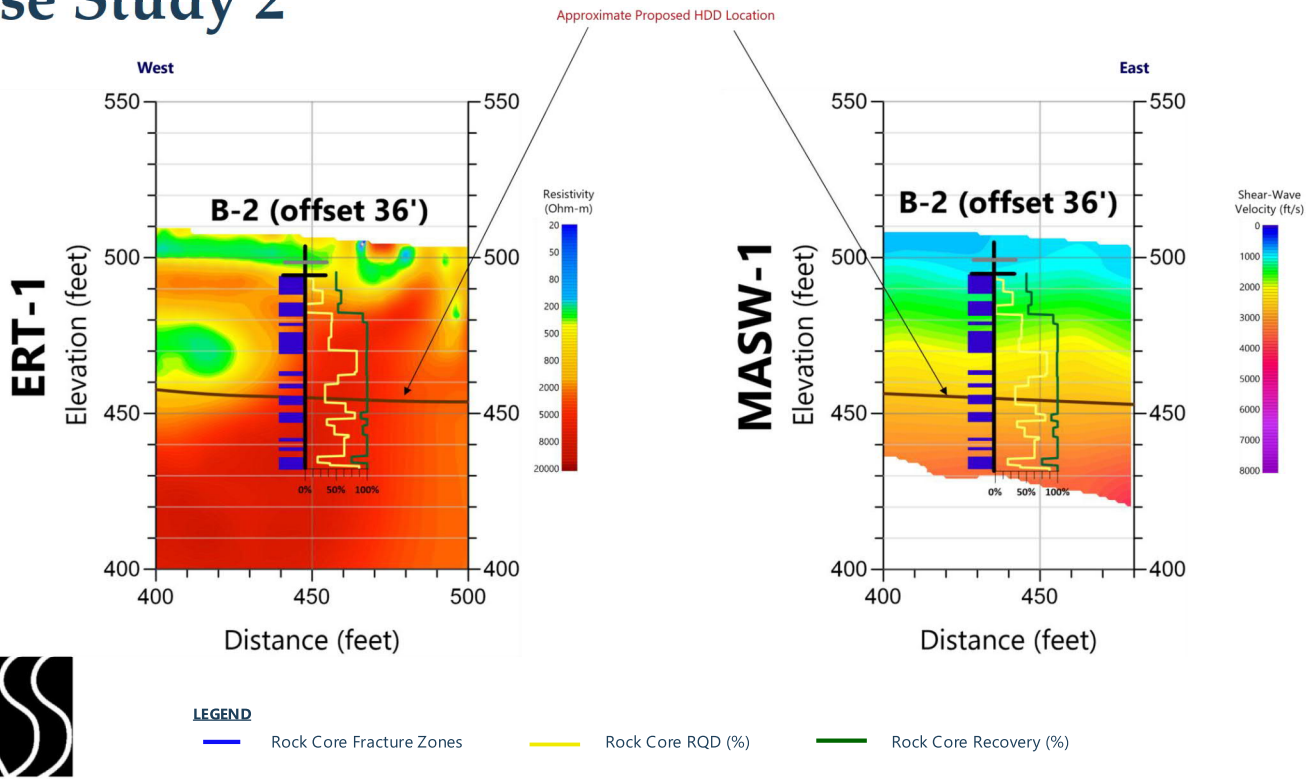

Case Study 3:

Line 467, Crooked Creek & Rocky River: North Carolina

Project Study Type: Horizontal Directional Drilling (HDD)

Methodology: Electrical Resistivity Tomography (ERT) and Two-Dimensional Multi-channel Analysis of Surface Waves (2D MASW)

Case Study 3 – Crooked Creek

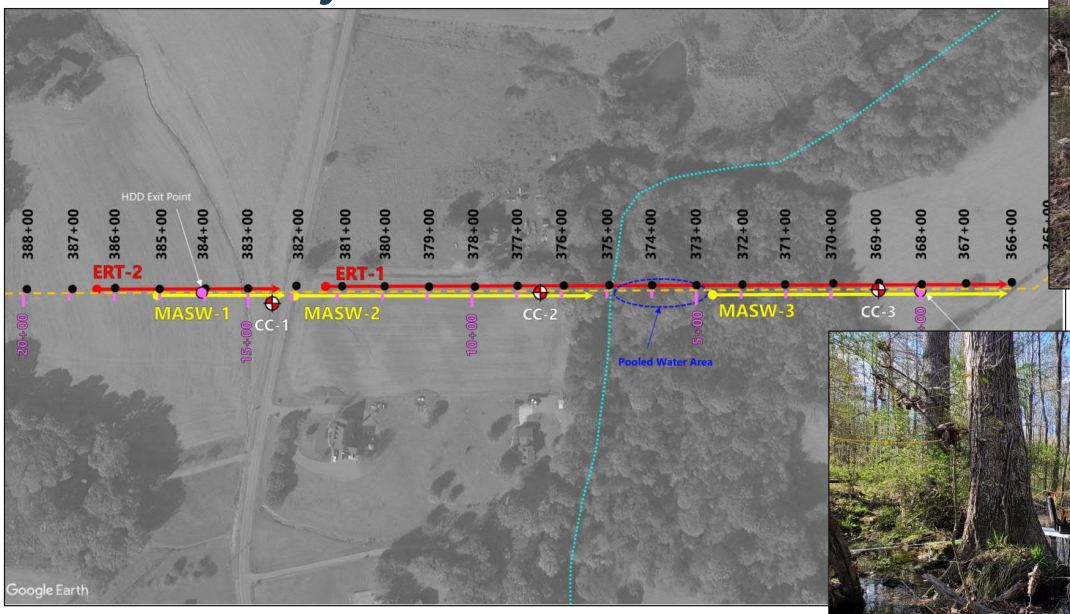

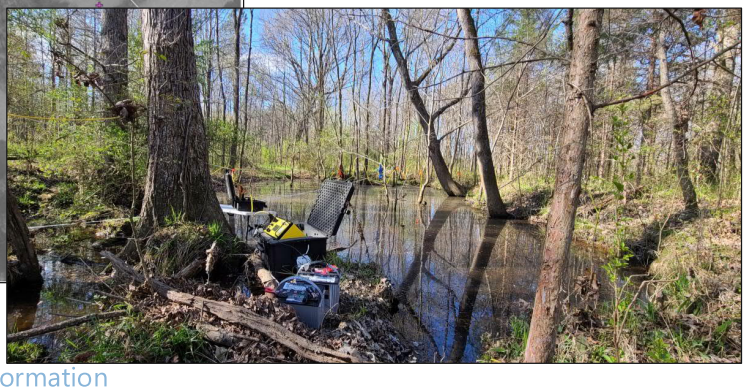

Primary Goals of the Geophysical Survey

- ERT – Depth to rock and general subsurface information
- 2D MASW – Depth of rock and material rigidity

Case Study 3 – Crooked Creek

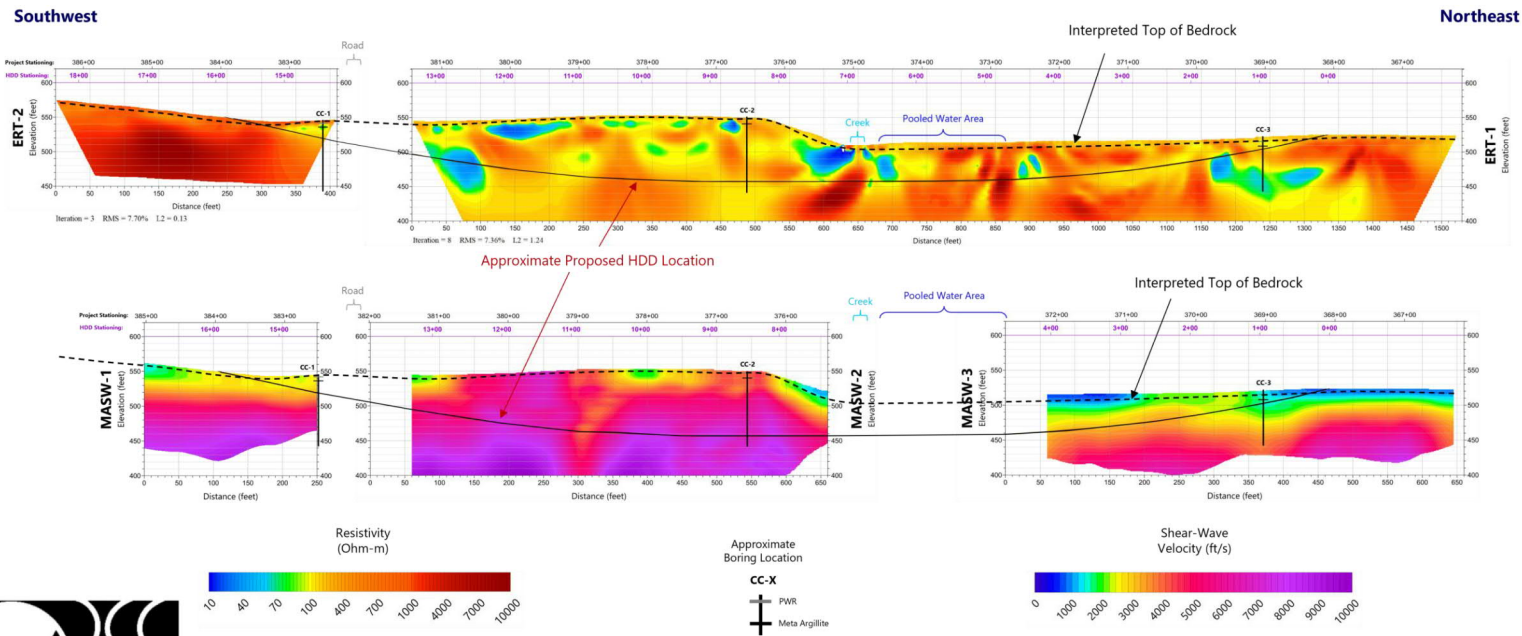

Case Study 3 – Crooked Creek

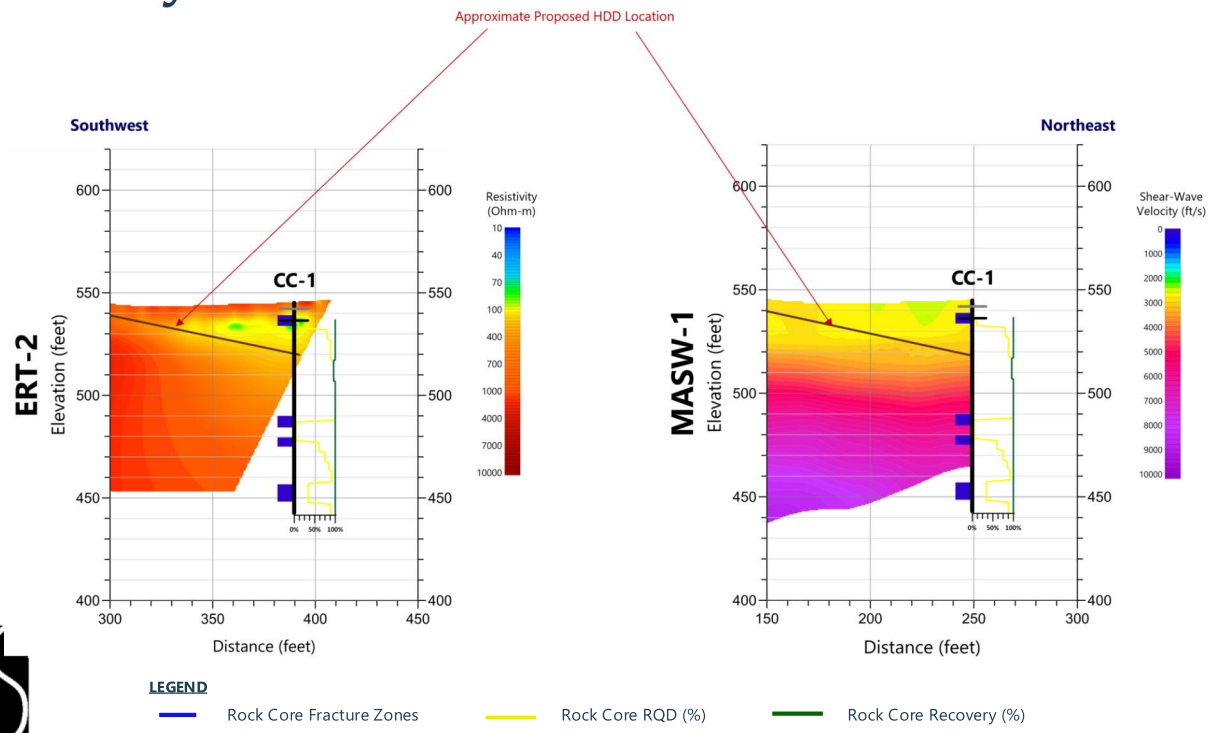

Case Study 3 – Rocky River

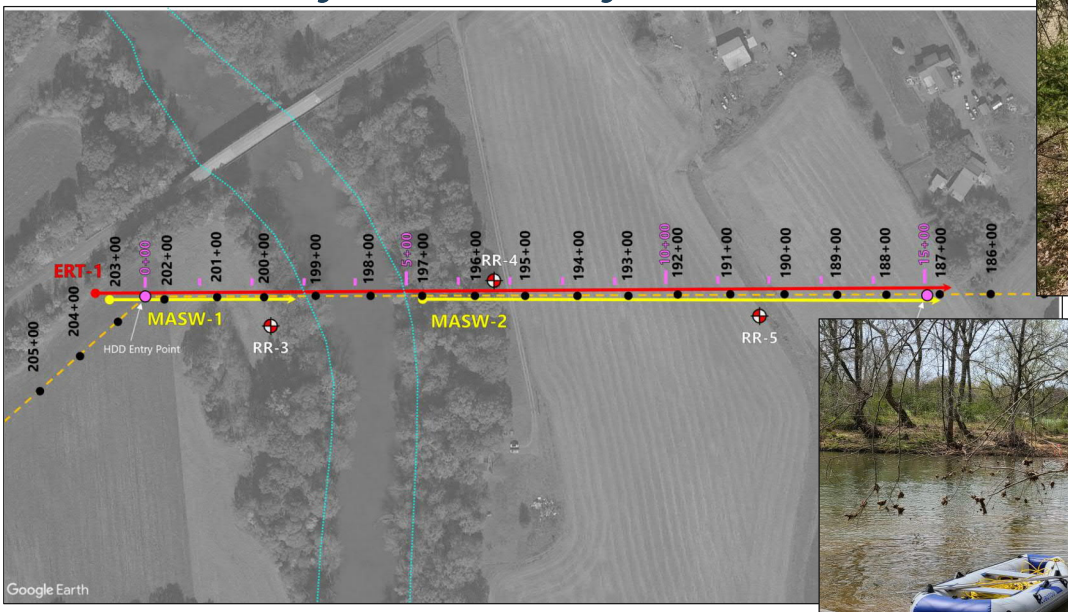

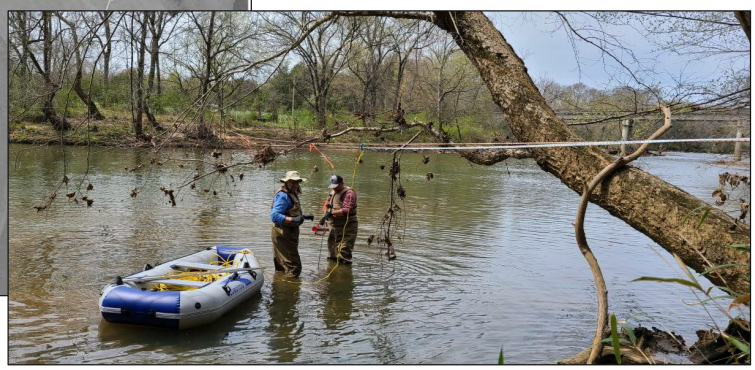

Primary Goals of the Geophysical Survey

- ERT – Depth to rock and general subsurface information
- 2D MASW – Depth of rock and material rigidity

Case Study 3 – Rocky River

Case Study 3 – Rocky River

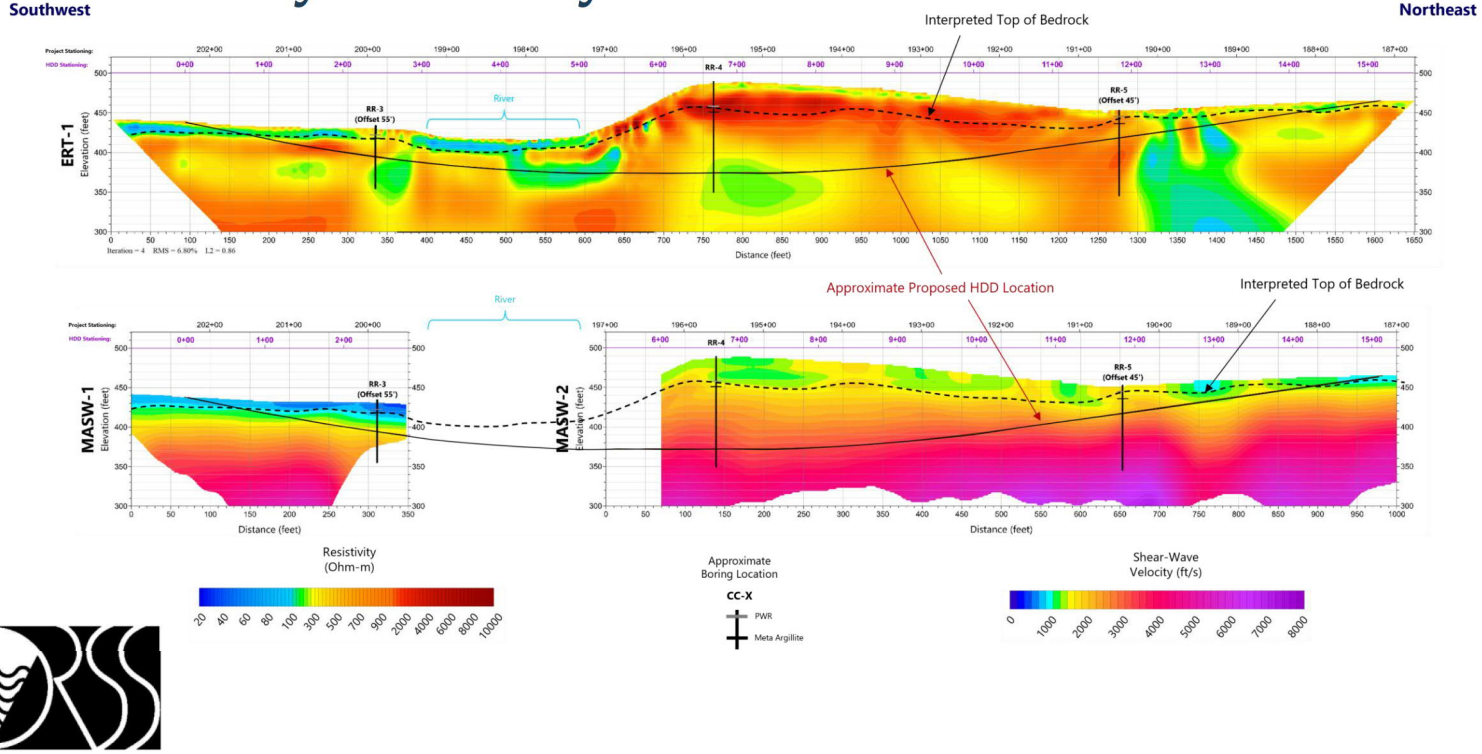

Case Study 3 – Rocky River

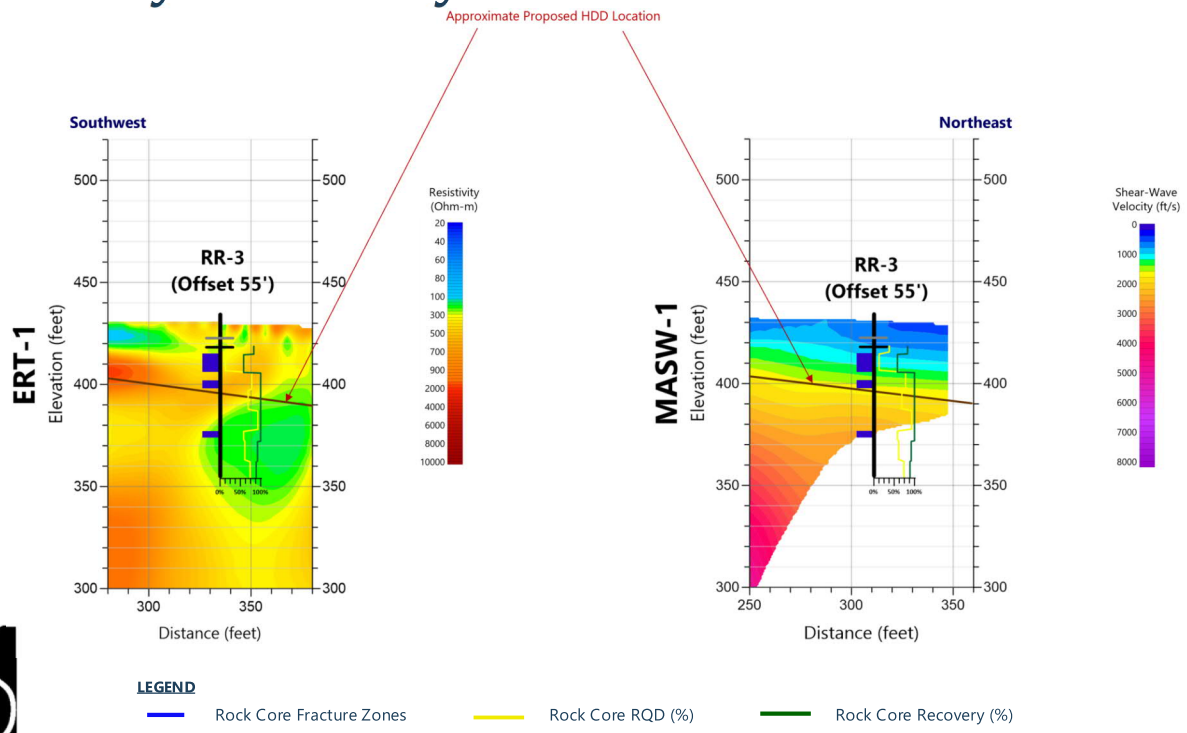

Case Study 4:

C367 Pipeline, East Fork Little Miami River: Ohio

Project Study Type: Horizontal Directional Drilling

Methodology: Electrical Resistivity Tomography (ERT), Frequency Domain Electromagnetics (FDEM), and 1D Multi-channel Analysis of Surface Waves/Microtremor Array Method (1D MASW/MAM)

So, what are the Concerns?

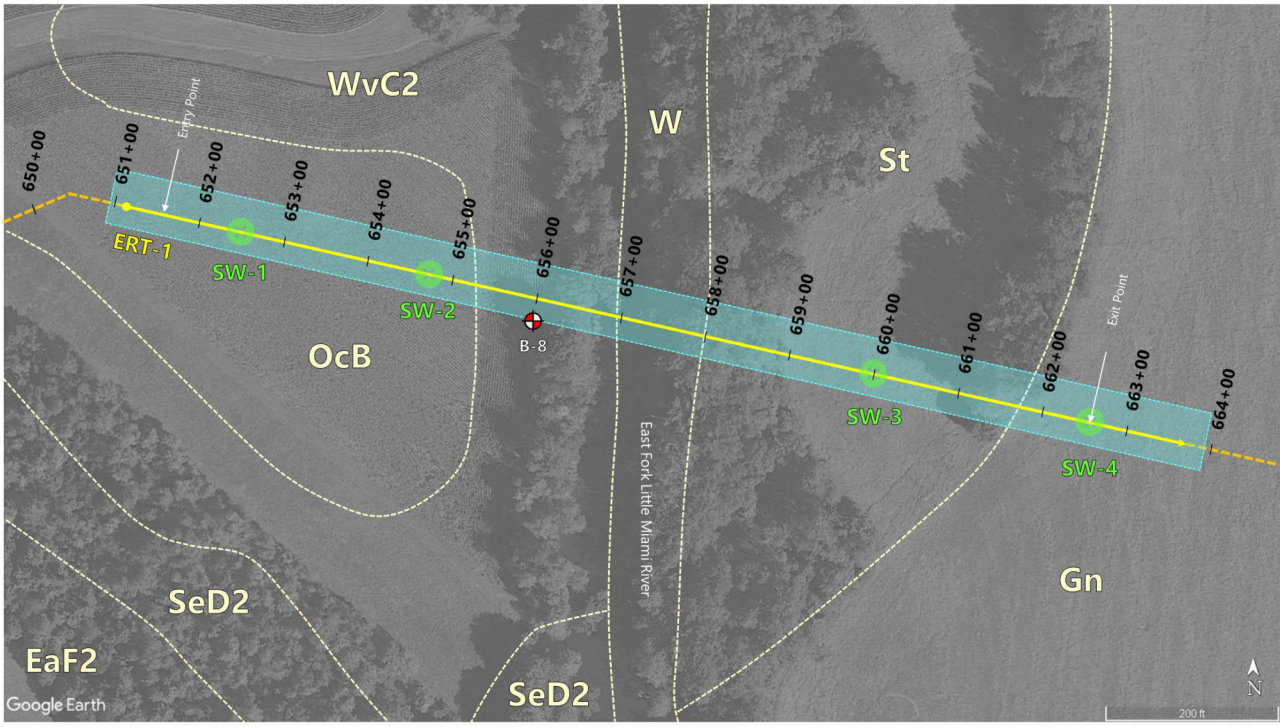

Google Earth Aerial September 2021

Geophysical Surveys – ERT, FDEM, and 1D MASW/MAM

Primary Goals of the Geophysical Survey

- ERT – Identify possible karst features, depth to rock, and general subsurface information.
- 1D MASW/MAM – Site classifications/shear wave velocity estimation
- FDEM – Measure the electrical conductivity of subsurface soil, rock, and groundwater.

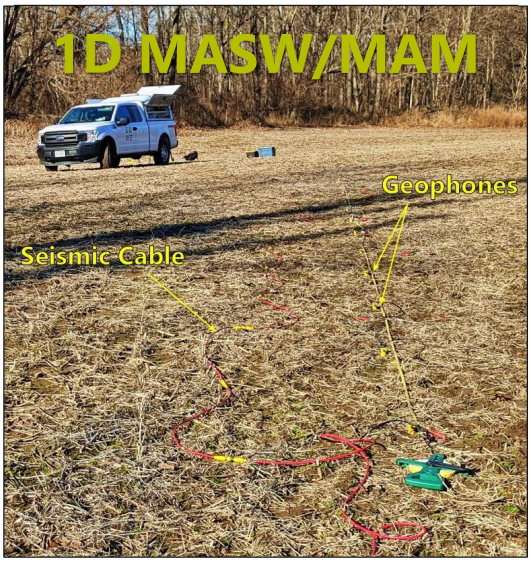

Example ERT/1D MASW/MAM Data

- 4 Layers:
  - Unconsolidated alluvium overburden.
  - Lean clay, silty sand, highly weathered shale with limestone float overburden.
  - Weathered shale with interbedded limestone.
  - Moderately weather shale with interbedded limestone.
- Anomalies:
  - Anomalies A, B, and C: Low resistivity zones within Layer 4 (weathered shale with interbedded limestone). Related to fracturing.
  - Anomaly C: Possible artifact generated from modeling inversion.

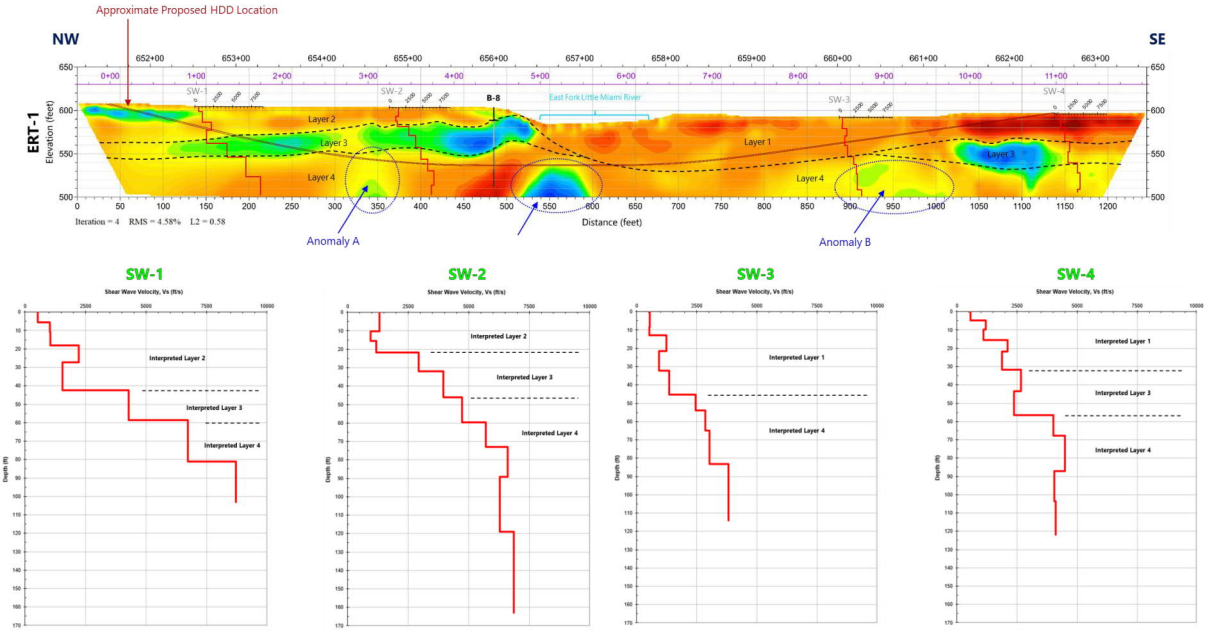

Example FDEM Data

- Conductivity:
  - FDEM terrain conductivity responses for weighted average exploration range between 10- to 30-mS/m
  - In-phase component of FDEM data responses range between –12- to 12-ppt
  - Variability in the distribution of in-phase responses was not observed which indicates lack of unknown metallic structures at site.
  - Observed lateral and vertical changes in conductivity are likely related to variations in soils vs buried obstructions (utilities, debris, etc.).

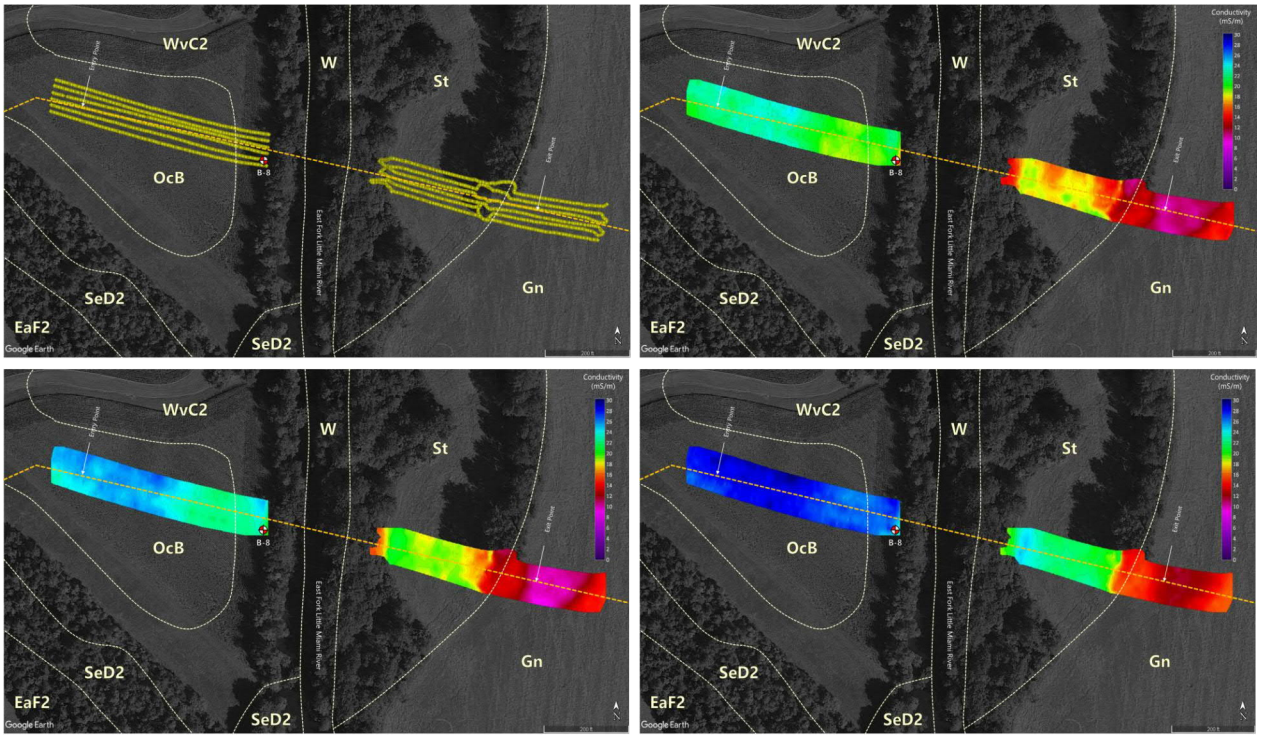

Case Study 5:

Creston Bridge Replacement: West Virgina

Project Study Type: Bridge Replacement and Material Properties Estimate

Methodology: Electrical Resistivity Tomography (ERT)

Case Study 5 – So, what are the Concerns? ERT Survey Design

AGI SuperSting R8 System

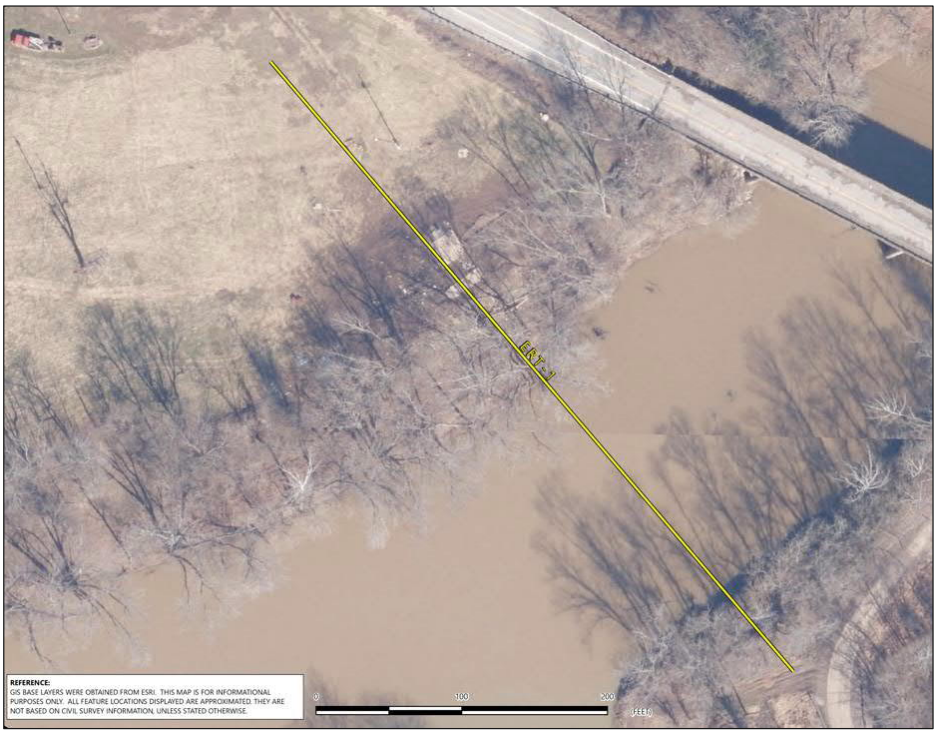

Case Study 5 – ERT Survey Design

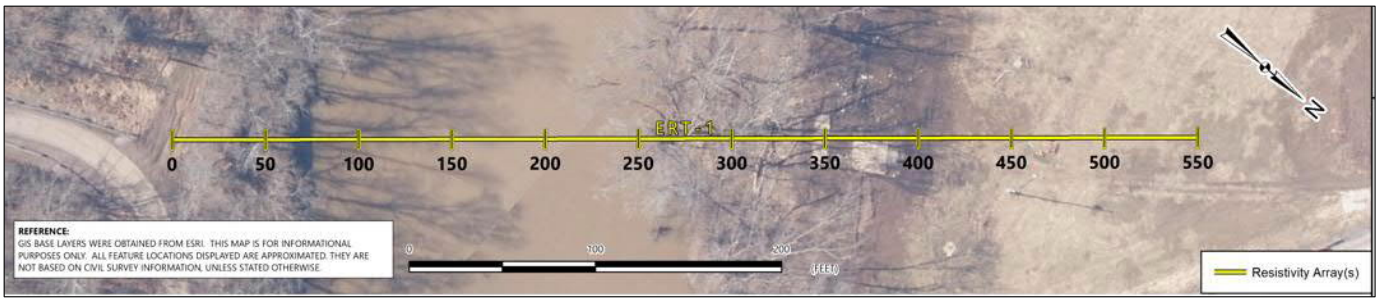

Google Earth Aerial February 2020

Case Study 5 – Example ERT Data

- Anomalies (2 Types)
  - Anomaly A: High resistivity areas indicating a steep riverbank or possible buried metallic artifact.
  - Anomaly B & C: Low resistivity areas corresponding to two cement foundations.
- Depth of partially weathered rock is interpreted to vary between 3 to 12 feet, but not deeper than approximately 15 feet.

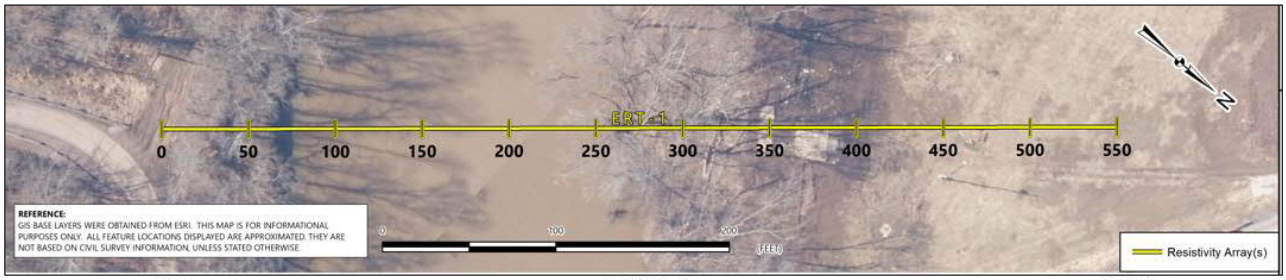

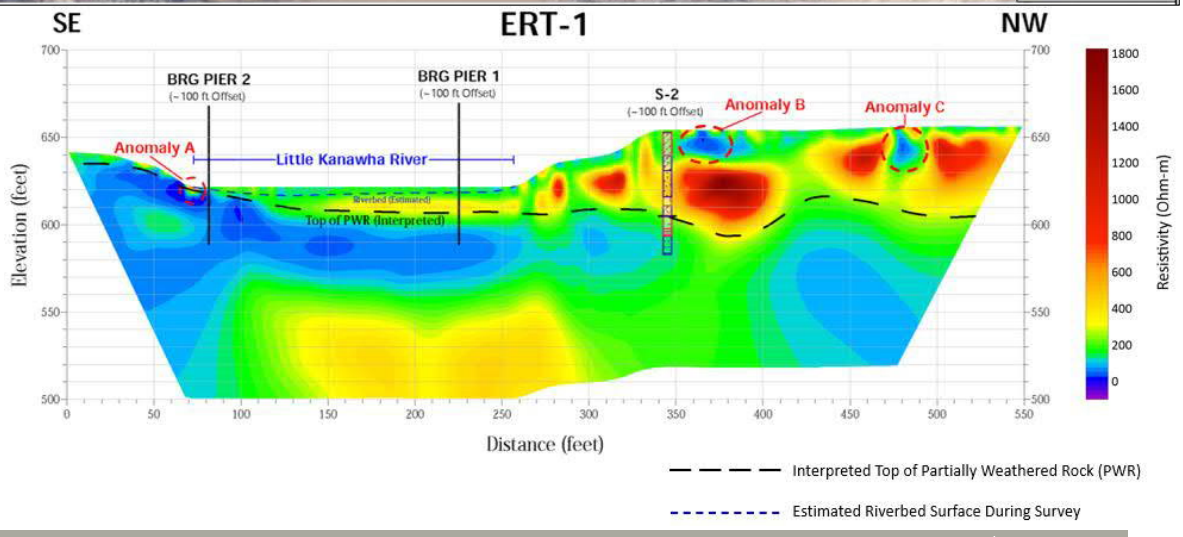

Conclusion

- River crossings can be problematic for a geotechnical program; however, there are geophysicists who are willing to get their feet wet. Coupling a geotechnical program with geophysics often provides a more robust model and understanding of the subsurface environment.
- Questions?

Thank you!

CHRONOLOGY OF OHIO RIVER VALLEY SOIL SEMINARS

ORVSS I	BUILDING FOUNDATION DESIGN AND CONSTRUCTION, October 16, 1970, Lexington, KY
ORVSS II	EARTHWORK ENGINEERING, START TO FINISH, October 15, 1971, Louisville, KY
ORVSS III	LATERAL EARTH PRESSURES, October 27, 1972, Fort Mitchell, KY
ORVSS IV	GEOTECHNICS IN TRANSPORTATION ENGINEERING, October 5, 1973, Lexington, KY
ORVSS V	ROCK ENGINEERING, October 18, 1974, Clarksville, IN
ORVSS VI	SLOPE STABILITY AND LANDSLIDES, October 17, 1975, Fort Mitchell, KY
ORVSS VII	SHALE AND MINE WASTES: GEOTECHNICAL PROPERTIES, DESIGN, AND CONSTRUCTION, October 8, 1976, Lexington, KY
ORVSS VIII	EARTH DAMS AND EMBANKMENTS: DESIGN, CONSTRUCTION AND PERFORMANCE, October 14, 1977, Louisville, KY
ORVSS IX	DEEP FOUNDATIONS, October 27, 1978, Fort Mitchell, KY
ORVSS X	GEOTECHNICS OF MINING, October 5, 1979, Lexington, KY
ORVSS XI	EARTH PRESSURE AND RETAINING STRUCTURES, October 10, 1980, Clarksville, IN
ORVSS XII	GROUNDWATER: MONITORING, EVALUATION AND CONTROL, October 9, 1981, Fort Mitchell, KY
ORVSS XIII	RECENT ADVANCES IN GEOTECHNICAL ENGINEERING PRACTICE, October 8, 1982, Lexington, KY
ORVSS XIV	FOUNDATION INSTRUMENTATION AND GEOPHYSICAL EXPLORATION, October 14, 1983, Clarksville, IN
ORVSS XV	PRACTICAL APPLICATION OF DRAINAGE IN GEOTECHNICAL ENGINEERING, November 2, 1984, Fort Mitchell, KY
ORVSS XVI	APPLIED SOIL DYNAMICS, October 11, 1985, Lexington, KY
ORVSS XVII	NATURAL SLOPE STABILITY AND INSTRUMENTATION, October 17, 1986, Clarksville, IN
ORVSS XVIII	LIABILITY ISSUES IN GEOTECHNICAL ENGINEERING AND CONSTRUCTION, November 6, 1987, Fort Mitchell, KY
ORVSS XIX	CHEMICAL AND MECHANICAL STABILIZATION OF SOIL SUBGRADES, October 21, 1988, Lexington, KY
ORVSS XX	CONSTRUCTION IN AND ON ROCK, October 27, 1989, Louisville, KY
ORVSS XXI	ENVIRONMENTAL ASPECTS OF GEOTECHNICAL ENGINEERING, October 26, 1990, Fort Mitchell, KY
ORVSS XXII	DESIGN AND CONSTRUCTION WITH SYNTHETICS, October 18, 1991, Lexington, KY
ORVSS XXIII	IN-SITU SOIL MODIFICATION, October 16, 1992, Louisville, KY
ORVSS XXIV	GEOTECHNICAL ASPECTS OF INFRASTRUCTURE RECONSTRUCTION, October 15, 1993, Fort Mitchell, KY
ORVSS XXV	RECENT ADVANCES IN DEEP FOUNDATIONS, October 21, 1994, Lexington, KY
ORVSS XXVI	SITE INVESTIGATIONS: GEOTECHNICAL AND ENVIRONMENTAL, October 20, 1995, Clarksville, IN
ORVSS XXVII	FORENSIC STUDIES IN GEOTECHNICAL ENGINEERING, October 11, 1996, Cincinnati, OH

CHRONOLOGY OF OHIO RIVER VALLEY SOIL SEMINARS (CONTINUED)

ORVSS XXVIII	UNCONVENTIONAL FILLS: DESIGN, CONSTRUCTION AND PERFORMANCE, October 10, 1997, Lexington, KY
ORVSS XXIX	PROBLEMATIC GEOTECHNICAL MATERIALS, October 16, 1998, Louisville, KY
ORVSS XXX	VALUE ENGINEERING IN GEOTECHNICAL CONSULTING AND CONSTRUCTION, October 1, 1999, Cincinnati, OH
ORVSS XXXI	INSTRUMENTATION, September 15, 2000, Lexington, KY
ORVSS XXXII	REGIONAL SEISMICITY AND GROUND VIBRATIONS, October 24, 2001, Louisville, KY
ORVSS XXXIII	GROUND STABILIZATION AND MODIFICATION, October 18, 2002, Covington, KY
ORVSS XXXIV	APPLICATIONS OF EARTH RETAINING SYSTEMS AND GEOSYNTHETIC MATERIALS, September 19, 2003, Lexington, KY
ORVSS XXXV	ROCK ENGINEERING AND TUNNELING, October 20, 2004, Louisville, KY
ORVSS XXXVI	GEOTECHNICAL INNOVATIONS IN TRANSPORTATION ENGINEERING, October 14, 2005, Covington, KY
ORVSS XXXVII	INNOVATIONS IN EXPLORATION OF SUBSURFACE VOIDS, October 27, 2006, Lexington, KY
ORVSS XXXVIII	CIVIL INFRASTRUCTURE AND THE ROLE OF GEOTECHNICAL ENGINEERING, November 14, 2007, Louisville, KY
ORVSS XXXIX	URBAN CONSTRUCTION, October 17, 2008, Covington, KY
ORVSS XL	GEOTECHNICAL ENGINEERING AND ENERGY INFRASTRUCTURE, November 13, 2009, Lexington, KY
ORVSS XLI	NATIONAL INFRASTRUCTURE: DAM AND LEVEE SAFETY, October 20, 2011, Louisville, KY
ORVSS XLII	LESSONS LEARNED: FAILURES AND FORENSICS, October 21, 2011, Cincinnati, OH
ORVSS XLIII	WALLS: ABOVE AND BELOW GRADE, November 19, 2012, Lexington, KY
ORVSS XLIV	THE APPLICATION OF GEOLOGY TO GEOTECHNICAL ENGINEERING PRACTICE, November 15, 2013, Louisville, KY
ORVSS XLV	GEOTECHNICAL ASPECTS OF WATERFRONT DEVELOPMENT, October 17, 2014, Cincinnati, OH
ORVSS XLVI	GROUTING SOLUTIONS TO GEOTECHNICAL PROBLEMS, December 16, 2016, Lexington, KY
ORVSS XLVII	GEOTECHNICAL ASPECTS OF THE LOUISVILLE-SOUTHERN INDIANA OHIO RIVER BRIDGES PROJECT, November 16, 2016, Louisville, KY
ORVSS XLVIII	INFRASTRUCTURE INNOVATION IN GEOTECHNICAL DESIGN, November 17, 2017, Cincinnati, OH
ORVSS XLIX	TOOLS FOR ASSESSING GEOTECHNICAL SITE CONDITIONS, November 29, 2018, Lexington, Kentucky
ORVSS L	50 YEARS OF GEOPROGRESS, November 13, 2019, Louisville, Kentucky
ORVSS LI	GEOHAZARDS – CHALLENGES TO GEOTECHNICAL ENGINEERING, November 2, 2021, Cincinnati, Ohio
ORVSS LII	IDENTIFYING, ASSESSING AND MANAGING RISKS THROUGHOUT THE OHIO RIVER VALLEY, November 2, 2022, Lexington, Kentucky

ORVSS LIII WHAT'S UP IN GEOTECH, November 8, 2023, Louisville, Kentucky

ORVSS LIV WATER IN GEOTECHNICAL ENGINEERING, November 13, 2024, Cincinnati, Ohio